

**HUB ASSEMBLIES FOR THE NEXT GENERATION OF BASCULE
BRIDGES**

**Glen Besterfield, Autar Kaw & Niranjana Pai
Department of Mechanical Engineering
Final Report
May 31, 2006**

**A Report on a Research Project Sponsored by the
Florida Department of Transportation
Contract BD544-17**

DISCLAIMER

The opinions, findings and conclusions expressed in this publication are those of the authors who are responsible for the facts and accuracy of the data presented herein. The contents do not necessarily reflect the views or the policies of the Florida Department of Transportation or the Federal Highway Administration.

Technical Report Documentation Page

1. Report No.	2. Government Accession No.	3. Recipient's Catalog No.	
4. Title and Subtitle Hub Assemblies For The Next Generation Of Bascule Bridges		5. Report Date May 31, 2006	
		6. Performing Organization Code USF	
7. Author(s) Glen Besterfield, Autar Kaw & Niranjn Pai		8. Performing Organization Report No.	
9. Performing Organization Name and Address Department of Mechanical Engineering University of South Florida Tampa, FL 33620-5350		10. Work Unit No. (TRAIS)	
		11. Contract or Grant No. BD544-17	
12. Sponsoring Agency Name and Address Florida Department of Transportation 605 Suwannee St. MS 30 Tallahassee, Florida 32399 (850)414-4615		13. Type of Report and Period Covered Final Report October 2004- March 2006	
		14. Sponsoring Agency Code FDOT	
15. Supplementary Notes			
16. Abstract <p>The objective of this project was to establish the basis for updating the current guidelines for design of bascule bridge hub assemblies with emphasis on recommendations for the various hub geometry parameters. Review of recent bascule bridge designs plans revealed that some FDOT guidelines for hub geometry are not consistently followed in practice.</p> <p>Simplified design equations and finite element models were used to determine the stresses developed in the hub assembly due to the shrink fit between the hub and trunnion. The analysis indicated that tensile hoop stresses developed in the hub may exceed the allowable static stress limits in many bridges designed based on the current FDOT design guidelines.</p> <p>A MathCAD worksheet was developed to generate preliminary hub assembly design to meet all the performance and strength requirements. Sample computations performed using design loads from representative bridges revealed that it is possible to obtain satisfactory designs by using the current FDOT recommendations for hub geometry.</p> <p>Structural finite element analysis result showed that the true behavior of the structure is more complex than indicated by the analysis used for design. Thermal finite element analysis revealed that current assembly procedure which allows heating of the hub, leads to acceptable levels of thermal stresses.</p> <p>Finally, hub geometry recommendations based on castability are presented. Also, guidelines for acceptance criteria of hub casting are proposed.</p>			
17. Key Word Movable bridge, Trunnion, Hub, Bascule bridge		18. Distribution Statement No restriction. This report is available to the public through NTIS, Springfield, VA 22161	
19. Security Classif. (of this report) Unclassified	20. Security Classif. (of this page) Unclassified	21. No. of Pages 115	22. Price

ACKNOWLEDGEMENTS

The investigation reported in this document was funded by a contract awarded to the University of South Florida, Tampa, FL, by the Florida Department of Transportation (FDOT). Mr. Thomas Cherukara was the Project Manager. We would like to acknowledge his numerous contributions to this study in the form of discussions and directions. He also provided many of the bridge plans and calculations reviewed as part of this project.

We would like to acknowledge the assistance obtained from Pete Amador of J.C. Machine shop and Lynn Taylor of Hardie Tynes, who for provided us with the name of foundries that cast bascule hubs.

We are grateful to George Hartay, Dan Zachariasen and Kim Kitzerow, from Rexnord (Milwaukee), and Dr. Hathibelgal Roshan, Robert Wabiszewski and Robert S. Judziewicz from Maynard Steel (Milwaukee) for providing their input on castability and acceptance criterion for hub castings.

We wish to thank Mr. Jim Phillips, Mr. George Patton and Mr. Sergey Kupchenko of EC Driver & Associates in Tampa, FL, for providing information on many of the sample bridges analyzed in this project and participating in technical discussions. Finally, we would also like to thank engineers from EC Driver and Associates, Parsons Brinkerhoff, Lichtenstein Consulting Engineers, Hardesty and Hanover and the Florida Department of Transportation, who took time from their busy schedules to attend the research meeting held at the University of South Florida, Tampa, FL, in June 2005.

EXECUTIVE SUMMARY

The objective of this project was to establish the basis for updating the current guidelines for design of bascule bridge hub assemblies. The primary focus of the project is to provide guidelines for the various hub geometry parameters, such as the hub radial thickness, hub length and flange outer diameter.

Review of current design guidelines revealed that FDOT hub geometry requirements result in significantly smaller hub sizes than recommended by AASHTO. Review of recent bascule bridge plans indicated that many of the bridges did not completely conform to the FDOT requirements for hub assembly design. This is partly because these guidelines are meant for bascule bridges with simple trunnions and do not apply to Hopkins frame and box girder types of bridges that were also included in the review.

Simplified design equations and linear finite element analysis results indicated that the tensile hoop stresses developed in the hub due to the interference fit with the trunnion may exceed the allowable static stress limits in hub designs based on current FDOT guidelines. A parameter study revealed that a hub design based on AASHTO, results in tensile hoop stresses that are within allowable limit with an FN2 fit between trunnion and hub. Hub hoop stresses always exceeds the allowable limit if the FN2 fit is replaced with an FN3 fit.

Performance and strength requirements for hub assembly were identified. A MathCAD worksheet that incorporated these requirements was developed to assist in preliminary design of hub assemblies. Review of preliminary designs based on bridge loading of representative bridges revealed that it is possible to obtain satisfactory designs based on current FDOT design guidelines with the methodology used in the worksheet.

Linear three-dimensional finite element models were developed to get a better understanding of the stresses developed in hub assemblies from the interference fit and service loads. The analysis highlighted regions in the hub that have stresses exceeding the allowable limits.

Non-linear two-dimensional plane strain finite element models were developed to study the behavior of contact pressure at the trunnion hub interference fit when the assembly is subjected to vertical loads. Design charts based on this model were developed and incorporated in the MathCAD worksheet used for preliminary design.

A complex non-linear three-dimensional finite element model of bolted joints in hub assemblies was developed to determine the ratio of loads carried by the friction, bolt bearing and direct bearing (between girder and hub) when the hub assembly is subjected to vertical service loads.

Thermal analysis of the current shrink fit procedure conducted using finite element model found the thermal stresses resulting from the current procedure of heating the hub to be within acceptable limits.

Finally, recommendations based on castability of hub geometry are presented along with preliminary recommendations for hub casting acceptance criteria.

TABLE OF CONTENTS

DISCLAIMER	ii
ACKNOWLEDGEMENTS	iv
EXECUTIVE SUMMARY	v
TABLE OF CONTENTS	vi
LIST OF FIGURES	ix
LIST OF TABLES	xi
LIST OF ABBREVIATIONS	xii
CHAPTER 1 INTRODUCTION	1
1.1 Introduction	1
1.2 Objectives	3
1.3 Tasks	3
1.3.1 Review of Recent Bascule Bridge Designs	3
1.3.2 Review of Fabrication Process	3
1.3.3 Structural Analysis	3
1.3.4 Thermal Analysis	4
1.3.5 Design Optimization	4
1.3.6 Recommendations	4
1.4 Summary	4
CHAPTER 2 LITERATURE REVIEW	5
2.1 Introduction	5
2.2 Review of Design Guidelines	5
2.3 Review of Recent Bascule Bridge Designs	7
2.3.1 Review of Hub Geometry	8
2.3.2 Review of Hub Assembly Design Computations	9
2.4 Meeting with Consulting Design Engineers	11
2.5 Assembly Practices	11
2.6 Parametric Modeling and Full Scale Testing [1]	12
2.7 Hub Assemblies Without Shrink Fit [33]	13
2.8 Miscellaneous Studies	13
2.9 Summary	14
CHAPTER 3 HUB CASTINGS	15
3.1 Introduction	15
3.2 Overview of Hub Casting Process	15
3.3 Recommendations from Foundry Engineers	15
3.3.1 Hub Geometry	16
3.3.2 Acceptance Criteria	18
3.3.3 Miscellaneous	19
3.4 Hub Casting Acceptance Criteria	20
3.4.1 ASTM A609 [44]	20
3.4.2 ASTM A802 [45]	21
3.4.3 ASTM E165 [46]	21
3.4.4 ASTM E709 [47] & ASTM E125 [48]	22
3.4.5 General	22
3.5 Summary	22

CHAPTER 4	SIMPLIFIED HUB DESIGN	24
4.1	Introduction.....	24
4.2	Loads.....	24
4.2.1	Shear	24
4.2.2	Torsion	25
4.2.3	Axial Loads.....	26
4.2.4	Bending Moment	26
4.2.5	Shrink Fit Assembly Loading.....	27
4.3	Materials	27
4.4	Trunnion Design	27
4.5	Hub Design	28
4.5.1	Hub Length	29
4.5.2	Hub Thickness	29
4.5.3	Hub Flange Thickness.....	32
4.5.4	Hub Flange Outer Diameter.....	33
4.5.5	Hub Ribs	33
4.5.6	Dowels	34
4.5.7	Bolts	35
4.6	Girder and Backing Ring	35
4.7	Shrink Fit Interference	35
4.8	Design for Service Behavior.....	36
4.9	Sample Analysis.....	38
4.10	Summary	39
CHAPTER 5	STRUCTURAL FINITE ELEMENT ANALYSIS	40
5.1	Introduction.....	40
5.2	Finite Element Model	40
5.3	Trunnion-Hub Shrink Fit Stresses	42
5.4	Hub-Girder Shrink Fit Stresses.....	44
5.5	Hub-Assembly Service Behavior.....	46
5.6	Discussion.....	49
5.7	Load Distribution	49
5.7.1	Finite Element Model of Bolted Assembly	50
5.7.2	Results.....	52
5.8	Contact Pressure Analysis.....	54
5.8.1	Finite element Model	54
5.8.2	Results.....	55
5.8.3	Design Chart	56
5.9	Summary	58
CHAPTER 6	THERMAL ANALYSIS	60
6.1	Introduction.....	60
6.2	Finite Element Model	60
6.3	Results.....	64
6.4	Effect of Hub Thickness	66
6.5	Summary	69
CHAPTER 7	RECOMMENDATIONS.....	70
7.1	Design Recommendations	70

7.1.1	Castability Considerations	70
7.1.2	Loading	70
7.1.3	Geometry & Fit	70
7.1.4	Assembly Procedure	71
REFERENCES		72
APPENDIX A HUB CASTING SHOP DRAWING NOTES [43]		76
APPENDIX B SAMPLE CALCULATIONS.....		80

LIST OF FIGURES

Figure 1.1	Box girder scheme (two bearings and two hubs)	1
Figure 1.2	Simple Trunnion (two bearings per trunnion).....	2
Figure 1.3	Overhang trunnion (with one bearing per trunnion) used with Hopkins Frame.....	2
Figure 2.1	Hub assembly nomenclature	6
Figure 2.2	Trunnion hub design guide [3].....	7
Figure 3.1	Tapered hub design	16
Figure 3.2	Casting geometry design to feed “hot spots”	17
Figure 3.3	Rib shapes found in bascule hubs	17
Figure 3.4	Possible rib profile	18
Figure 4.1	General loading on Hub-Girder Assembly.....	25
Figure 4.2	Trunnion hub design nomenclature.....	28
Figure 4.3	Effect of hub thickness on contact pressure	30
Figure 4.4	Effect of hub thickness on tensile hub hoop stress.....	32
Figure 4.5	Effect of hub thickness on contact pressure	37
Figure 5.1	S.R.706 trunnion-hub-girder-backing ring assembly	41
Figure 5.2	Finite element mesh of trunnion-hub-girder-backing ring assembly	41
Figure 5.3	Radial stress (psi) in the hub after trunnion-hub assembly	43
Figure 5.4	Hoop stress (psi) in the hub after trunnion-hub assembly.....	44
Figure 5.5	Radial stress (psi) in the hub after trunnion-hub-girder assembly	45
Figure 5.6	Hoop stress (psi) in the hub after trunnion-hub-girder assembly.....	45
Figure 5.7	Dead load modeling as force on around girder circumference	46
Figure 5.8	Radial stresses (psi) due to shrink fit and dead load + impact	47
Figure 5.9	Hoop stresses (psi) due to shrink fit and dead load + impact.....	48
Figure 5.10	Radial stresses (psi) on girder due to shrink fit and dead load + impact.....	48
Figure 5.11	Finite element mesh of bolted hub assembly	51
Figure 5.12	Hub assembly loading	52
Figure 5.13	Axial stress σ_z (contact pressure) due to bolt preload on backing ring (top) and hub (bottom)	53
Figure 5.14	Finite element mesh of model used to determine contact pressure.....	55
Figure 5.15	Contact Pressure distribution at trunnion-hub interface: (a) immediately after shrink fit (b) upon application of vertical load	56
Figure 5.16	Normalized contact pressure versus applied load	57
Figure 5.17	Reduction in contact pressure at A per unit load per unit hub thickness (ΔC_{PRES}) versus trunnion radius	58
Figure 6.1	Fracture toughness and yield strength as a function of temperature [50]	61
Figure 6.2	Yield strength of steel as a function of temperature [51].....	61
Figure 6.3	Modulus of elasticity of steel as a function of temperature [51].....	62
Figure 6.4	Coefficient of thermal expansion of steel as a function of temperature [52]...62	62
Figure 6.5	Specific heat of steel as a function of temperature [51].....	63
Figure 6.6	Thermal conductivity of steel as a function of temperature [51]	63
Figure 6.7	Areas of hub subjected to heat in finite element model	64
Figure 6.8	Temperature distribution (°F) in the hub during heating after	65

Figure 6.9	Von Mises stress (psi) in the hub during heating after (a) 0.25 hours (b) 1.5 hours	67
Figure 6.10	Radial displacements (in.) after 6 hours of heating.....	68
Figure 6.11	Von Mises stress (psi) in the hub during heating after 0.25 hours.....	68
Figure 6.12	Radial displacements (in.) after 6 hours of heating.....	69

LIST OF TABLES

Table 2.1	Hub assembly geometry for recent bascule bridges.....	10
Table 3.1	Criteria for classification of indications per ASTM A609 [44]	20
Table 3.2	Visual inspection acceptance criteria [45].....	21
Table 3.3	Types of discontinuities per ASTM E125 [48]	23
Table 4.1	Materials used for hub assemblies	27
Table 4.2	Tensile hoop stress due to FN2 shrink fit.....	31
Table 4.3	Results from sample bridges using proposed design equations	38

LIST OF ABBREVIATIONS

AASHTO	American Association of State Highway and Transportation Officials
FDOT	Florida Department of Transportation
LRFD	Load and Resistance Factor Design
LRFDM	AASHTO. LRFD Movable Highway Bridge Design Specifications
O.D.	Outer Diameter
SDG	FDOT Structures Design Guidelines
USF	University of South Florida

CHAPTER 1 INTRODUCTION

1.1 Introduction

Bascule bridge designs used in Florida have changed over the years as bridge sizes have increased to handle the higher traffic demands. Design of large bascule bridges capable of handling up to four lanes of traffic brings new challenges that have not been addressed by current design guidelines. For example, some recent bascule bridges utilize a box girder design (see Figure 1.1) for the main girders instead of the commonly found plate girders, and simple trunnion (Figure 1.2) or Hopkins frame designs (Figure 1.3) of the past. Assembly requirements of such designs place constraints on the hub sizes. As a result, many of these bridges deviate from current AASHTO and FDOT guidelines on hub geometry and hub assembly designs (see Section 2.3 for details).

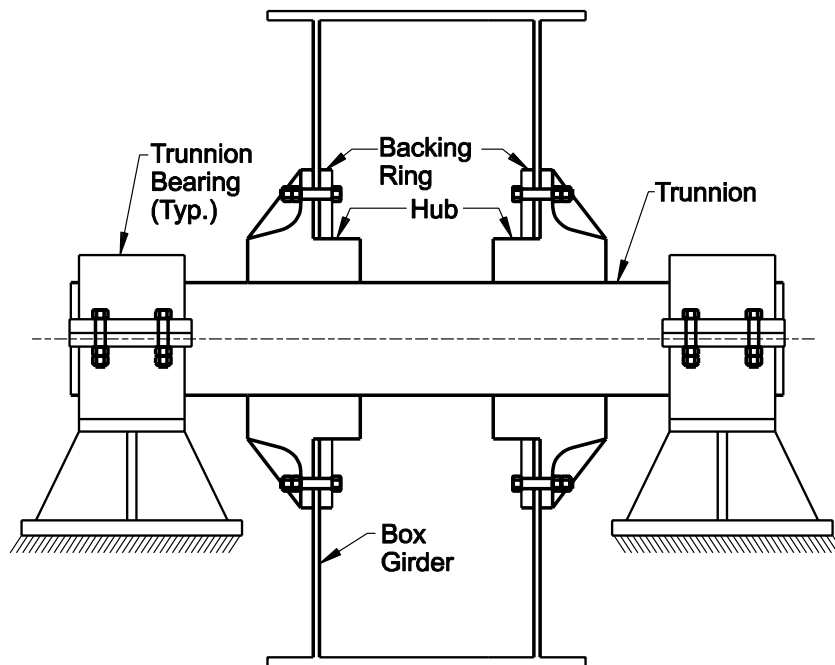


Figure 1.1 Box girder scheme (two bearings and two hubs)

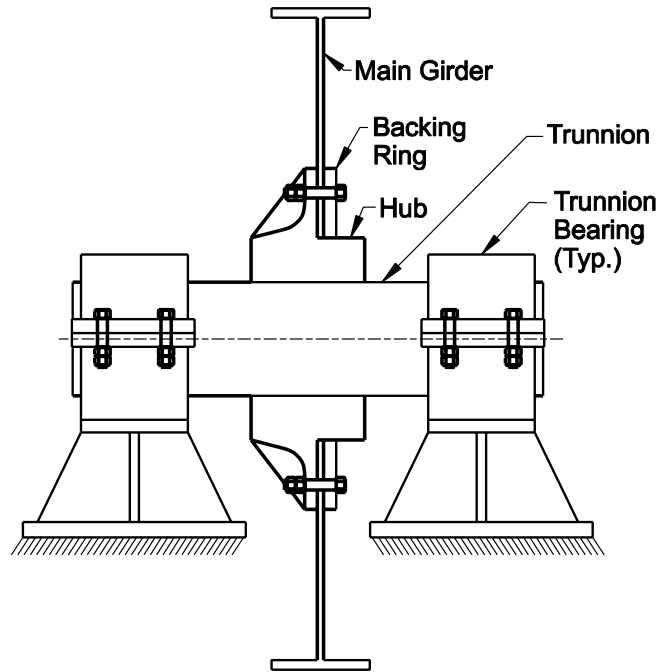


Figure 1.2 Simple Trunnion (two bearings per trunnion)

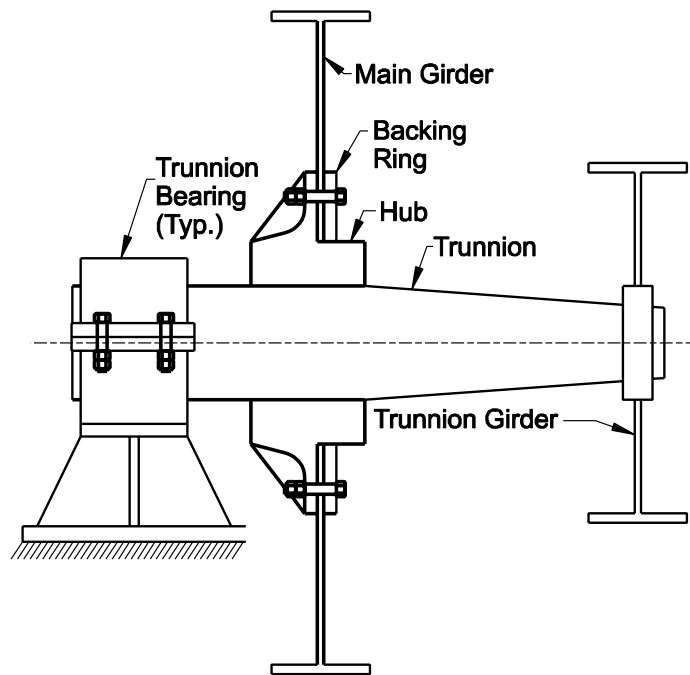


Figure 1.3 Overhang trunnion (with one bearing per trunnion) used with Hopkins Frame

1.2 Objectives

The objective of this project is to determine the influence of the hub geometry on the structural performance of the bridge in service. The impact of the proposed hub geometry on the assembly process is also considered because of hub failures experienced during the hub-girder shrink fitting procedure [1]. The finding may be used to update current guidelines used for design of bascule bridge hub assemblies. Tasks performed to reach the stated objectives are listed in the next section.

1.3 Tasks

1.3.1 Review of Recent Bascule Bridge Designs

Several recent bascule bridge plans and design computations were reviewed to document the current state of the practice for hub assembly design. Specifically, deviations from existing AASHTO [2] and state [3] guidelines on hub geometry were identified. Discussions were also held with several design engineers on the current state of the practice. These findings are presented in Chapter 2.

Chapter 2 also reports on procedures used to obtain the shrink-fit between the trunnion-hub and girder. In addition, several studies related to trunnion-hub-girder assembly process are summarized in the chapter.

1.3.2 Review of Fabrication Process

Typical bascule hubs are fabricated by casting. It was considered important to get input from foundry engineers on geometric features that affect castability of the hub. Chapter 3 presents a summary of the findings from discussions with foundry engineers on topics of hub geometry. Recommendations for hub casting acceptance criteria are also presented in the chapter.

1.3.3 Structural Analysis

Simplified design procedures used to analyze structural behavior of the hub are presented in Chapter 4. Chapter 5 presents the results of structural analysis conducted using two-dimensional and three-dimensional finite element modeling. The aim of the

analysis is to better understand the performance of hub assemblies during shrink fit assembly and in the final service state. The chapter also presents results from a detailed finite element analysis model that includes bolted joints. The model is intended to provide insight into likely behavior of the hub assemblies without a shrink fit between the girder and the hub.

1.3.4 Thermal Analysis

Thermal stresses developed during shrink fitting process have caused hub cracking in the past [1]. Chapter 6 presents results from thermal analysis of hub geometry performed using a three-dimensional finite element model to determine the temperature distribution in the hub during the currently utilized shrink fit process. The temperature distribution is subsequently used to solve for thermal stresses.

1.3.5 Design Optimization

Sample calculations performed using a MathCAD worksheet are included in the Appendix. The worksheet is used to determine the “optimum” solution that satisfies all strength, performance, service and castability requirements.

1.3.6 Recommendations

The primary findings from the study are summarized in Chapter 7. These may be presented to the AASHTO technical committee on Movable Bridges for possible inclusion in future specifications.

1.4 Summary

The objective of the study is to update bascule hub assembly design guidelines based on findings from structural analysis, thermal analysis and discussion with foundry engineers on castability of hubs. Tasks used to achieve this objective were outlined in this chapter.

CHAPTER 2 LITERATURE REVIEW

2.1 Introduction

This chapter summarizes findings from a literature review related to bascule bridge design. Basic information about movable bridge design is available in bridge design handbooks such as [4] and [5] and other books on modern movable bridge design [6]. These books cover general aspects of bascule bridge design in the context of movable bridge design and the broader subject of bridge engineering. For specific design guidelines, the design engineer must follow the specifications published by AASHTO ([2] & [7]) and states such as Florida [3]. Often topics presented in general machine design textbooks [8] and handbooks [9], provide additional guidelines for design of many machinery components of bascule bridges.

Current hub design guidelines are presented in Section 2.2. Section 2.3 presents hub geometries of several recent bascule bridge designs. Summary of findings from a meeting with several design engineers is presented in Section 2.4. This is followed by a brief overview of current assembly practices in Section 2.5. Research related specifically to hub assemblies of bascule bridge design has been restricted to studies conducted at the University of South Florida (USF) since 1998. Section 2.6 through 2.8 summarizes the relevant findings from these studies.

2.2 Review of Design Guidelines

At present, design of bascule bridges are based on LRFD Movable Highway Bridge Design Specifications (hence forward referred to as LRFDM) published by AASHTO [2]. LRFDM provides general guidelines for design of the trunnion-hub-girder assembly. In Florida, Structures Design Guidelines (SDG) [3], published by the Florida DOT, is used in addition to LRFDM.

LRFDM specifies that trunnions must be designed to transfer span and machinery loads to trunnion bearings. Other design guidelines for trunnions address issues such as fatigue performance, torque transfer and deflection considerations.

Basic design guidelines applicable to all machinery hubs are also provided in LRFDM. It recommends ratio of hub length to bore diameter of 1.0 (see Figure 2.1 for nomenclature). It also recommends minimum hub thickness to be 40% of the bore diameter. Applied torque must be carried by either shrink fits, keys or splines. Items relating specifically to trunnion hubs are limited. LRFDM recommends an FN2 shrink fit between the hub and girder, and FN2 – FN4 fit for hub and trunnion.

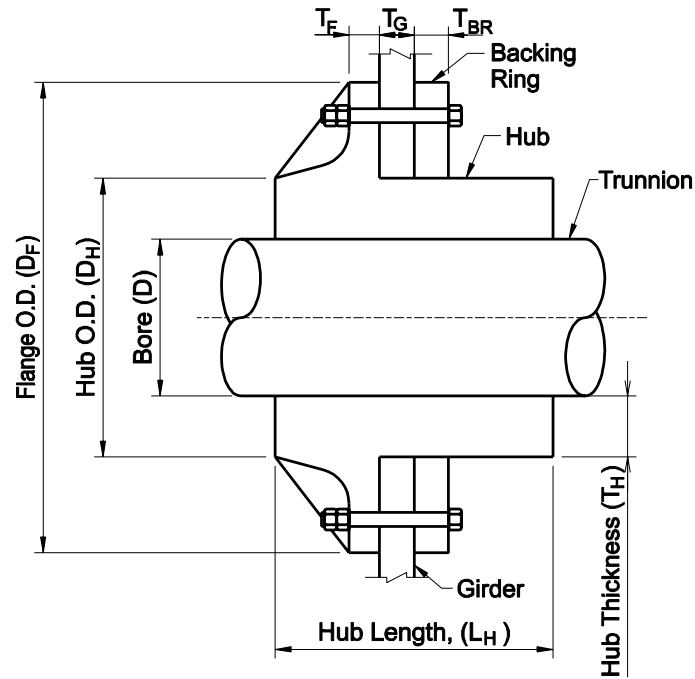


Figure 2.1 Hub assembly nomenclature

SDG provides guidelines specific to trunnion hub geometry (see Figure 2.2). These are aimed towards bascule bridges utilizing simple trunnion designs. These guidelines provide more details than those from LRFDM, such as minimum bolt size, backing ring thickness and girder thickness. These guidelines match the LRFDM guidelines for the hub length. However, the hub thickness is half of that recommended by LRFDM (20% of bore compared to 40% of bore).

LRFDM guidelines seem to be based on typical hub designs used in machinery applications. The primary function of the hub in most machines is power transmission, which requires thick hubs and interference fit to provide adequate contact pressure in order to develop friction between the hub and shaft for torque transfer. Through

discussions with FDOT officials, it was found that SDG guidelines recognize that in bascule bridge applications, the amount of torque to be resisted is relatively small, and the primary function of the hub is to transfer the span loads and machinery operation loads.

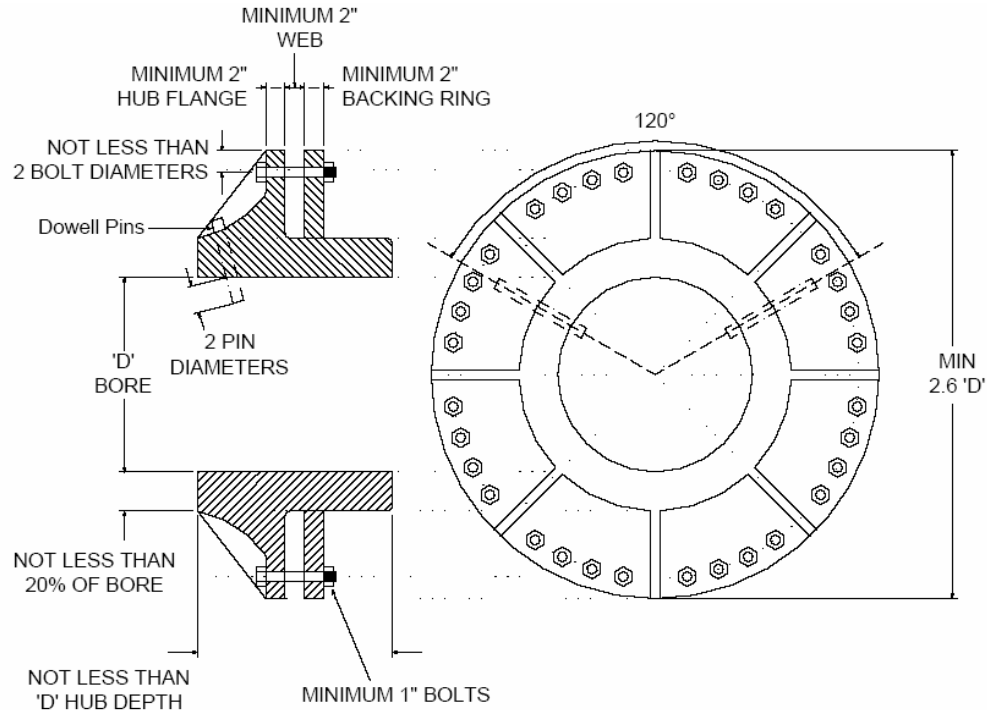


Figure 2.2 Trunnion hub design guide [3]

2.3 Review of Recent Bascule Bridge Designs

Several recent bascule bridge design plans were reviewed to determine the extent to which the SDG and LRFDM guidelines are followed in practice. All but one of these designs were of bridges located in Florida. The only exception was the bascule span of Woodrow Wilson Memorial Bridge located in Maryland. This was included in the survey since it is a relatively new bridge and is one of the largest bascule bridges in the country.

A detailed list of the documents reviewed is provided in the reference section [10-24]. These plans were obtained from the FDOT project manager and EC Driver and

Associates. In addition to bridge plans, a limited number of hub assembly design computations and fabrication specification for hub assemblies were also reviewed.

2.3.1 Review of Hub Geometry

Bridges reviewed in the above group include the three common types of bascule bridge design configurations found in Florida. These are bridges with Hopkins frame, simple trunnion with plate girders, and simple trunnion with box girders (see Figures 1.1 through 1.3). Table 2.1 lists geometric parameters for twelve reviewed bascule bridges. The dimension listed include the hub bore, hub length, hub outer diameter, web thickness and other features specified by FDOT guidelines (see Figure 2.2).

Since the FDOT guidelines are intended for simple trunnion designs, the hub geometry requirements cannot be directly applied to box girder type bascule bridges. While it is reasonable to expect Hopkins type trunnion hub design requirements to be similar to that for simple trunnion, hub requirements for bascule bridges with box girders are different. In such bridges, the span and machinery load is transferred through two hubs to each trunnion instead of one hub per trunnion used in the other two designs. In effect, the load per hub is halved from an equivalent simple trunnion design. Consequently, for certain ratios, such as hub bore to hub length, it is more reasonable to compare combined ratio of the two hubs that occur on each trunnion to the FDOT requirements rather than any individual hub.

Design items that deviate from FDOT requirements are marked with asterisks in Table 2.1. It can be seen that many of these bridges deviate from FDOT guidelines for one or more items. One of the guidelines relevant to the current study is the ratio of the hub length to bore diameter. The recommended ratio of 1 is seldom found in practice. Instead, it varies from 0.75 to 1.22 for Hopkins frame bridges, 0.57 to 1.35 for simple trunnion bridges, and 0.46 to 0.50 per hub for bascule bridges with box girders. Note that the ratio is close to 0.50 for box girder bridges, which is expected since the load is transferred through two hubs per trunnion. Also, with one exception, the ratio of hub length to bore is close to 0.9 or above for simple trunnion type bridges listed in Table 2.1. The guideline specifying hub thickness (20% bore) is generally satisfied. Four of the twelve bridges listed utilize hub thickness of 40% of bore or more, which is the

recommendation found in LRFDM. Seven of the twelve bridges from Table 1.1 meet the requirement of the ratio of flange outer diameter to bore of 2.6. The actual ratio varies from 1.48 for the SR-44 to 2.8 for the Royal park and Hatchett Creek bridges. Other items, such as the minimum bolt size, dowel requirements and bolt spacing are satisfied for the most part.

2.3.2 Review of Hub Assembly Design Computations

A limited number of design computations [25-30] were reviewed to determine the current practice in hub design. All computations with the exception of those for Johns Pass [30] were based on older ASD or LFD design methodology [7 & 31]. Johns Pass design utilized LRFD [2 & 32] specifications.

LRFDM specifies that trunnion and hub designs must be based on the highest of the following load cases: (Dead Load + Dead Load Dynamic Load Allowance), (Dead Load + Live Load + Live Load Dynamic Load Allowance) and (Dead Load+ Wind Load). For designs reviewed, in many cases, the governing condition for hub design involved a special maintenance mode with one bearing removed, and subjected to dead load and 20% impact. Torsion and wind loads generally were small and not found to govern the designs.

The older designs simply check for bearing stresses in the hub and determine the interference required for FN2 or FN3 fit. The newer designs [28 & 29] consider stresses developed from shrink fit. In both cases where the shrink fit stresses are computed, the tensile Hoop stress in the hub was found to exceed the allowable limit by 20%.

The sole LRFD design reviewed [30] included an additional check for fatigue in the trunnion as required by LRFDM. Hub design checks were limited to torque capacity from the shrink fit and other standard stress checks (such as dowel size, bearing stresses etc.). Hub geometry seemed to be based on SDG and LRFDM ratios.

Table 2.1 Hub assembly geometry for recent bascule bridges

No.	Bridge	Type	Bore 'D' (in.)	Length (in.)	Hub O.D. (in.)	Web Thickness (in.)	Backing Ring Thickness (in.)	Flange O.D. (in.)	Bolt Dia. (in.)	Bolt Circle Dia. (in.)	No. of Dowels	Flange Thickness (in.)
1	Royal Park	Simple	24	26	43.3	1.3*	2.9	67.3	1.375	58.5	2	2.9
2	SR 706	Simple	26	24*	40	1.5*	2	72*	1.5	66	3	2
3	Woodrow Wilson	Simple	34	30.25*	62	2.25	3.5	92*	2	84	3	3.5
4	Hallandale	Simple	25.6	27.6	45.3	1.6*	2	69.9*	1.75	62.2	2	3
5	Ulmerton	Simple	20	27*	28*	1.75*	2	53*	1.5	45	Keyway*	3
6	SR-44	Simple	21	12*	24*	1.5*	0.5*	31*	0.875*	27.5	Keyway*	1*
7	SW 2nd Ave. Bridge over Miami River	Hopkins /Box	35.4	17.7*	53.1	3	3.9	84.6*	1.375	76.8	N/A	3.9
8	SR 804	Hopkins	33.5	25.2*	50.2	3	3	66.9*	1.375	61	3	3
9	Hatchett Creek	Hopkins	23.2	28.2	41.8	1.2*	1.2*	65.0	1.5	55.9	2	3
10	NW 12th Ave. over Miami River	Box	25.56	12.25*	37.5	1.25*	2	53.5*	1.125	48.75	2	2
11	17th Street	Box	25.6	11.8*	37.4	0.9*	2.0	53.5*	1.125	48.8	2	2
12	Johns Pass	Box	26.75	14*	50	1.5*	2	71*	1.25	64	2	2

*indicates deviation from current FDOT or AASHTO guidelines

2.4 Meeting with Consulting Design Engineers

As part of the current project, a meeting attended by engineers from USF, FDOT and many consulting engineering firms with bascule bridge design experience was held in June 2005 at the USF campus in Tampa. The objective of the meeting was to obtain input from consulting engineers regarding current design guidelines. Most out of state designers preferred to conform to LRFDM guideline regarding ratio of hub thickness to bore ratio of 40%. FDOT representative clarified that one of the rational behind the smaller hub thickness specified in SDG was the relatively small amount of torque that the hub assembly is subjected to in comparison to typical power transmitting application on which the LRFDM guidelines seem to be based on.

It was clarified by FDOT officials that the present guidelines were empirical in nature and not based on any extensive theoretical analysis. Other issues raised for discussion by FDOT representative was the possibility of trunnion bearings getting seized, which would require the trunnion and hub assembly to be designed for higher torque, the need to minimize the spacing between trunnion bearings, and using certain minimum dowel sizes for trunnion hub assemblies.

2.5 Assembly Practices

Documents containing specifications for assembly of trunnion-hub assemblies and also girder assembly were reviewed for four recent bridges [34-38]. The documents indicate that two types of trunnion-hub-girder assembly procedures are used in practice. In the first case, the trunnion is assembled into the hub and the trunnion-hub assembly is inserted into the girder [34 & 35]. In the second case the hub is first shrink fit into the girder and then the trunnion is fit into the hub-girder assembly [36 & 37].

The most significant change in the assembly procedure from earlier practice [1] is that liquid nitrogen is no longer used to obtain the shrink fit. Instead, the specifications only allow the use of dry ice and alcohol to cool the components. The components to be shrunk are required to be cooled for at least 12 hours.

The use of heat for shrink fitting is also permitted. Review of the contractor's document [38] indicated that it is possible to achieve the desired clearance for fit by

heating the hub to 300°F and 400°F using gas burners placed at the bottom of the hub around the hole while using insulation blankets to cover the component.

2.6 Parametric Modeling and Full Scale Testing [1]

The following sections summarize findings from past research on bascule hub assemblies. The first of these was undertaken in response to instances of hub cracking during shrink fitting of trunnion-hub-girders. The objective of the study was to determine the cause of these failures. The observed failures were thought to occur due to fracture propagation of existing cracks. The likelihood of such cracking was measured using critical crack length.

The study involved development of finite element models to simulate the assembly process and experiments to verify predicted thermal stresses. Thermal finite element model used to determine the temperature distributions during the assembly process. Thermal stresses corresponding to these temperature distributions were subsequently determined using structural finite element model.

Critical crack lengths for two types of assembly processes were obtained. The first, called Assembly Procedure 1 (AP1) involves cooling the trunnion in liquid nitrogen and shrink fitting it into the hub. Subsequently, the trunnion-hub assembly is cooled in liquid nitrogen and shrink fit into the girder. The second assembly procedure, AP2, involves shrink fitting the hub into the girder first, followed by shrinking fitting of the trunnion into the hub-girder assembly. Based on the numerical analysis of these procedures in representative bridges, the authors concluded that AP2 was a safer assembly procedure.

Current Florida guidelines do not allow the use of liquid nitrogen for shrink fitting. Instead, the state of the practice has moved to use of heat to expand the outer component. If necessary, the use of dry-ice and alcohol to cool the inner component is permitted.

2.7 Hub Assemblies Without Shrink Fit [33]

A possible means to avoid failures during shrink fitting of trunnion-hub-girder assemblies is by eliminating the shrink fit between the girder and the hub. The elimination of the shrink fit required the use of a slip-critical bolted joint between the hub and the girder. Analysis of several existing bridge hub assemblies revealed that this to be a feasible option with existing hub sizes.

With the use of liquid nitrogen being discontinued for shrink fitting, failure during assembly are unlikely (see Chapter 7), and the design scheme without hub girder interference fit is not necessary.

2.8 Miscellaneous Studies

Several masters theses have been published by students at the University of South Florida related to trunnion-hub-girder assembly process. These are summarized in a chronological order below.

Denninger [39] developed a Visual Basic program to carry out some of the design computations for bascule hub assemblies. These included features to determine torque capacity based on wind loading, determining interference stresses and bolt pattern design.

Collier [40] looked at cooling the trunnion-hub-girder assembly in stages as a means to minimize thermal shock and resulting thermal stress during the shrink fit process. A finite difference model of two cylinders was used for both thermal and structural analysis. The study concluded that cooling the trunnion-hub assembly in refrigerated air prior to cooling in liquid nitrogen increased the critical crack length by up to 200%.

Berlin [41] performed experiments and finite element analysis to study the possibility heating the girder to assemble the trunnion-hub-girder. The study concluded that heating can produce the necessary clearance for the assembly process. The placement of heating coil was identified as being an important factor in determining the geometry of the heated girder.

Paul [42] studied the effect of hub radial thickness, trunnion bore and interference fit on the critical stresses and critical crack lengths encountered during the shrink-fit assembly process. Thermal and structural finite element models were used to determine

the stresses. Design of experiments methodology was utilized to identify radial thickness as the most significant among the parameters considered.

2.9 Summary

This chapter presented the current state of the art for bascule hub assembly design. Recent bascule bridge plans and computation were reviewed to identify factors that need to be addressed. It was found that some of the most recent bridges designed and built in Florida do not satisfy the AASHTO requirement for hub thickness. Finally, findings from research related to hub assembly were summarized. All the research was in some way aimed at avoiding potential hub cracking during shrink fitting of the trunnion-hub-girder assembly.

CHAPTER 3 HUB CASTINGS

3.1 Introduction

Bascule hubs are typically cast using A148 Grade 90-60 steel. As a part of the current research, meetings were held with foundry engineers experienced in bascule hub sized casting to discuss castability and other issues related to hub castings. Findings from meetings held with two major providers of bascule sized hubs are presented in this chapter.

3.2 Overview of Hub Casting Process

Casting is a manufacturing process that involves pouring molten metal into moulds to form the desired geometry [9]. Due to the physics of the metal flow involved, bascule sized hubs are generally oriented horizontally with rib facing up while being cast (Figure 3.1). Depending on the metal flow configuration, certain geometric features, such as sharp corners can produce casting defects. The job of the foundry engineer is to design the casting, such that the final hub geometry is free from such defects. This is achieved by designing the mould to be larger than the final hub, and machining the casting to obtain the final geometry. The hub casting design accounts for metal flow characteristics, solidification process and other metallurgical aspects of steel. Sophisticated software (such as Magma from Magmasoft) is often used to aid in analysis of casting designs. Such software can predict mechanical properties of the castings, also locations of areas with defects. The casting designer must ensure that such defects occur only in regions outside the final machined part.

3.3 Recommendations from Foundry Engineers

The following recommendations were made by the foundry engineers contacted as part of the project. The recommendations have been grouped into the following three

main categories: a) hub geometry, b) casting acceptance criteria and c) miscellaneous issues.

3.3.1 Hub Geometry

The following are some of the items that a designer must be aware of while finalizing the hub geometry.

General: Typical hub geometry was considered to be relatively simple. Items of interest to a designer, such as hub length and hub thickness were not thought to significantly affect the castability.

Tapered hub: Tapers at ends of hubs (see Figure 3.1) should be avoided if possible, since they increase machining costs. Such designs are generally found in shallower hubs (box girder type bridges) and are required for locating dowels.

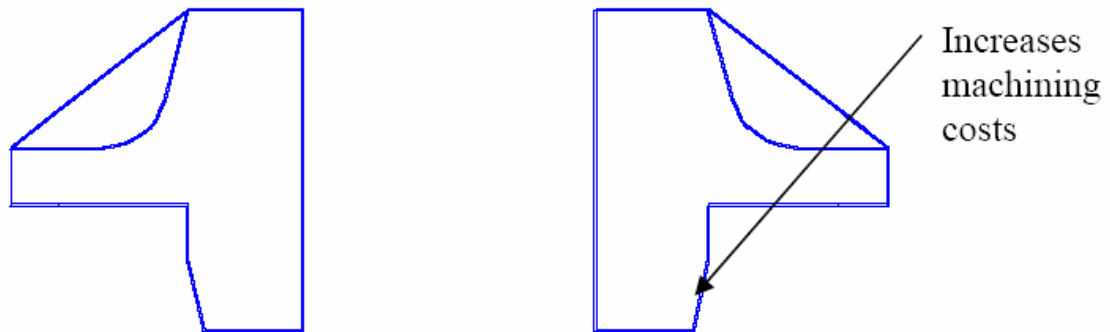


Figure 3.1 Tapered hub design

Hub thickness: It may be advantageous to have the upper portion of the hub to be thicker than the lower parts (see Figure 3.2). This is because castings are designed with wider upper sections to feed “hot spots”, which are regions in a casting which solidify last (generally thicker sections). Since steel contracts as it cools, it is important to provide sufficient metal flow to ensure this shrinkage is compensated. Consequently, the hub top must have a wider section to feed the hot spot. The wider portion at top is machined off to obtain the final geometry. If hubs are designed to be wider at the top so that hot spots can be fed (see dotted line in Figure 3.2), the amount of machining can be reduced. From a design perspective, the wider hub can produce higher contact pressures and lower

interference fit stresses locally, both of which are desirable. However, it may reduce the room available for bolting.

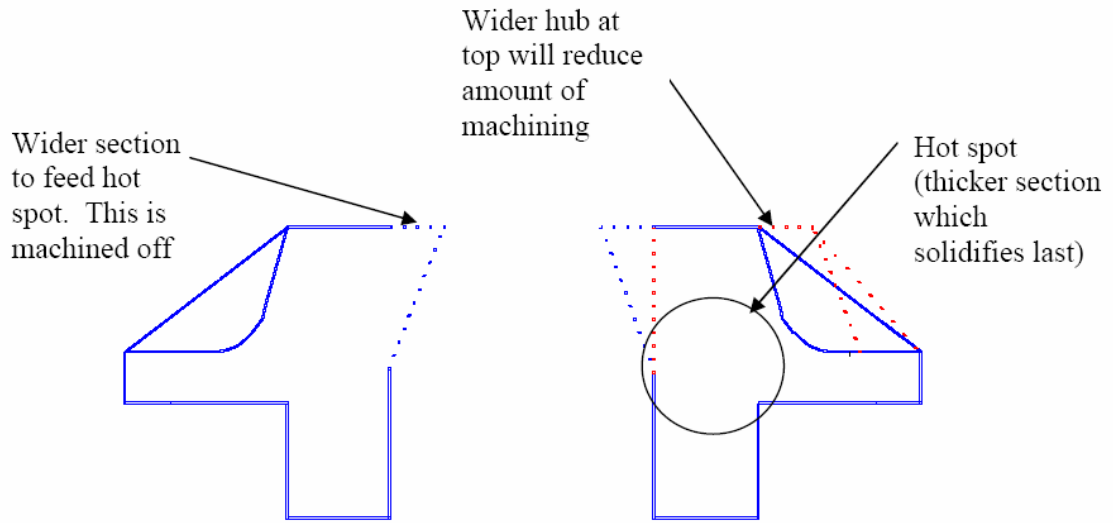


Figure 3.2 Casting geometry design to feed “hot spots”

Number of ribs: While the number of ribs does not have a significant impact on the casting quality, some engineers preferred hub designs with six ribs over those with eight ribs due to lower gating costs associated with fewer ribs.

Rib design: The rib shape scheme shown in Figure 3.3b is preferred to the one shown in Figure 3.3a since it ensures better metal flow by eliminating the sharp edge.

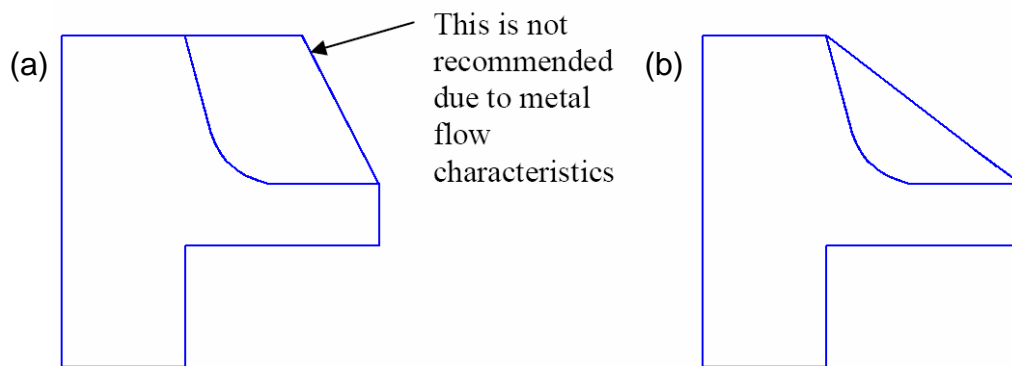


Figure 3.3 Rib shapes found in bascule hubs

Rib thickness: A minimum thickness of 1½” is recommended for good quality casting.

Rib profile: A tapered rib profile (see dashed line in Figure 3.4) can provide better castings due to better metal flow. While this has the desirable result of stiffening the hub's response to flange bending, it may have the drawback of reduced room for bolting.

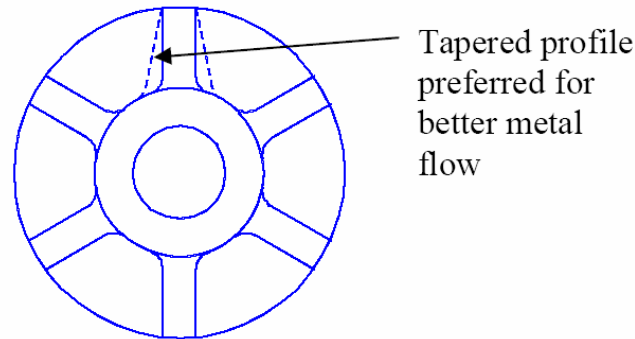


Figure 3.4 Possible rib profile

Fillet Radii: Existing fillet radius specified was considered to be adequate. In general, fillet radius should be approximately equal to the rib thickness.

3.3.2 Acceptance Criteria

The biggest concern that all foundry engineers shared was the absence of clear acceptance criteria for bascule hub castings. Currently, a typical inspection requirement for casting reads as follows:

“Castings shall be ultrasonically tested in accordance with ASTM A609, Method A, Quality Level 3. Castings that do not pass this test may be rejected. Perform visual surface examinations per ASTM A802, liquid penetrant exams in accordance with ASTM E165 or magnetic particle exams in accordance with ASTM E709 in the manufacturer's shop for each casting.”

The above specification fails to note the acceptance criteria for the surface inspection performed per ASTM 802, ASTM E165 or ASTM E709. The only requirement is for the hub casting to pass the ultrasonic test per ASTM A609 at Quality Level 3. The foundry engineers pointed out that ultrasonic inspections provide little information about defects near the surface (1/8” to 1/4”) due to an inherent limitation of the method. Castings that pass the above test can show inclusions after rough machining. Steel fabricators find the presence of any “indications” unacceptable even though this is

consistent with what could be expected from casting that passes “Level 3” ultrasonic inspections. This results in large expenses to the foundry on off-site repair of castings using specialized welding procedures approved by ASTM.

The foundries stressed the need for defining uniform acceptance specification in terms of accepted international standards (such as ASTM). This is also expected to result in a more uniform bid process since the cost of the casting cannot be adequately estimated without well defined acceptance specifications. Based on input from the foundries, acceptance criteria for surface inspections are proposed in Section 3.4.

3.3.3 Miscellaneous

The following suggestions to help improve the current process were also made during the discussions.

Castability review: The engineers suggested that a castability review be performed prior to finalizing the design so any potential problems can be addressed prior to releasing the design for bid. Such a review is expected to require about 60 hrs. The foundries have the ability to use three-dimensional CAD models developed during typical mechanical design for such an analysis. Unfortunately, most current bridge drawings are 2D line drawings.

Drawings: Some engineers suggested that the contract plans should include three drawings of the hub: the casting drawings, rough machined part drawings and finish machined part drawings, with clearly defined acceptance criteria for each stage of the process.

Critical Sections: It was pointed out that all castings inherently have defects and current inspection methods have their limitations. This is recognized by many clients in the heavy machinery industry, where the design drawings identify the critical sections of the castings that must pass higher inspection requirements. Such information assists the foundry engineer to design castings that provide the highest quality in these critical areas.

Residual stresses: Hub casting made of A148 Grade 90-60 steel are normalized and tempered, consequently residual stresses should not be a significant consideration in hub design.

3.4 Hub Casting Acceptance Criteria

The following minimum acceptance criteria are proposed for the different types of inspections performed on hub castings. These are based on review of shop drawings for castings of a swing bridge (145th Street Bridge over the Harlem River) [43]. Inspections are performed in accordance with ASTM standards, which are briefly summarized below for background.

3.4.1 ASTM A609 [44]

ASTM A609 provides standards and procedures for the pulse-echo ultrasonic examination of heat-treated carbon, low-alloy, and martensitic stainless steel castings by the longitudinal-beam technique. The standard outlines the specification for two testing procedures and recommends standard measurement data to be included for reporting. In accordance with the first method of testing, the quality of the tested material is assessed based on the criteria described in Table 3.1. The areas in the table refer to the surface area, measured from the center of the search unit, on the casting over which a continuous indication exceeding the amplitude reference line or a continuous loss of back reflection of 75% or greater is maintained. The current hubs are required to meet Quality Level 3. It is recommended that this be changed to Level 1 in order to be consistent with other recommendations for surface inspections, presented later.

Table 3.1 Criteria for classification of indications per ASTM A609 [44]

Ultrasonic Testing Quality Level	Area, in. ² [cm ²]	Length, max, in. [mm]	Current Recommendation	Proposed Recommendation
1	0.8 [5]	1.5 [40]	Level 3	Level 1
2	1.5 [10]	2.2 [55]		
3	3 [20]	3.0 [75]		
4	5 [30]	3.9 [100]		
5	8 [50]	4.8 [120]		
6	12 [80]	6.0 [150]		
7	16 [100]	6.9 [175]		

3.4.2 ASTM A802 [45]

ASTM A802 provides the acceptance criteria for the surface inspection of steel castings by visual examination. A detailed description of the defects is provided in the standards. Up to four levels of acceptance are specified for each feature examined. These are listed in Table 3.2 along with the recommended level for hub castings.

Table 3.2 Visual inspection acceptance criteria [45]

Surface Feature	Level I	Level II	Level III	Level IV	Recommendation
Surface texture	A1	A2	A3	A4	A4
Nonmetallic inclusions	B1	B2	B4	B5	B4
Gas porosity	C2	C1	C3	C4	C2
Fusion discontinuities		D1	D2	D5	D2
Expansion discontinuities			E3	E5	E3
Inserts			F1	F3	F1
<i>Metal removal marks:</i>					
Thermal	G1	G2	G3	G5	G2
Mechanical	H1	H3	H4	H5	H3
Welds	J1	J2	J3	J5	J2

3.4.3 ASTM E165 [46]

ASTM E165 provides procedures for penetrant examination of materials. Nondestructive testing methods are described for detecting discontinuities that are open to the surface such as cracks, seams, laps, cold shuts, laminations, through leaks, or lack of fusion. These are applicable to in-process, final, and maintenance examination. They can be used in the examination of nonporous, metallic materials, both ferrous and nonferrous, and of nonmetallic materials. Unlike other ASTM standards described above, this standard does not classify indications into different levels. Evaluation and

interpretation of the discontinuity based on the size of the indication must be specified separately. For bascule hubs, it is recommended that acceptable sizes of indications be consistent with those specified for visual inspections (Table 3.2).

3.4.4 ASTM E709 [47] & ASTM E125 [48]

ASTM E709 describes techniques for nondestructive method for detecting cracks and other discontinuities at or near the surface in ferromagnetic materials. Dry and wet magnetic particle examinations are described, and may be applied to raw material, semi finished material (billets, blooms, castings, and forgings), finished material and welds, regardless of heat treatment or lack thereof.

ASTM E125 provides a standard reference for 8 types and degrees of discontinuities that could occur in steel and other types of ferrous castings. These discontinuities are detectable by the dry powder magnetic particle method. Pictures of these discontinuities, with various degrees of severities, are provided for comparison with magnetic particle indications observed on actual castings. Table 3.3 describes five of the eight discontinuities with recommended acceptance levels.

3.4.5 General

In addition to the above inspection specifications, the hub casting specification must address other requirements, such as acceptable repair procedures. Appendix A contains a sample of shop drawing listing these and other requirements that must be included as part of any casting specification.

3.5 Summary

This chapter presented geometry related recommendations that affect castability of the hub. Some recommendations were based on economical considerations, while other based on the nature of casting process. The need for clear acceptance criteria for hub casting was stressed by the foundries. A preliminary set of recommendations is made here based on discussion with foundry engineers.

Table 3.3 Types of discontinuities per ASTM E125 [48]

Category	Type of Discontinuity	Degrees of Severity	Description	Recommendation
I	Linear discontinuities (hot tears and cracks)	5	Ragged lines of variable width. May appear as a single jagged line or exist in groups. They may or may not have a definite line of continuity. They usually originate at the casting surface and generally become smaller as they go deeper.	1/4 " max
II	Shrinkage	5	Appears as a jagged area or irregular patches. Shrinkage is a subsurface discontinuity that may be brought to the surface by machining or other methods of metal removal.	Degree 3
III	Inclusions	5	Isolated, irregular or elongated variations of magnetic particles occurring singly, in a linear distribution or scattered at random in feathery streaks.	Degree 3
IV	Internal chills and unfused chaplets	5	A uniform line or band outlining the object and indicating lack of fusion between the metal object and the casting.	Degree 2
V	Porosity	2	Appears as rounded and elongated clusters of magnetic particles of various sizes; scattered at random.	Degree 1

CHAPTER 4 SIMPLIFIED HUB DESIGN

4.1 Introduction

As seen in Chapter 2, recommendations for hub geometry presented in FDOT design guidelines differ from those found in LRFDM. Moreover, there is limited or no theoretical analysis presented in the literature to substantiate the geometric guidelines presented for trunnion hubs. These guidelines seem to be primarily based on rules of thumb adopted from the machine design community. This chapter presents simplified analysis of hub using a basic mechanics of material approach to establish if the current guidelines satisfy basic strength and stiffness requirements. Appendix A includes sample calculations illustrating hub assembly design.

4.2 Loads

General loading that acts on a trunnion hub assembly (see Figure 4.1) are shear (V), torsion (T), axial load (P), and bending moment (M). Depending on the assembly process, the influence of friction force developed due to the interference fit between the hub and the backing ring must also be considered [33]. Details of these loads are discussed below.

4.2.1 Shear

The primary loads resisted by the trunnion-hub-girder connection are the span and machinery loads transferred from the girder to the trunnion bearings. This is obtained from determining the controlling limit state load case combinations of dead load, dead load dynamic allowance, live load, impact, wind etc. as specified by AASHTO (See Table 3.4.1-1 in Ref. [32], Section 2 in Ref. [2], Section 6.8.1.3.2 in Ref. [2]). For machine design, the relevant load cases are service limit load case, fatigue limit load case and extreme event limit load case.

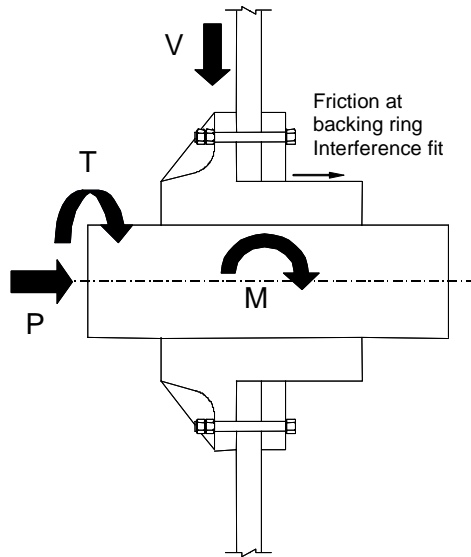


Figure 4.1 General loading on Hub-Girder Assembly

4.2.2 Torsion

The maximum torsion that the hub-girder connection can be subjected to is equal to the torsional resistance provided by the trunnion bearings due to friction. When the net unbalanced torque exceeds the friction at the trunnion bearings, the bascule span undergoes rigid body rotation (such as when opening or closing the span).

Friction factors used to compute frictional torque are specified as 18% for plain radial type bearing (see Section 5.8.2 in Ref. [2]) and 0.4% for roller bearings. Earlier AASHTO specifications [7] required the load acting at the circumference to be 1/5 the maximum radial load for bearings with bronze bushing and 1/100 the maximum radial load for anti-friction bearings (see Section 2.6.17 in Ref. [7]). Since torsion loads are obtained as percentages of shear loads (radial), influence of torsional impact loads is included when the corresponding shear loads are increased to account for dynamic effects.

As discussed in Chapter 2, FDOT officials raised the question about designing for the case where bearings seize. The possibility of bearing seizure must be considered in bridges utilizing bronze bushing for trunnion bearings. Typically, bronze bushings used on bascule bridges consist of two halves. Each half has a lip with holes for screws to mount it to the bearing base. A locational clearance fit (LC1) is provided between the bearing base and the bushing. In case of bearing seizure, the screws attaching the bronze

bushing to the bearing block are intended to shear off and allow for continued operation of the bridge [Ref. 6, pg. 148]. To ensure safety of hub assemblies, it is proposed that the torsional resistance provided by combination of the trunnion-hub shrink fit and dowels at the trunnion, and bolt circles and hub-girder shrink fit at the hub exceed the torque required to shear the screws connecting bronze bushing to bearing block. This must be considered during design of the trunnion bearing.

4.2.3 Axial Loads

The axial load acting on the connection is specified as 15% of the maximum bearing reaction per Section 6.8.1.3.2 in Ref. [2]. The source of this axial load is not specified in LRFDM. Some likely sources for the loads are wind and misaligned moving components. However, these are generally significantly smaller than the 15% of bearing reaction load specified in the code.

Current designs [25-30] do not seem to consider axial loads when designing the shrink fit and dowels between hub and trunnion. Unless trunnions utilize stepped sections to transfer axial thrusts, the axial load acting on the span will need to be transferred to the trunnion bearing through friction or dowels. Therefore, it seems necessary to design the shrink fit and dowels to resist combined torsion and axial loads. If using the arbitrary axial load of 15% of bearing reactions leads to unreasonable requirements for shrink fit and dowels, it is proposed that the axial load may be reduced to loads that can be reasonably expected from sources such as wind and misalignments.

4.2.4 Bending Moment

The hub-girder assembly is subjected to small bending moment that is generally neglected in design. The bending moment is a function of the member stiffness, and in cases where the moment has been determined, for example using finite element models, it may be included in the analysis, if desired. If the bending moment is found to be significant, for example in bridges with Hopkins trunnion, the bolted connection design must account for eccentric bolt loading and bolt fatigue.

4.2.5 Shrink Fit Assembly Loading

In addition to the general loads described above, the hub assembly is subjected to loads due to shrink fit between the trunnion and hub, and hub and girder. During assembly the components are subjected to transient thermal stresses due to the temperature gradient that develops from heating of the outer member and cooling the inner member. In addition, once the assembly reaches steady state ambient temperature, it is subjected to radial and hoop stresses due to the interference fit between the assembled members.

4.3 Materials

The following table (Table 4.1) summarizes materials commonly used for the various components of the trunnion-hub assembly [4- 24]. The modulus of elasticity of all these materials is assumed to be 29,000 ksi [32].

Table 4.1 Materials used for hub assemblies

Component	Material	Minimum Yield Point (ksi)
Trunnion	ASTM A668, CLASS D or G	37.5 (CLASS D) / 50 (CLASS G)
Hub	ASTM A148, GRADE 90-60	60
Backing Ring	ASTM A709, GRADE 50	50
Dowels	ASTM A668, CLASS D or K ASTM A108	37.5 (CLASS D) / 80 (CLASS K) 36 (A108)
Bolts	ASTM A325, ASTM A449	120 (DIA<1"), 105 (DIA>1") (A325) 150 (A449)

4.4 Trunnion Design

Trunnions are designed to transfer span and machinery load from the girder to the trunnion bearings. LRFDM recommends utilizing a bore of 20% of the outer diameter (see Figure 4.2 for nomenclature). Trunnion designs check deflection, bending stresses,

torsion, shear, bearing at hubs and bearing at dowels. LRFDM also requires a check for fatigue endurance based on bending moment and torsion. Many trunnion designs utilize stepped design to resist axial thrust. In designs reviewed, the stress concentration factor utilized to design the trunnion was based on stress concentration effect at this step. Details of trunnion design requirement can be found in LRFDM.

4.5 Hub Design

As stated above, the LRFDM guidelines provide sufficient details on the trunnion design procedure. The following analysis is aimed at quantifying requirements for hub geometry which are generally designed purely using rules of thumb (i.e., minimum dimensions or ratios specified in SDG or LRFDM). Most designs reviewed as part of this project were restricted to torque capacity based on fit, dowel sizing and bearing stress checks.

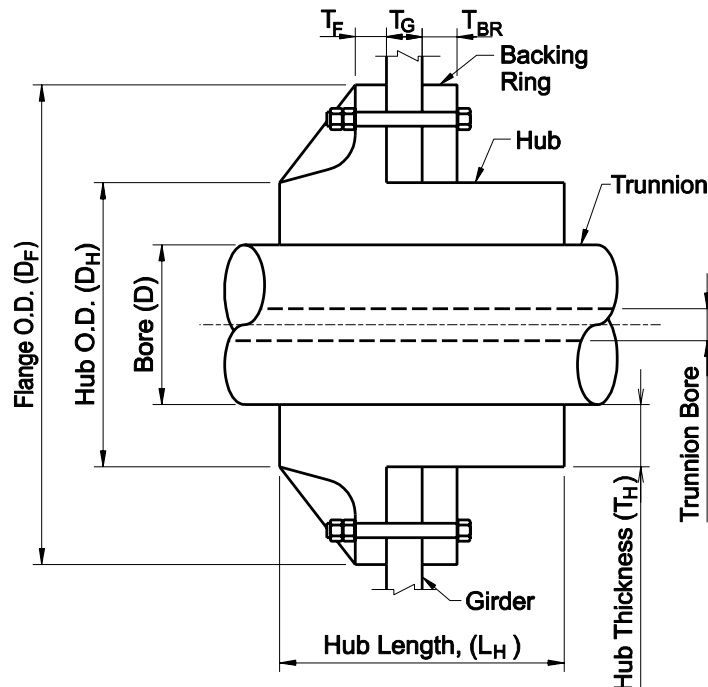


Figure 4.2 Trunnion hub design nomenclature

Hubs must be designed to satisfy the following requirements:

- i) Functional requirements – The hub must be capable of transferring span and machinery loads to the trunnion bearing. This includes torsion loads, which must be resisted by friction at the shrink fit assembly.
- ii) Strength requirements – All stresses must be within allowable under applied loading (static and dynamic) including shrink fit.
- iii) Fabrication & assembly requirements – Hub geometry should meet the castability requirements identified in Chapter 3 and also bolt spacing requirements identified in AASHTO [32].
- iv) Serviceability requirements – Hub must be designed to maintain contact with trunnion under all applied loading to avoid failure due to fretting and wear.

4.5.1 Hub Length

The current LRFDM and SDG requirements specify that the hub length may not be less than the bore (see Figure 4.2). Hub length influences the following items:

- i) Torque capacity of the shrink fit. The torque capacity increases linearly with greater hub length. This is because the total contact force and friction at the shrink fit assembly depends on the contact pressure and the contact area. The latter increases linearly with the hub length.
- ii) Bearing stresses between the hub and trunnion. Bearing stress from applied shear load (V in Figure 4.1) reduces linearly with greater hub length. This is because the load is spread over a larger area.
- iii) The distance between trunnion bearings may increase if the hub length is increased. This increases the bending moment linearly, but the trunnion deflections increase to the third power of length. The resulting moment and deflection would affect the trunnion design.

4.5.2 Hub Thickness

LRFDM recommends a minimum hub thickness of 40% of the bore, which results in the hub outer diameter (O.D.) being 1.8 times the bore. Current SDG requirement for

hub thickness is 20% of bore, which results in hub O.D. being 1.4 times the bore. This dimension influences the following items:

- i) *Radial and hoop shrink fit stresses between the hub and trunnion:* Figure 4.3 shows contact pressure between hub and trunnion as a function of hub O.D. to bore ratio obtained using equations for shrink fit between cylinders [49]. The contact pressures have been normalized with respect to contact pressure obtained using current SDG guideline. It can be seen that the rate of increase of contact pressure is initially high but decreases as the hub gets thicker. Increasing the hub thickness from 20% bore to 40% bore increases the contact pressure by 40%. The increased contact pressure results in higher friction, therefore higher torque and axial load transfer capacity.

Table 4.2 lists the ratio of the maximum hub interference fit hoop stress to the allowable static tensile load (15 ksi) for A148 steel [2] for 12 bridges previously presented in Chapter 2. The stress is based on maximum interference for an FN2 fit. With the exception of Woodrow Wilson and Johns Pass bridge, which utilize hub flange inner diameter to bore ratio of 1.8 (as specified in LRFDM) all bridges exceed the allowable static tensile stress limit. The amount exceeded varies from 6% to 62% depending on the hub thickness. Hub tensile hoop stresses exceed allowable limit for all bridges with an FN3 fit between the hub and trunnion.

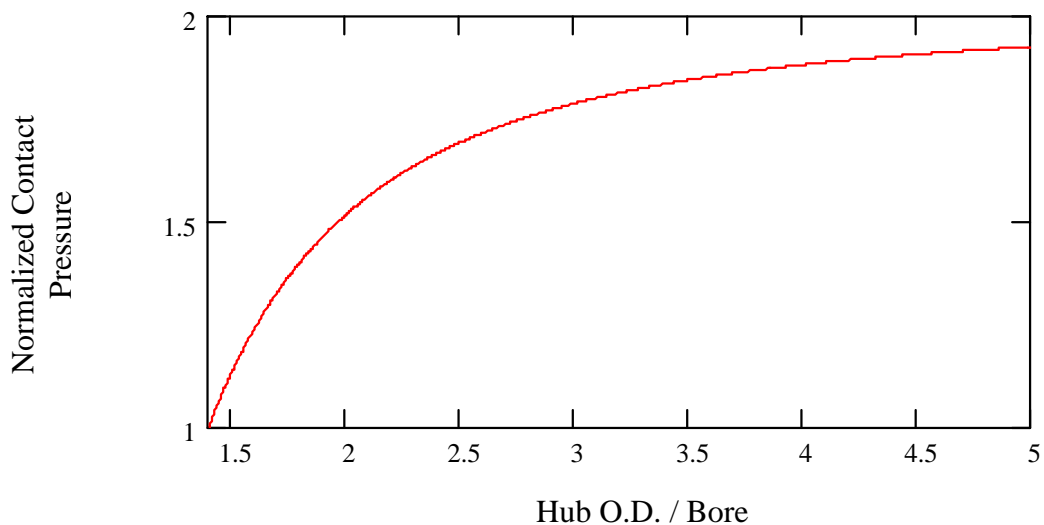


Figure 4.3 Effect of hub thickness on contact pressure

Table 4.2 Tensile hoop stress due to FN2 shrink fit

No.	Bridge	Ratio of Hub Hoop Stress to Allowable
1	Royal Park	1.13
2	SR 706	1.14
3	Woodrow Wilson	0.99
4	Hallandale	1.07
5	Ulmerton	1.43
6	SR-44	1.61
7	SW 2nd Ave/ Bridge over Miami River	1.06
8	SR 804	1.12
9	Hatchett Creek	1.06
10	NW 12th Ave. over Miami River	1.19
11	17th Street	1.19
12	Johns Pass	0.99

Figure 4.4 shows the effect of hub thickness on the tensile hoop stress developed in the hub. The graph has been normalized with respect to the stresses developed for a ratio of hub O.D. to bore of 1.4 (SDG recommendation). It can be seen that hoop stresses can be reduced by about 15% by changing the ratio of hub O.D. to bore from 1.4 to 1.8. With this change, many of the bridges where the hoop stresses are currently exceeded will satisfy the allowable stress requirements.

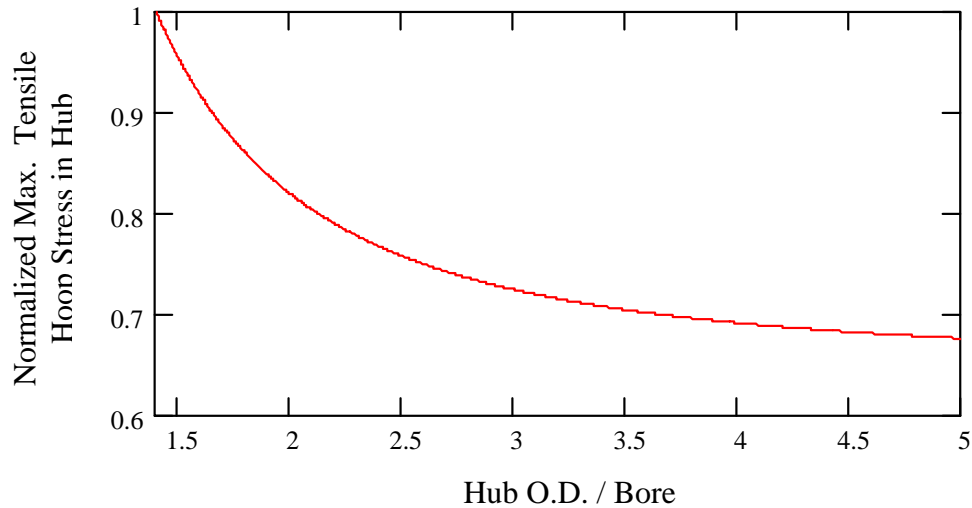


Figure 4.4 Effect of hub thickness on tensile hub hoop stress

It must be pointed out that the above analysis is based on modeling the hub and trunnion as cylinders. Finite element analysis results (see Chapter 5) indicate that actual stresses vary due to stiffeners. Also, locally, tensile hoop stress on the hub is reduced due to shrink fit between girder and backing plate, which induces compressive hoop stresses in the hub.

- ii) *Flange capacity to resist axial loads and torsion:* Current LRFDM code requires bolted joint at the hub flange to be designed to resist torsion. This torsion and any axial load must pass through the circular section of the hub at the hub outer diameter, which has an area of $(\pi D_H T_F)$. Assuming both the torsion and axial load result in shear stress at the section, a large hub O.D. results in larger section area and proportionately smaller shear stress. This however, is not an important consideration for most designs since sample calculations have shown these stresses to be insignificant.

4.5.3 Hub Flange Thickness

SDG recommends a minimum flange thickness of 2". The flange thickness affects the following items:

- i) *Resistance to torsional and axial loads acting on the hub assembly:* As stated in the previous section, if these loads are assumed to act as shear in

the cross-section at hub O.D., then stress is reduced linearly as the thickness is increased. Note that the above analysis ignores the contribution of stiffeners.

- ii) *Bearing stress at bolt holes:* The bearing stresses decrease linearly as the thickness is increased. Although it is possible to lower the bearing stress by using a thicker flange, a more economical solution would be to increase the number of bolts. The additional bolts share the applied loads and reduce the bearing stress on each bolt hole.
- iii) *Shrink fit stresses in hub and trunnion regions around the flange:* Compressive radial loads increase in the trunnion, while hoop stresses in the hub are reduced locally.
- iv) *Bolt preload distribution:* A thick hub flange helps in distributing the bolt preload since the preload is generally spread as a cone of 45° (see Figure 5.13), in which case the thicker flange distributes the load over a larger area on the girder (see Chapter 5).

4.5.4 Hub Flange Outer Diameter

Hub flange outer diameter is currently specified per SDG as being at least 2.6 times the bore (see Figure 2.2). This affects the following items

- i) *Torsional resistance of bolts:* This increases if the bolts they are spaced further from the center.
- ii) *Bolt spacing requirement as specified in AASHTO.*
- iii) *Bearing stress between the hub and the girder bolted faces* (vertical surface).
- iv) *Shrink fit stresses:* Radial and hoop stress on trunnion increase locally in the areas next to the hub regions with the flange.

4.5.5 Hub Ribs

There seem to be no specific guidelines on number and size of ribs to use on hubs. Most designs reviewed utilize rib thickness close to the flange thickness. Ribs affect the following items:

- i) *Torsion transfer from hub flange to trunnion:* Ribs will contribute to transferring a part of the torsion from the hub to the flange. However, as discussed earlier, hub flanges are generally capable of handling the shear stress resulting from torsion and axial loads. The sharing of these loads between the various components can be determined using finite element analysis, but is of limited use for design since these loads do not govern the design.
- ii) *Bending of flange under applied axial loads:* In absence of ribs, any axial load acting on the hub flange will result in bending stresses in the area at the root of the flange. The magnitude of these stresses can be roughly estimated by treating the flange to be similar to a cantilever beam loaded at a location of bolt circle. Calculations with sample bridge loading revealed that these bending stresses easily exceed allowable limits. Adding ribs to the flange changes the response of the flange to axial loads from being similar to a cantilever beam to a plate supported at three sides (two ribs and root of flange). The resulting bending stresses with plate bending are well below allowable. For completeness, the shear stresses at the rib interface along length of the hub must be checked to ensure the loads transferred from the flange can be resisted. Sample calculations revealed that in current bridges, all resulting stresses are well below allowable limits.

4.5.6 Dowels

SDG guidelines show that at least two dowels are required between the trunnion and hub (see Figure 2.2). These are generally installed with an FN2 fit and designed to resist torsion, but may need to be designed to also resist axial loads. The following items are affected by dowels:

- i) *Torsion capacity of hub-trunnion interface*
- ii) *Axial load capacity of hub-trunnion interface*
- iii) *Bearing stress on dowel, trunnion and hub*
- iv) *Shear stress in dowel*

- v) *Stress Concentrations:* Dowels cause local stress concentration on hub and trunnion and slightly lower the capacity of the trunnion and hub. However, due to relatively small size of the dowel hole, stress concentrations due to other features (such as steps on trunnion) are likely to be more severe.

4.5.7 Bolts

SDG requires minimum 1” bolt diameters. Bolts affect the following items:

- i) *Torsion transfer between hub and girder*
- ii) *Shear transfer between girder and hub* (bearing and friction joint, see Chapter 5)
- iii) *Bearing stresses on hub flange, girder and backing ring*
- iv) *Bolt stresses* (shear, tension, fatigue checks).

4.6 Girder and Backing Ring

Current SDG requirements for girder and backing ring thickness specify a minimum 2” thickness. In context of hub assemblies, these affect the following items:

- i) *Bearing stresses at bolt holes*
- ii) *Bearing stresses at interface with hub*
- iii) *Shrink fit stresses in mating area with hub*

4.7 Shrink Fit Interference

LRFD recommends FN2 to FN4 fits for hub to trunnion and FN2 fit for hub to girder. This seems to be based on industry practice in typical machinery design. However, as seen in above sections, in many cases the resulting hoop stresses in the hub are high and sometimes exceed allowable static stresses. In general, it is important to stay below the specified allowable limits since the design analysis is simplified and does not account for many items that can potentially increase stresses, such as the true hub geometry (see Chapter 5), fabrication issues including machining finish, run out, tolerances, temperature loads, dynamic loads and misalignments.

4.8 Design for Service Behavior

The discussion presented above on hub geometry items qualitatively described the relationship between the geometric parameters (such as flange thickness) and stresses. With the exception of shrink fit stresses and flange bending stresses, most items are simple to compute and vary linearly with the geometric parameter. It is therefore easy to obtain optimum hub geometry by computing dimensions that result in allowable stresses for all the items listed the previous sections. Sample calculations illustrating such a process are presented in the Appendix B and can be used for preliminary designs. The final design however must account for empirical knowledge, which is the basis for the minimum dimensions specified in SDG and LRFDM specifications.

The analysis of hub design requirement presented in earlier sections identified the following items that are currently not considered in general design of hub assemblies:

- i) Hoop stresses developed due to shrink fit
- ii) Shrink fit contact pressure requirement to resist axial loads
- iii) Dowel size required to resist axial loads

Hub designs can be checked to ensure the resulting geometry satisfies these requirements in addition to those in current design guidelines. Item (iii) is relatively easy to address since it simply involves sizing the dowel to resist combined shear from torsion and axial load on hub (see Figure 4.1).

In many cases, the tensile hoop stress due to an FN2 shrink fit may exceed the allowable limit (see Table 4.2) Some designs utilize FN3 fits between the hub and trunnion, where the tensile stress will exceed the allowable limits even more severely. There are a few options that can be used individually or in combination to reduce the hoop stress from interference fit. These are

- i) Reduce the interference fit from FN2 to FN1 or FN3 to FN2. This is the most effective means to reduce the hoop stress since the stresses vary linearly with amount of interference.
- ii) Increase the hub thickness (see Figure 4.4). This can reduce hoop stress to certain extent. However, the reduction in stress is limited.

Reducing the interference fit from FN2 to FN1 or FN3 to FN2 reduces the contact pressure, which in turn affects the torsional and axial capacity of the trunnion-hub joint.

However, any reduction in contact pressure due to a lighter fit can be compensated by increasing the hub thickness and if necessary increasing the hub length. The second option is not always desirable since it would affect the trunnion design. Figure 4.4 shows the normalized contact pressure for an FN1 fit as a function of hub thickness. The contact pressures shown are normalized with respect to current SDG recommended ratio of 1.4 and FN2 fit. It can be seen that the contact pressure with an FN1 fit can be increased to about 76% of that with an FN2 fit by increasing the hub O.D. to bore ratio to 2.0. In many cases, where the torsional loads are small, this amount of contact pressure may be sufficient to resist the torsion and axial loads. The resulting assembly would also have significantly lower tensile hoop stresses. The optimum solution is to use the maximum fit that still keeps the stresses within allowable limits. This process is illustrated in the sample calculations presented in Appendix B.

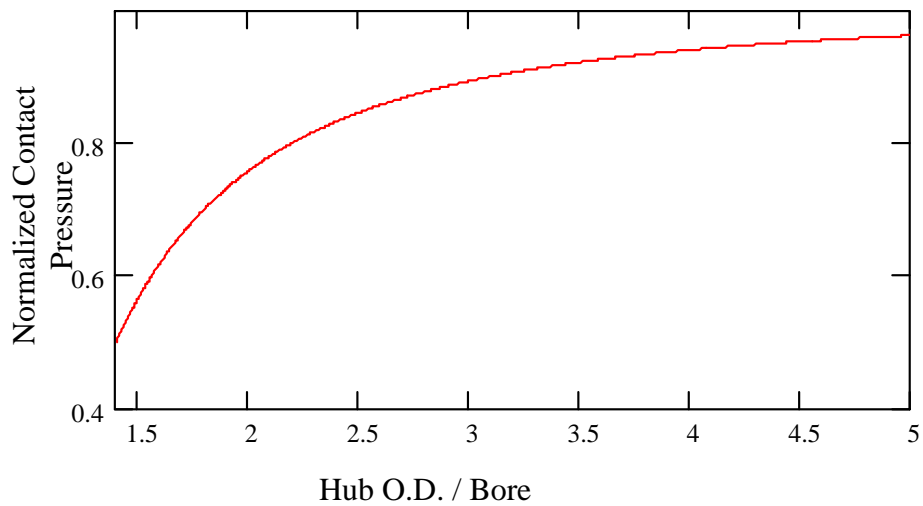


Figure 4.5 Effect of hub thickness on contact pressure

A lighter interference fit that provides the necessary resistance to torsion and axial loads is unlikely to affect performance of the bridge in any way other than to reduce hoop stresses in the hub. In some cases, an FN1 fit is adequate to ensure a solid interface between the trunnion and the hub under all applied loads (see section 4.9).

4.9 Sample Analysis

A MathCAD worksheet (see Appendix B) was developed to carry out the computations based on the qualitative analysis presented above. This worksheet along with the Excel worksheet developed in the earlier project can be used to determine preliminary design of hub assemblies that satisfy all the functional and stress requirements.

Data from sample bridges were used to compare preliminary design generated using the MathCAD worksheet with final designs. The results are shown in Table 4.3. The ratios shown are with respect to the trunnion diameter computed in the preliminary design. The last column indicates the ratio of actual trunnion diameter used in the final design to the preliminary diameter. The final trunnion bore is 1 to 26% bigger than the preliminary design.

The sample computations performed indicated that in bridges with box girders an FN1 fit between the hub and trunnion may be sufficient to meet all the performance requirements. These designs are governed by the contact pressure requirement to avoid separation between the hub and trunnion under applied service shear loads (see Section 5.8).

Table 4.3 Results from sample bridges using proposed design equations

Bridge	Type	Trunnion-Hub Shrink Fit	D	(L _H /D)	D _H /D	D _F /D	D _{Design} /D
Royal Park	Simple	FN2	521 mm	0.80	1.40	1.96	1.17
Hatchett Creek	Hopkins	FN2	583 mm	0.80	1.40	1.96	1.01
NW 12th Ave. over Miami River	Box	FN1	21.16"	0.40	1.40	1.96	1.21
		FN2	21.16"	0.40	1.40	1.96	1.21
Johns Pass	Box	FN1	21.15"	0.40	1.40	1.96	1.26
		FN2	21.15"	0.40	1.40	1.96	1.26

The results shown here indicate that the hub length ratios (0.4 to 0.8) and flange outer diameter ratios (1.96) required to meet all performance requirements are smaller than the present requirement of 1 and 2.6 respectively. The analysis presented above is

applicable to all three types of bascule bridges commonly found in Florida (simple trunnion, Hopkins and box girder).

4.10 Summary

This chapter presented a qualitative analysis of the various structural factors that influence hub design. Numerical analysis of the structure is presented in the Appendix using MathCAD and following chapters using finite element models.

CHAPTER 5 STRUCTURAL FINITE ELEMENT ANALYSIS

5.1 Introduction

Simplified analysis of the trunnion hub shrink fit stresses presented in Chapter 4 showed that the tensile hoop stress due to shrink fit between the trunnion and the hub exceeds the allowable limit by between 6% and 62% in existing designs. Analytical equations used to determine the tensile hoop stress in the hub are based on shrink fitting analysis of two cylinders. The actual geometry of the hub is more complicated, and bound to affect the stress distribution resulting from the shrink fit. Consequently, a three-dimensional finite element model was developed to determine the stresses developed in the trunnion, hub, girder and backing ring due to the shrink fit. The stresses computed are steady state stresses and do not account for transient thermal stress developed due to heating or cooling of the assembly. Transient thermal stresses are briefly studied in Chapter 6. The objective of the following structural analysis is to better determine the extent by which the stresses in the hub assembly are exceeded.

5.2 Finite Element Model

Figure 5.1 shows the trunnion-hub-girder-backing ring assembly from SR-706, while Figure 5.2 shows the finite element mesh of the same assembly. The finite element model was developed using ANSYS Version 8.0, a general purpose finite element analysis program. The model consists of (a) trunnion (b) hub (c) girder (d) backing ring. Each of these is modeled with 8 node brick element (SOLID45). It can be seen from Figure 5.2 that the geometry has been simplified to include only the most important features. Details such as bolts, dowels and variations in trunnion diameter have been neglected for simplicity. Significant dimensions reflected in the model are the 5" trunnion bore, 26" trunnion diameter, 40" hub outer diameter and 72" hub-flange diameter. The trunnion overhang on each side of the hub is taken as 7". All the nodes on

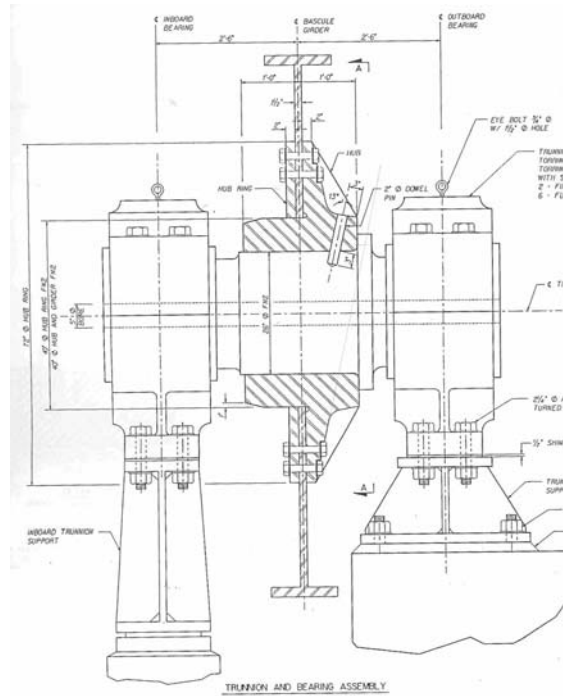


Figure 5.1 S.R.706 trunnion-hub-girder-backing ring assembly

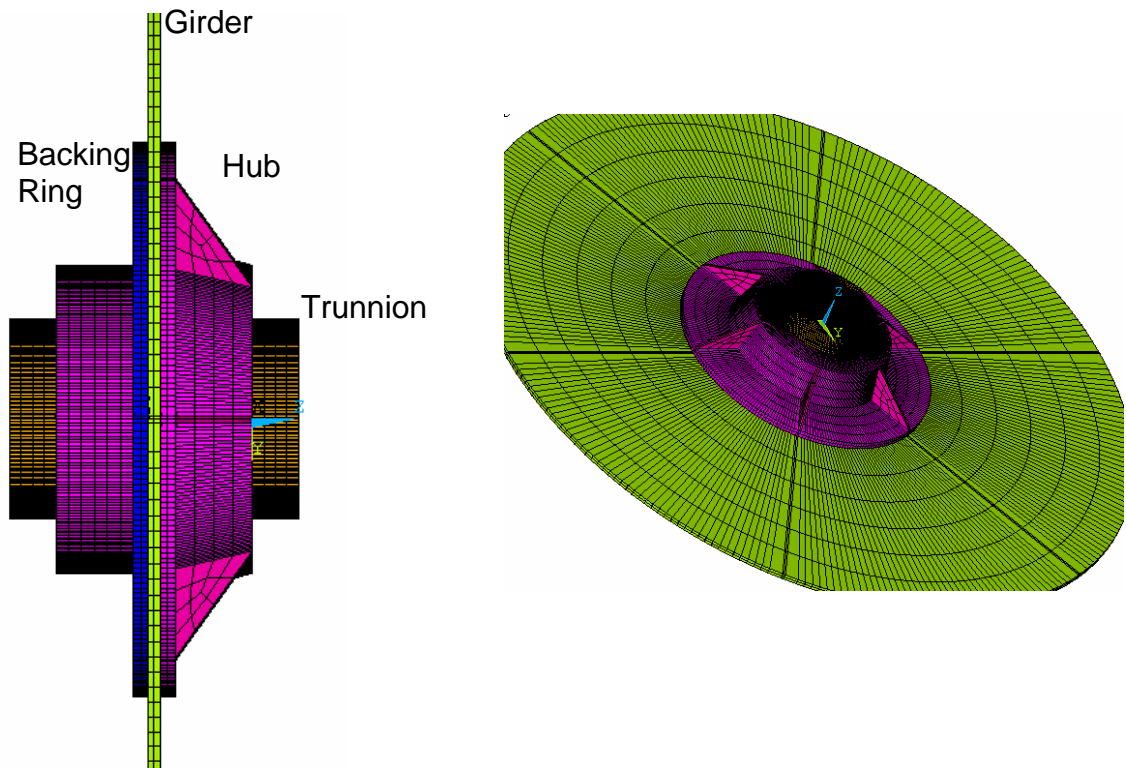


Figure 5.2 Finite element mesh of trunnion-hub-girder-backing ring assembly

the two end faces of the trunnion are constrained to model the fixed support provided by trunnion bearings.

The components are modeled as being made of steel ($E=29,000$ ksi). The interface between components in regions where they bear against each other is modeled as being perfectly bonded through the use of coincident nodes. Interference between various components is modeled by applying a temperature load to obtain the amount of deformation specified by the fit (FN3 between hub and trunnion, and FN2 between girder and hub & girder and backing ring). The temperature load to simulate interference is applied to the trunnion, girder and backing ring (not to the hub).

Due to symmetry, only half the geometry is modeled with symmetry boundary conditions applied along the plane of symmetry. This results in significant reduction in solution time and storage space. The use symmetry boundary conditions and coincident nodes to model contact results in an efficient, linear model, that avoid the complexities and longer run times associated with non-linear models that include contacts utilized in previous studies [1, 33]. The model consists of approximately 41,000 nodes and 33,000 elements and run time per load case is about an hour on a 3.0 GHz Pentium 4, 2.5 GB RAM PC running Windows XP.

5.3 Trunnion-Hub Shrink Fit Stresses

As stated in Chapter 2, two types of assembly procedures were encountered during the review of fabrication processes. The finite element model simulates the case where the trunnion is first shrink fit into the hub. Subsequently the trunnion-hub assembly is shrink fit into the girder. This section provides results from the trunnion-hub assembly process.

Figure 5.3 shows steady state radial stresses developed in the hub. Elements at the inside surface of the hub that mate with the trunnion are excluded since stress values plotted there are combined stresses of trunnion and hub stress (since they share nodes). The average stress inside of the hub is between -6.5 ksi and -7.7 ksi. This is in fairly good agreement with the closed form solution obtained using theory of elasticity, which predicts a stress of -7.2 ksi. While the averages are close to predictions from simplified equations, it is seen that stress distribution in the region of the hub flange is slightly

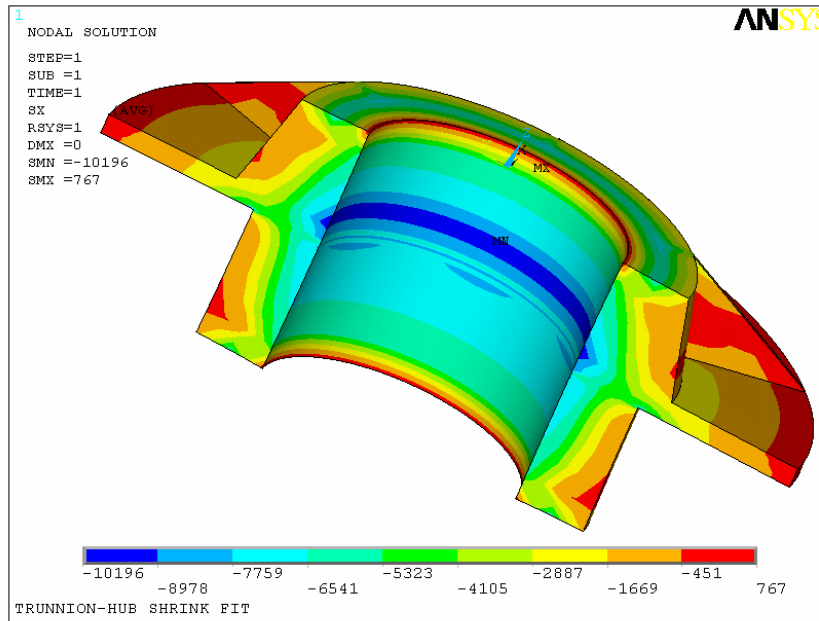


Figure 5.3 Radial stress (psi) in the hub after trunnion-hub assembly

different. This is a result of the higher radial stiffness in the area of the flange. All stresses are below the allowable limit of 15 ksi for ASTM A148 steel typically used for hubs.

Figure 5.4 shows the hoop stress developed in the hub due to the trunnion-hub assembly. The hoop stress is positive, indicating tension. It is maximum at the hub bore and reduces in the outside regions. Peak tensile stresses (20.4 ksi to 23.2 ksi) significantly exceed the allowable limit of 15 ksi in region at the top and bottom of the hub. Tensile stresses of about 18 ksi were predicted using closed form equations from elasticity. However, it is clear that true hoop stresses can be slightly higher. Although the stresses exceed the allowable limit, the hub is no danger of failure because the steel is Grade 90-60, and these stresses are well below the yield. In addition, regions of high stresses are localized and even if the stresses exceed the yield limit, the steel is likely to simply yield in order to redistribute the loads. A review of principal stresses (not shown) indicates that the maximum principle stress varies from about 23 ksi tension to 13 ksi compression.

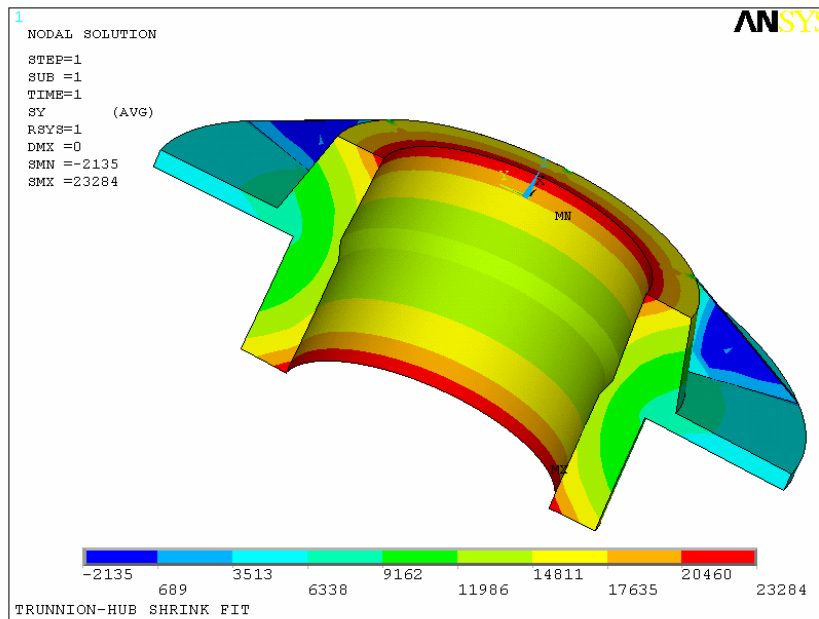


Figure 5.4 Hoop stress (psi) in the hub after trunnion-hub assembly

5.4 Hub-Girder Shrink Fit Stresses

Figure 5.5 shows radial stresses on the hub at the end of the trunnion-hub-girder-backing ring assembly process. The results show that radial compressive stress on the inside surface of the hub increases from a maximum of 12.3 ksi to 15.6 ksi in the area mating with the girder and backing ring. At the same time, the outside area shows tensile radial stresses between .41 ksi and 6.6 ksi in a localized area under the flange where the girder mates.

Figure 5.6 shows hoop stresses in the final assembled configuration. It can be seen that regions where the girder and backing ring mate with the hub have tensile stresses in the range of 24.3 ksi to 27.5 ksi. As with the trunnion-hub assembly, these are well above the allowable limit of 15 ksi specified in AASHTO [2]. Review of the principal stresses (not shown) indicates a range of 15 ksi compression on the inside of the hub to 28 ksi tension on the outside.

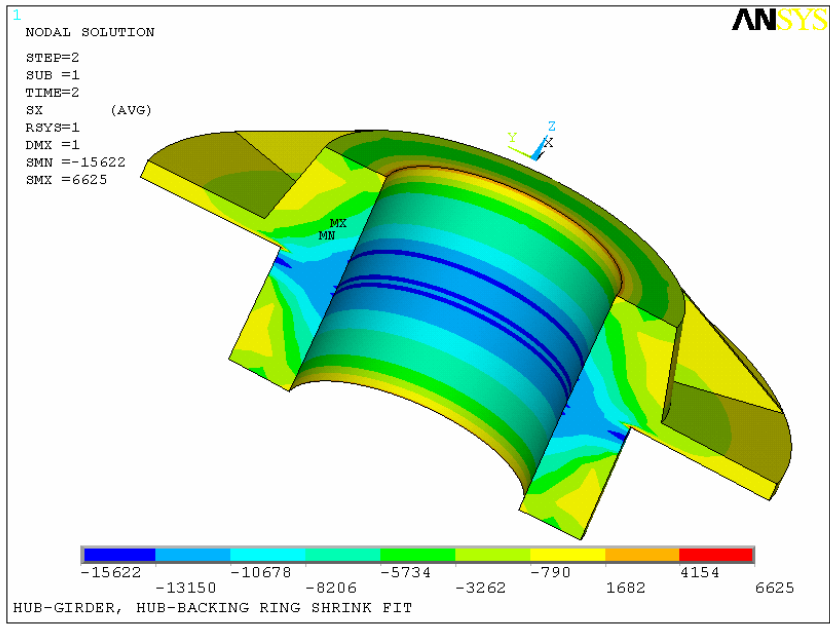


Figure 5.5 Radial stress (psi) in the hub after trunnion-hub-girder assembly

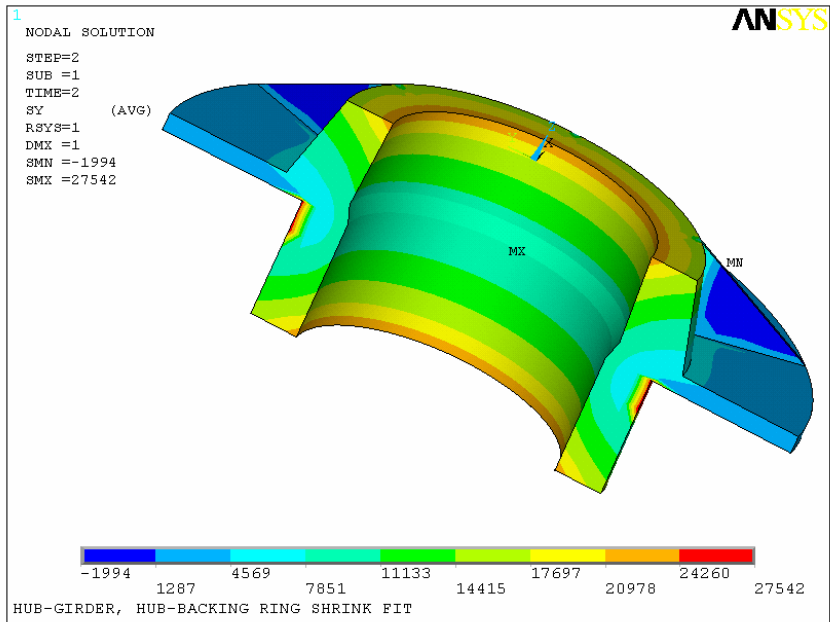


Figure 5.6 Hoop stress (psi) in the hub after trunnion-hub-girder assembly

5.5 Hub-Assembly Service Behavior

The above analysis shows that the stresses in the hub exceed allowable tensile limits. The model developed above was subjected to a vertical load of 220 kips to simulate the loading due to dead load + 20% impact with one bearing removed for maintenance. This was found to be the load case that governs design of the hub in the computations reviewed (see Chapter 2). Load due to torsion is typically very small, especially when spherical roller bearings are used, and therefore ignored in the analysis. The total load was distributed uniformly amongst the top nodes on the circumference of a circle representing the girder (see Figure 5.7).

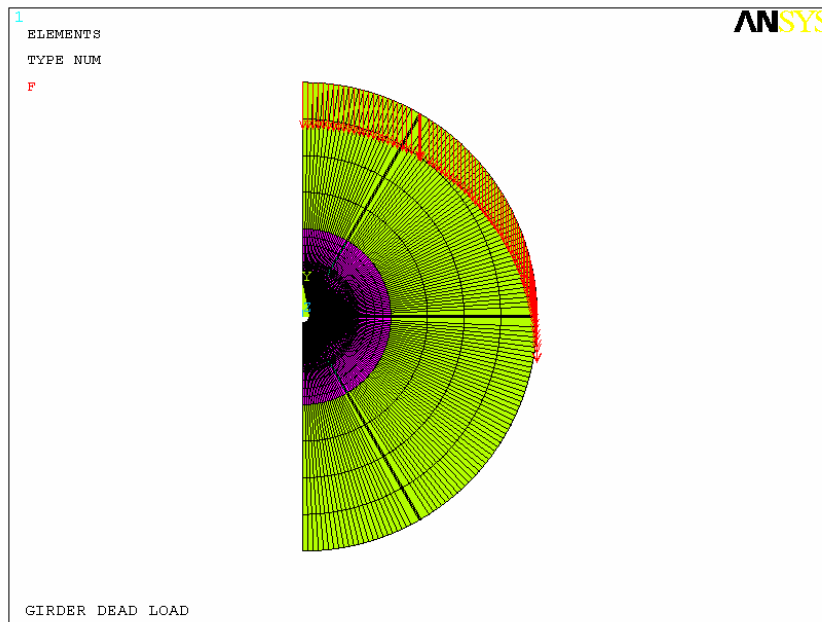


Figure 5.7 Dead load modeling as force on around girder circumference

Figure 5.8 shows radial stresses developed in the hub due to combination of dead load and the shrink fit. As one might expect, the dead load increases the compressive stresses in the top region of the hub (from 15.6 ksi in Figure 5.5 to 24.1 ksi). At the same time, the tensile radial stress in the localized region below the hub flange also increases (but to a lesser extent) on the outside regions from maximum of 6.6 ksi to 9.6 ksi in Figure 5.8.

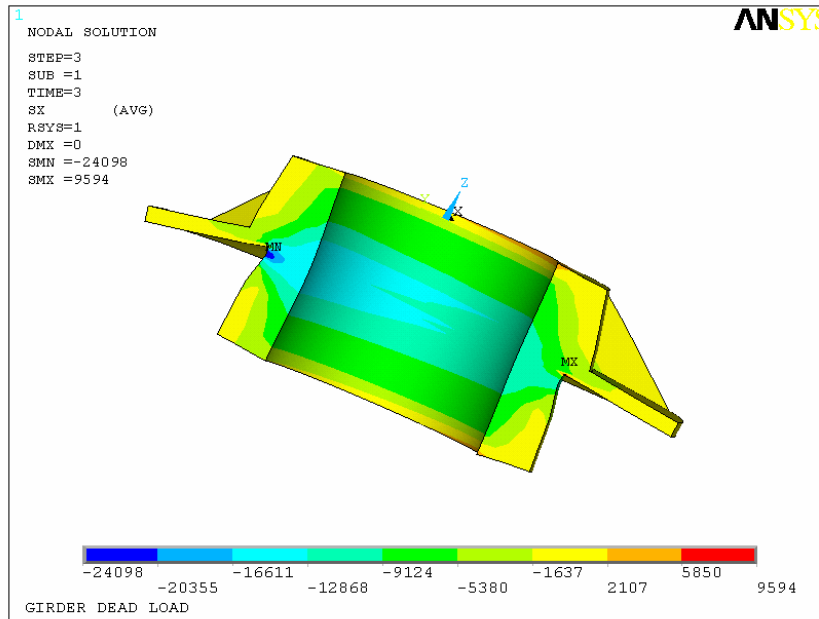


Figure 5.8 Radial stresses (psi) due to shrink fit and dead load + impact

Figure 5.9 shows hoop stress in the combined loading case. The tensile hoop stress peaks in the region of load application at about 29.8 ksi. The tensile stress in this case is nearly twice the allowable limit. Furthermore the maximum compressive principle stress (not shown) for this load case is 23.6 ksi and maximum tensile principle stress is 30.5 ksi. The tensile stress is significantly above the allowable limits.

The primary purpose of the FN2 shrink fit between the girder and hub is to ensure that load is transferred directly to the hub through the solid interface, thereby eliminating the possibility of fretting as the bridge opens and closes. Figure 5.10 shows radial stresses in the girder developed under combined loading (dead load, impact and shrink fit). It can be seen that the entire part of the girder bearing on the hub has compressive radial stresses, indicating a closed joint. As one might expect, the compression at the lower part of the girder is significantly lower than at the upper part. This result indicates that in this case, the FN2 fit maintains contact between the hub and the girder. Note that peak local compressive stresses in the girder are 34.1 ksi. Hoop stress results (not shown) show the maximum tensile hoop stress to be 19.8 ksi, which is above the allowable limit.

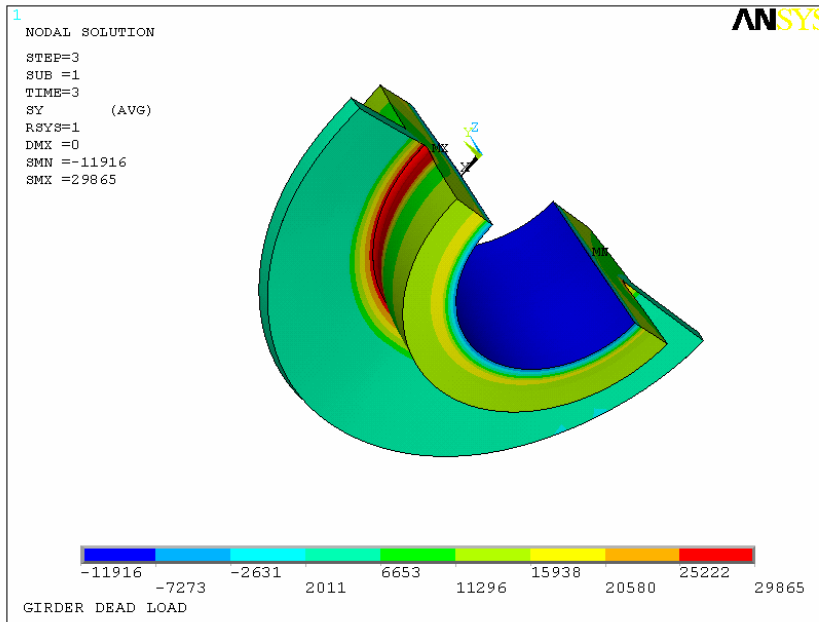


Figure 5.9 Hoop stresses (psi) due to shrink fit and dead load + impact

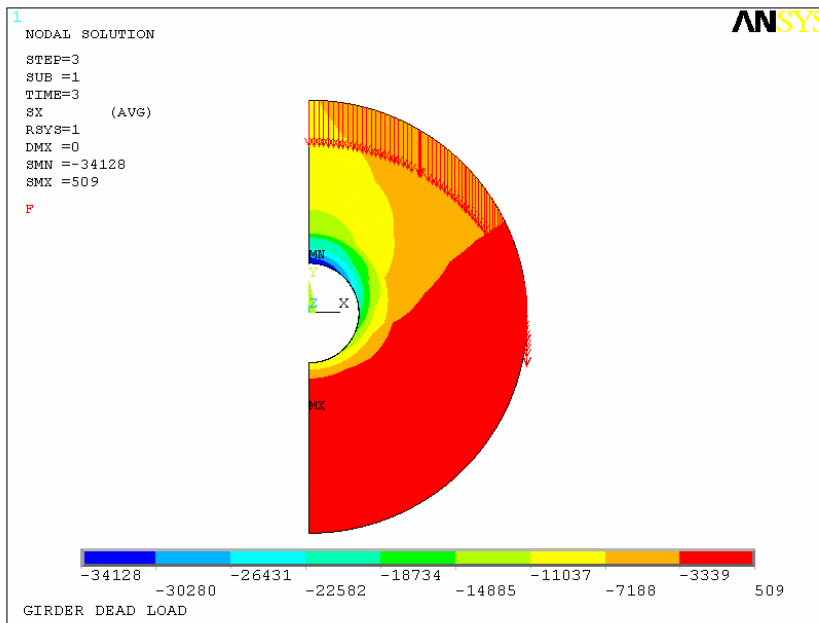


Figure 5.10 Radial stresses (psi) on girder due to shrink fit and dead load + impact

5.6 Discussion

The results presented here clearly show the possibility of hub assemblies having higher stresses than allowed by AASHTO specifications. These results can also be verified through use of closed form equations for hoop and radial stresses in a shrink fit assemblies. In spite of the possibility of being subjected to high loads, bascule bridge hub assemblies have performed satisfactorily over the years. This is most likely due to the inherent conservative design assumptions used for materials and governing loads cases. In addition, since these assemblies are made of steel, they are capable of redistributing loads by localized yielding. Finally, the case of the results presented for hub assembly subjected to dead load, the above model allows load transfer only through the bearing area between the girder and the hub. In reality, hub-assemblies utilize bolted joints which provide slip resistance and resistance in bearing, both of which are likely to distribute the load more evenly (directly through the flange and also the through the backing ring). Results presented in the following section show that the load transferred in bearing is in fact only about a fifth of the total, with the remaining load transfer occurring through the backing ring and the hub flange.

It is reasonable to conclude from the above analysis that the hub assemblies do not have the same amount of factor of safety as is obtained for other components using standard bridge design procedures. The primary cause for this is the shrink fit utilized between the components. Means to improve the safety margins include optimizing the shrink fit to obtain only the amount of compressive stresses required to function safely (without fretting). Other options include providing redundancy for load transfer, as is already done in such assemblies through the use of bolted joints.

5.7 Load Distribution

Service load analysis presented in the previous section used a simplified assumption of the entire vertical load being transferred through direct bearing between girder and hub. The analysis presented in the following section aims to better quantify the distribution of the vertical load between direct bearing of girder and friction transfer to backing ring and hub flange.

The analysis presented above indicates that interference between the hub and trunnion results in large tensile hoop stresses. It was shown in Chapter 4 that these stresses reduce as the thickness of the hub is increased. In case of the FN2 interference fit between the girder and hub, the girder is significantly larger than the hub and therefore the resulting hoop stresses are smaller and hence, tensile hoop stress is generally not an issue. However, in some cases, the interference fit between the girder and hub may need to be eliminated for ease of assembly and to avoid high thermal stresses that may occur during the shrink fitting process. In this case, it is useful to have some basic understanding of how the shear load (see Figure 4.1) is transferred from the girder to the hub. There are three possible means for this load transfer:

- i) Direct transfer through interference fit interface: Here the load is transferred directly from the girder to the hub resulting in bearing stresses on the girder and hub.
- ii) Transfer from girder to backing ring through friction between the bolted faces.
- iii) Transfer from girder to hub flange through friction between the bolted faces.

In typical case each of these items is designed to be capable of carrying the entire load. Understanding the relative amounts of load carried by these members can be used to determine a better estimate of reserve capacities of these members and refine the design if necessary. A non-linear three-dimensional finite element model was developed to estimate the load sharing between these three components.

5.7.1 Finite Element Model of Bolted Assembly

Figure 5.11 shows the mesh of the finite element model of bolted hub assembly developed using ANSYS Version 8.0. The dimensions of the model are based Hatchett Creek bridge (see Table 2.1). Unlike the previous model used to study shrink fit stress, the present model includes bolts. Bolts are represented as cylinders with bolt heads (no threads). Hub, trunnion, girder and backing plate are modeled using 8 node solid element SOLID45 with 3 displacement degrees of freedom at each node. Bolts and curved regions that can make contact with the bolt in hub flange, girder and backing ring are modeled with SOLID95, which is a 20 node solid element with 3 displacement degrees of freedom per node. Contact elements (CONTAC174 and TARGET170) elements are

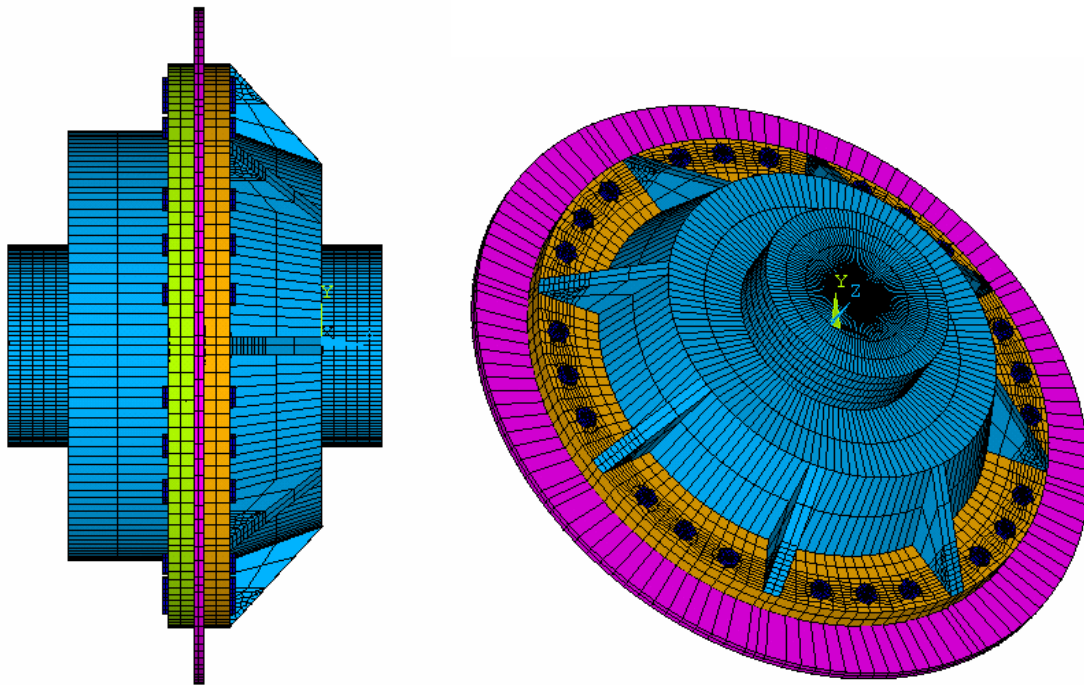


Figure 5.11 Finite element mesh of bolted hub assembly

overlaid on contact regions between the hub flange and girder, girder and backing plate, bolt heads and hub flange, bolt head and backing plate and between cylindrical surface of bolt and bolt hole walls in the hub flange, girder and backing plate. Interference fit between trunnion-hub-girder was not modeled since it does not affect load transfer. Areas that have contact due to interference fit were modeled with common nodes, effectively joining the components. Only half the geometry is modeled due to symmetry. The model consists of a total of about 34,000 nodes and 21,000 elements.

All materials are assumed to be steel with modulus of elasticity of 29,000 ksi. The coefficient of friction between all contact surfaces is taken to be 0.5. In addition to the symmetry boundary condition at the plane of symmetry (see Figure 5.12), the model is fixed at the two trunnion end faces. The solution is obtained in two load steps. First, the bolt preload is developed in the assembly by modeling the bolt geometry with an initial interference. Second, a vertical load is applied to the outer girder nodes (see Figure 5.12). The model is non-linear due to inclusion of contact and friction to model the slip resistance and bearing resistance of bolts. The non-linear solution process

involves multiple iterations and is therefore very time consuming. A typical run on a 3.0 GHz Pentium 4 PC running Windows XP and 2.5 GB of RAM was about 6-10 hours.

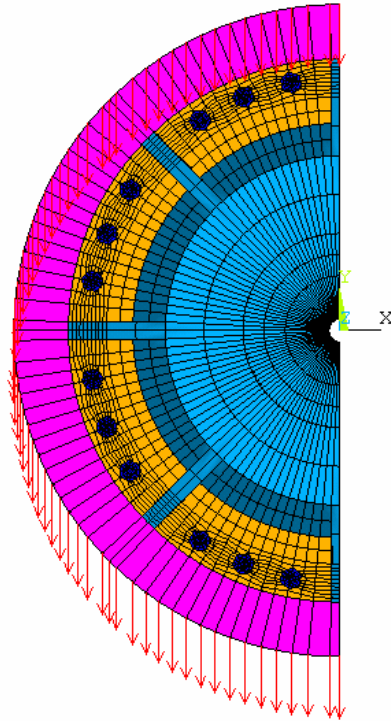


Figure 5.12 Hub assembly loading

5.7.2 Results

As stated in the previous section, the solution was obtained in two steps. First, the preload was developed by modeling an initial interference between the bolt head and hub flange. The amount of preload developed can be adjusted by varying the amount of initial interference. Figure 5.13 shows the axial stress along the z axis on the backing ring and the hub. This represents the pressure distribution resulting from the bolt preload of about 16.7 kips per bolt on 1.5” diameter bolts (total 200 kips). The average contact pressure expected from the 200 kip preload is about 200 psi. It is seen that the contact pressure is concentrated around the bolts and is more than five times higher than the average. The model does not include washers, which are likely to help distribute the load a little more uniformly.

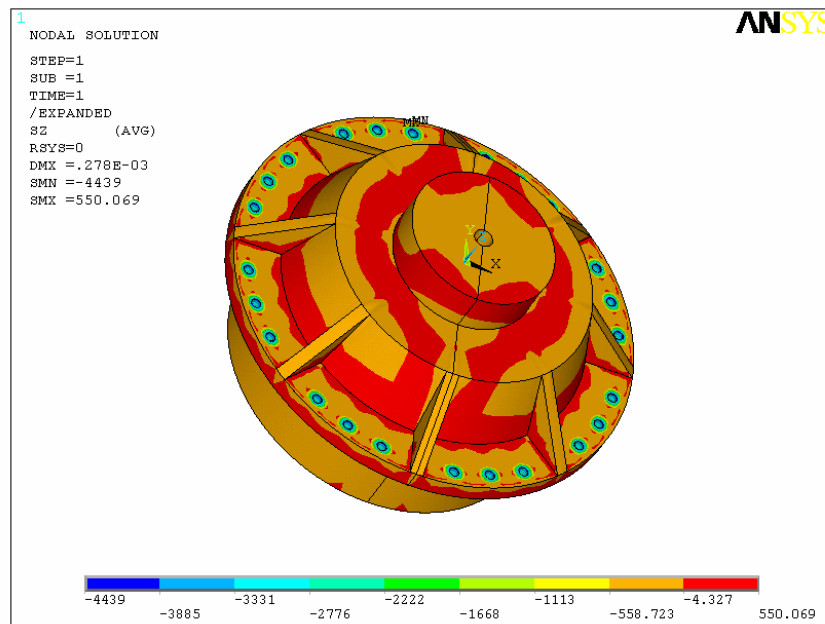
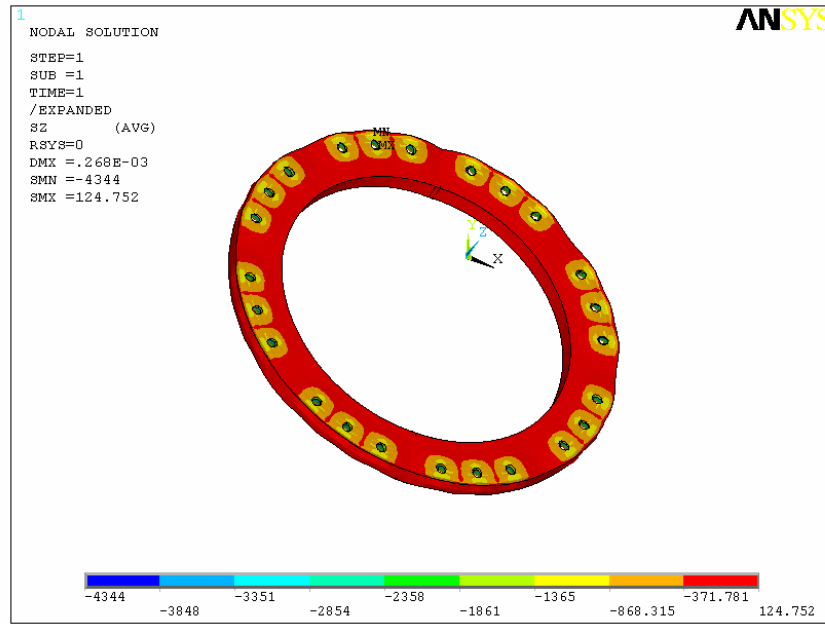


Figure 5.13 Axial stress σ_z (contact pressure) due to bolt preload on backing ring (top) and hub (bottom)

A vertical load was applied on the girder as shown in Figure 5.12. The load was incremented slowly until the non-linear solution stopped converging. Results were obtained until the vertical load reached 66 kips, which is about a third of the applied preload. Since the slip resistance of the bolted joint is about 200 kips (two slip surfaces

with coefficient of friction of 0.5 each and bolt preload of 200 kips), there is no slip and the hub-backing ring-girder joint behave as one body. Review of nodal forces indicate that about 31 kip (47%) was transferred through the friction at hub flange, 24 kips (36%) through the friction at backing plate and the remaining 11 kips (17%) directly by girder bearing on the hub. These ratios are approximately the same as the ratio of cross section area of the three components. The results indicate that the ratio of thickness of all three bolted members (backing ring, girder and hub flange) and corresponding the load distribution is nearly equal with the hub flange carrying more load due to larger area of the hub. A more uniform load can be obtained by increasing the girder and backing plate thickness to match the effective thickness of the hub flange (including the hub area below the flange).

5.8 Contact Pressure Analysis

Current design specifications require a shrink fit (FN2 thru FN4) fit between the trunnion-hub and hub-girder. The shrink fit serves two main purposes. First, it provides the contact pressure required to generate the friction between the trunnion and hub to resist applied torsional and axial loads. Secondly, it prevents wear by maintaining positive contact between the hub and trunnion under applied loading. Analysis to determine if the fit performs the first function is relatively simple and has been explained in Chapter 4 and illustrated in the sample calculations presented in Appendix B. The analysis required to determine if the second requirement is being satisfied is more complex. Such an analysis must provide the contact pressure on the trunnion-hub face when the shrink fit is subjected to vertical loads. Closed form solutions for such problem are not readily available. Consequently, a finite element model was used to obtain numerical data that can be used to estimate the change in contact pressure due to an applied load on the trunnion hub girder assembly.

5.8.1 Finite element Model

Figure 5.14 shows the finite element mesh of the model developed using ANSYS. It is a two-dimensional plain strain (1" thick) representation of trunnion, hub and girder, all of which are made of as steel ($E=29,000$ ksi). Due to symmetry, only half the

geometry has been modeled. Four node PLANE42 elements are used for the trunnion, hub and girder. Contact elements (CONTACT172 and TARGET169) are used to model contact between the trunnion and the hub, and hub and the girder. The model consists of a total of 1602 nodes and 1554 elements. In addition to symmetry boundary conditions, all the nodes at inside bore of the trunnion are constrained along the radial directions. Due to the use of contact elements, the solution process is non-linear.

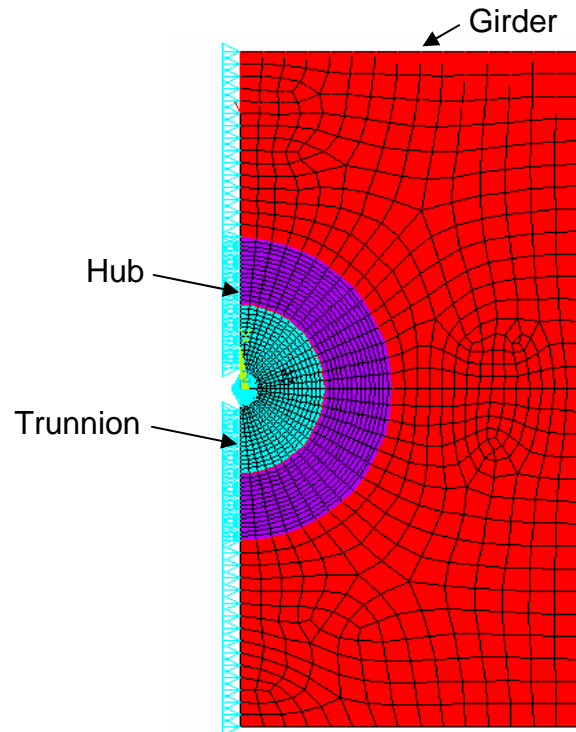


Figure 5.14 Finite element mesh of model used to determine contact pressure

5.8.2 Results

The analysis was performed in two steps. First, the shrink fit between the trunnion-hub and hub-girder was obtained by applying temperature load to the trunnion and the girder (not the hub). The resulting contact pressure and hoop stress were found to be within 3% of closed form solutions obtained from equations for thick cylinders (see Appendix B). Subsequently, a vertical load was applied uniformly over the top of the girder. Figure 5.15 shows contact pressure distribution drawn normal to the trunnion-hub contact area immediately after the shrink fit and also upon application of vertical load. In the first case (Figure 5.15a), the contact pressure is uniform. In the second case (Figure

5.15b), the contact pressure is higher at the top and lower at the bottom. Figure 5.16 shows a graph of the applied load versus minimum contact pressure between the hub and trunnion (which occurs at the lowest point on the trunnion). The load has been normalized with respect to the maximum load at which the contact pressure drops to zero. The contact pressure has been normalized with respect to the initial contact pressure (from shrink fit only). It is seen that the contact pressure reduces linearly as the applied load is increased and eventually becomes zero. Linear behavior is not surprising since there is no separation between the parts.

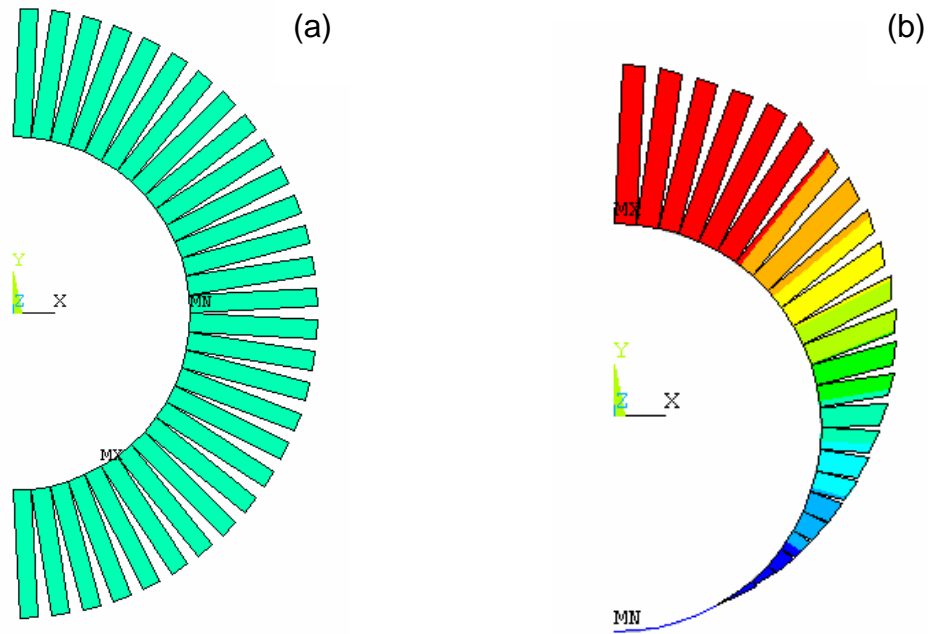


Figure 5.15 Contact Pressure distribution at trunnion-hub interface: (a) immediately after shrink fit (b) upon application of vertical load

5.8.3 Design Chart

The above analysis indicates that contact pressure at the trunnion reduces linearly as the vertical load is increased until separation occurs. The contact pressure reduction per unit applied load per unit hub thickness, ΔC_{PRES} , (units psi-in/ (kip)) was determined for various hub sizes. Figure 5.17 shows the relationship between ΔC_{PRES} and trunnion

outer radius. ΔC_{PRES} pressure reduces approximately linearly from 24.1 psi-in/ (kip) to 15.3 psi-in/ (kip) as the trunnion outer radius goes from 10 inches to 15 inches.

Additional runs were made to study the effect of hub outer diameter, girder height (vertical) and girder width on the reduction in contact pressure. The hub outer diameter had no influence on the change in pressure. This is expected since the assembly behaves like a single body as long as there is contact between all parts, and changing the hub outer diameter does not alter the load transfer paths. The girder height was varied from 6 to 14 times the trunnion radius. ΔC_{PRES} increases by about 20% as the girder height is increased over this range. Finally, ΔC_{PRES} increases by 20% as the girder width is increased from 8 to 40 times the trunnion radius. To account for this variation, it is proposed that the ΔC_{PRES} value obtained from the chart be multiplied by an adjustment factor C_{CP} during design. A value of $C_{CP} = 1.3$ is used for the sample computations presented in Appendix B.

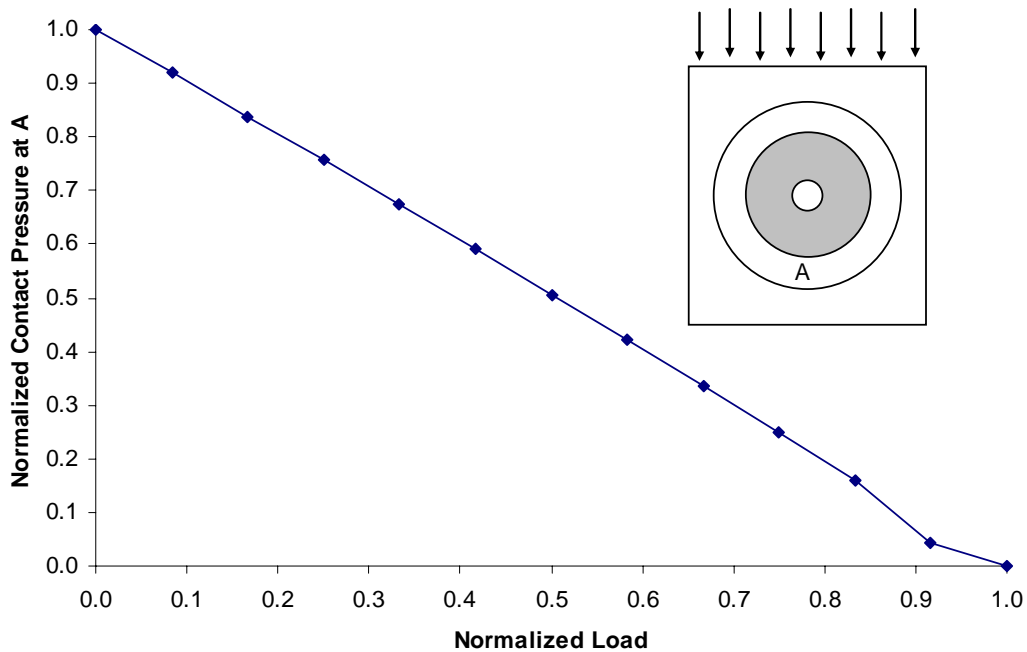


Figure 5.16 Normalized contact pressure versus applied load

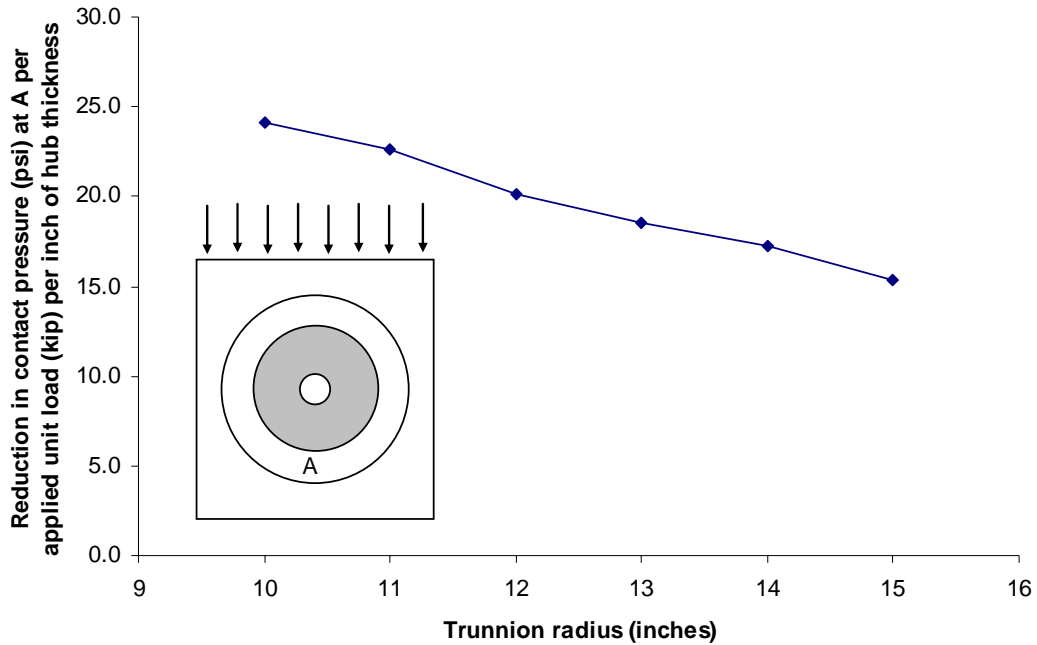


Figure 5.17 Reduction in contact pressure at A per unit load per unit hub thickness (ΔC_{PRES}) versus trunnion radius

The main utility of this chart is that the expected reduction in contact pressure due to the applied service shear load can be computed using the chart by multiplying the ΔC_{PRES} obtained from the chart with the shear load (kip) and dividing by the hub length (inches). This information can be used to check if the shrink fit at the trunnion-hub is sufficient to maintain contact when the vertical service load is applied to the hub assembly. The use of this procedure for design is illustrated in Appendix B.

5.9 Summary

This chapter presented the results of structural finite element analysis of the hub assembly. The analysis verified results obtained using simpler closed form solutions presented in Chapter 4. The analysis predicts tensile stress above allowable limits based on a factor of safety of 4.0. In all cases, the tensile stresses are below the yield limits.

A more refined analysis of the hub assembly was performed using a model that included bolted joints. The analysis provided estimates of load distribution of the applied shear at the hub-girder-backing ring interface. Finally, a two-dimensional model was

used to obtain a design chart for estimating the change in contact pressure at the trunnion-hub joint under applied vertical loading.

CHAPTER 6 THERMAL ANALYSIS

6.1 Introduction

Components of hub-assemblies develop thermal stresses during the shrink fit process as a result of either cooling (with dry ice and alcohol) or heating. Computation of these stresses requires thermal analysis to determine the temperature distribution and subsequently structural analysis to determine the thermal stresses. Based on review of contractor's documents [38] and simple hand calculations, it was established that the required amount of diametral clearance (0.025") can be obtained by heating the components. To assemble the trunnion and hub, the hub is heated to between 300°F and 400°F at the bottom around the center of the hub using gas burners or any suitable heating source (e.g. induction heating), while other parts of the hub are covered with an insulating blanket. Similarly, to assemble the trunnion-hub assembly with the girder, the latter would be heated until the required clearance is obtained.

In general, heating a steel component to achieve the shrink fit is preferable to cooling. This is because the fracture toughness of steel is higher at high temperatures (see Figure 6.1). Figure 6.2 shows that the yield strength of steel decreases at high temperature. Therefore thermal stresses must be kept below the reduced yield stress to avoid permanent deformation. Since the modulus of elasticity of steel reduces with increase in temperature (see Figure 6.3), the thermal stresses produced due to thermal deformations are also lowered. Variation of other material properties with temperature is shown in Figures 6.3 through 6.6 for steels. Properties shown in Figures 6.2 through 6.6 are considered to be representative of steel grades used for typical structural applications with yield strength less than 70 ksi [53].

6.2 Finite Element Model

A finite element model of the hub was developed to estimate of the thermal stresses developed during the heating process. Material properties of steel were varied

with temperature as shown in Figures 6.3 through 6.6. The density of steel was maintained at 0.284 lbs/in^3 over the range of temperature. The mesh is similar to the one

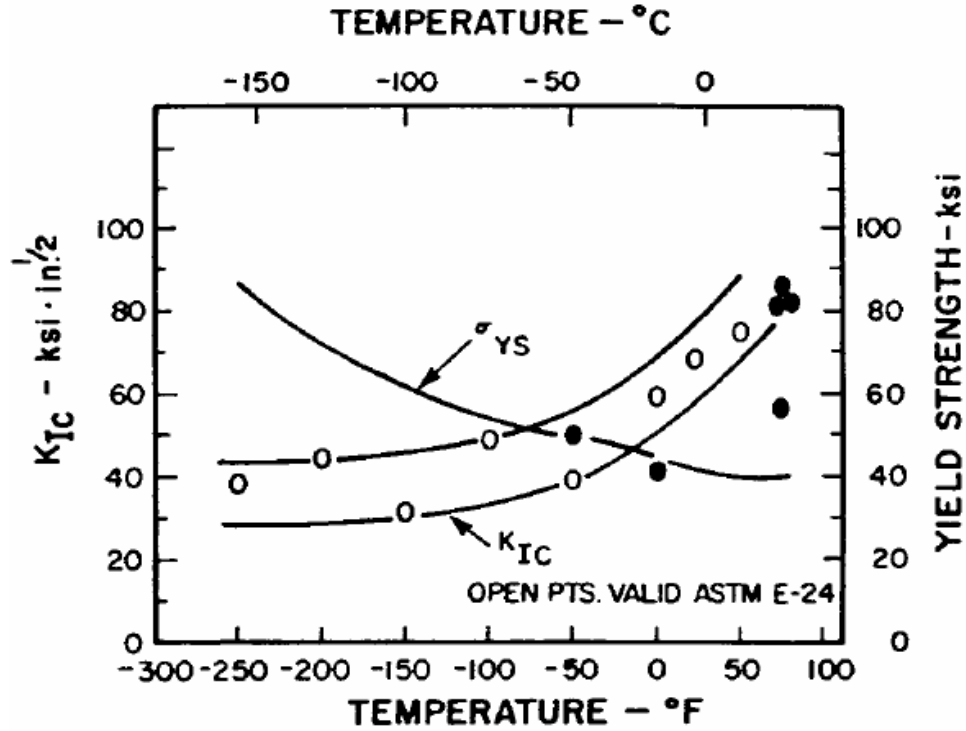


Figure 6.1 Fracture toughness and yield strength as a function of temperature [50]

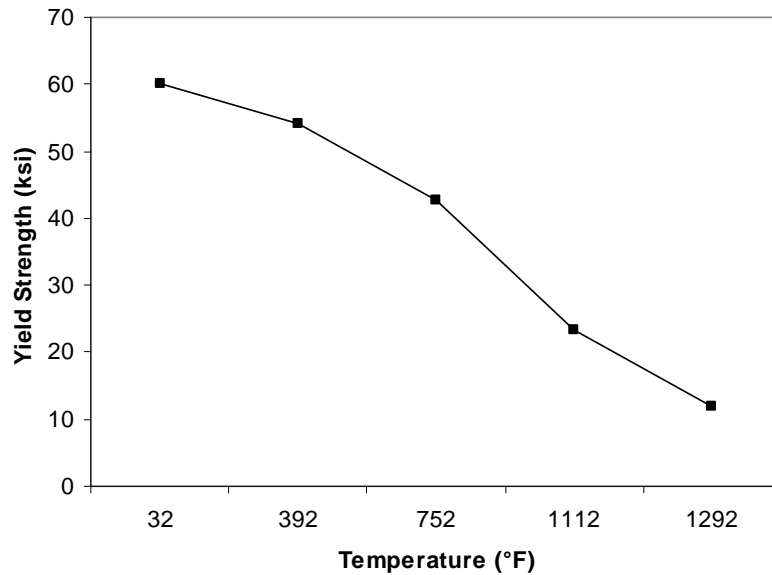


Figure 6.2 Yield strength of steel as a function of temperature [51]

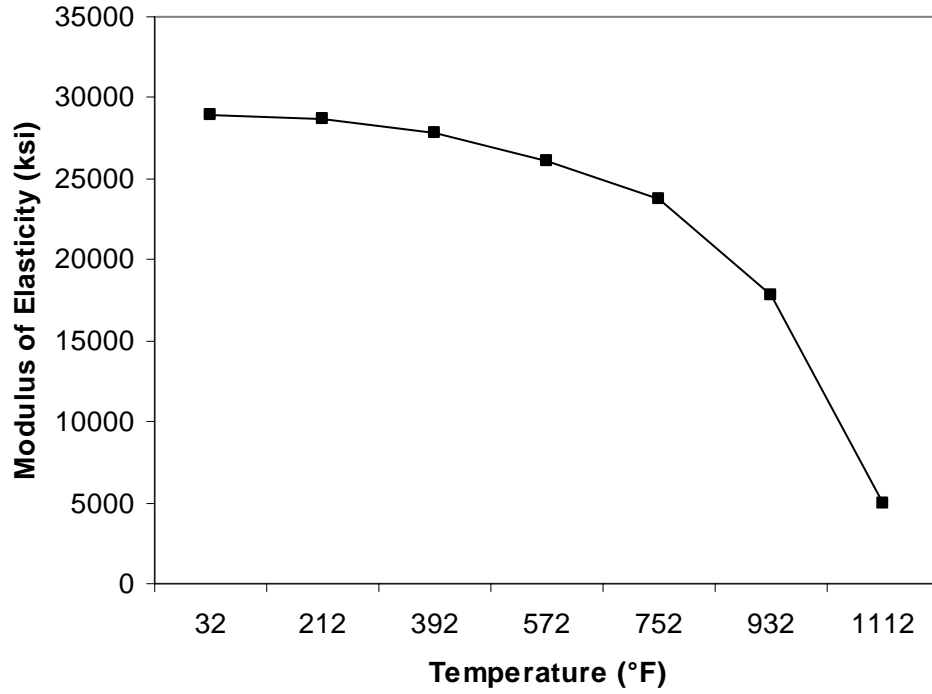


Figure 6.3 Modulus of elasticity of steel as a function of temperature [51]

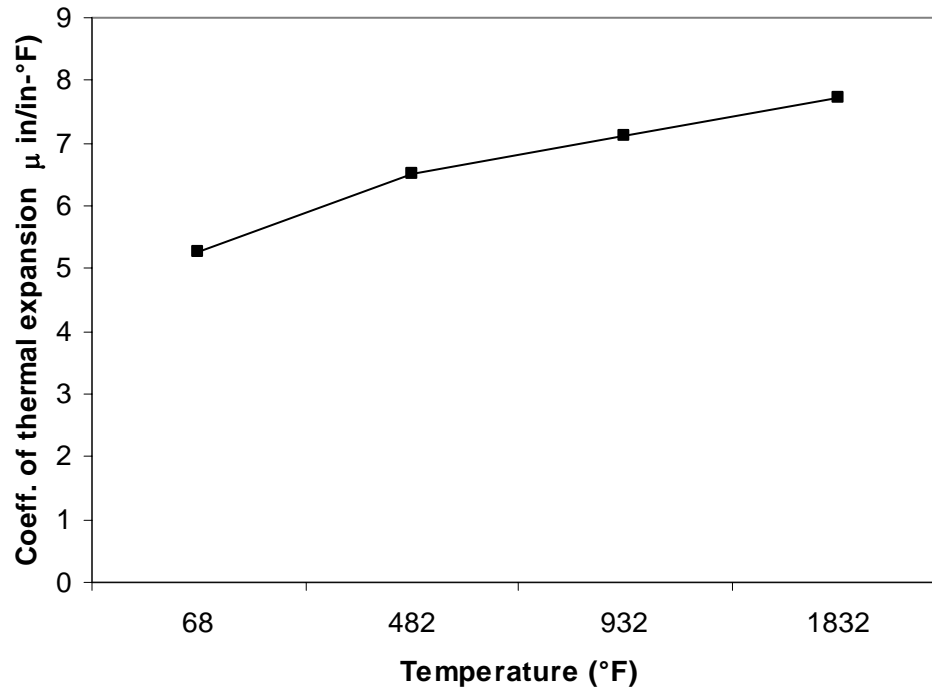


Figure 6.4 Coefficient of thermal expansion of steel as a function of temperature [52]

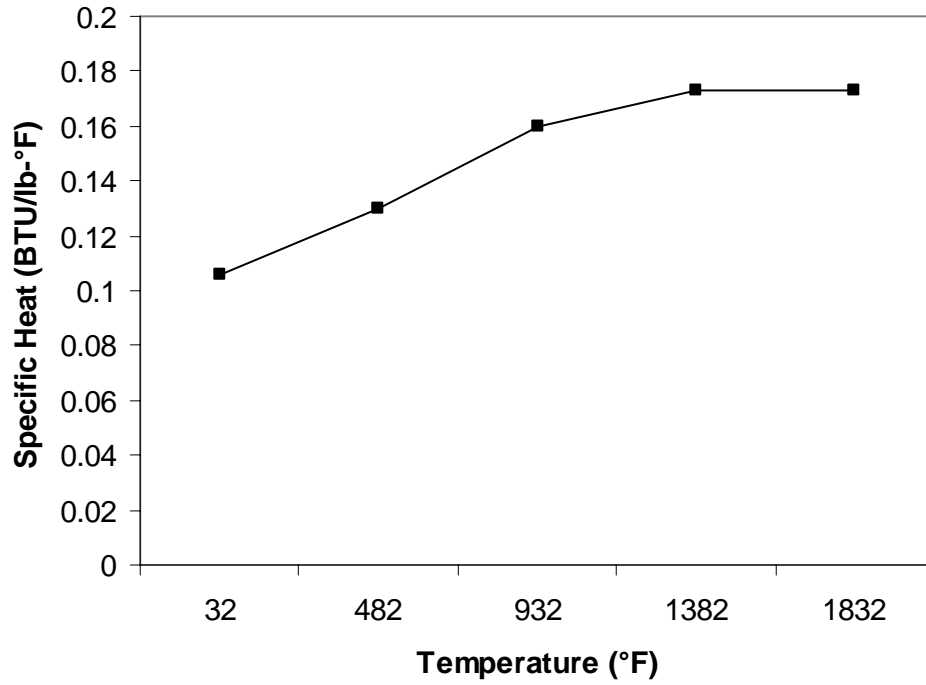


Figure 6.5 Specific heat of steel as a function of temperature [51]

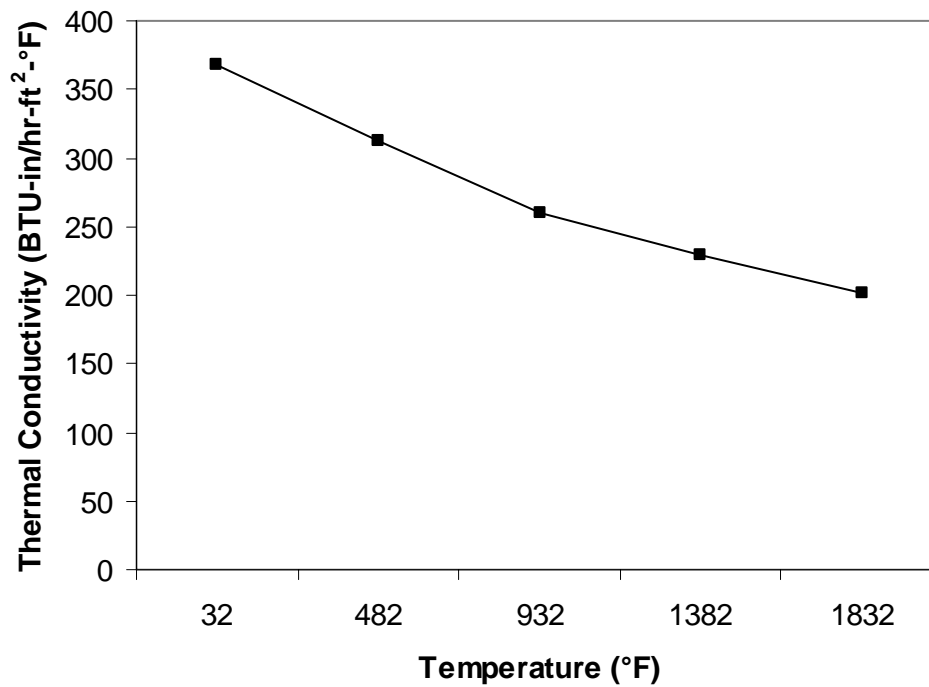


Figure 6.6 Thermal conductivity of steel as a function of temperature [51]

used for the structural analysis (see Figure 5.2). SOLID70, an 8 node thermal brick element is used for the thermal analysis, while SOLID45 is used for the structural analysis. Three nodes spaced equally at the hub bore are constrained to provide stability. The model assumes that the hub top is being heated at the three red regions shown in Figure 6.7 at the bottom of the hub. These regions are assumed to be at a temperature of 1000°F, which is more than twice the amount needed for hub assembly.

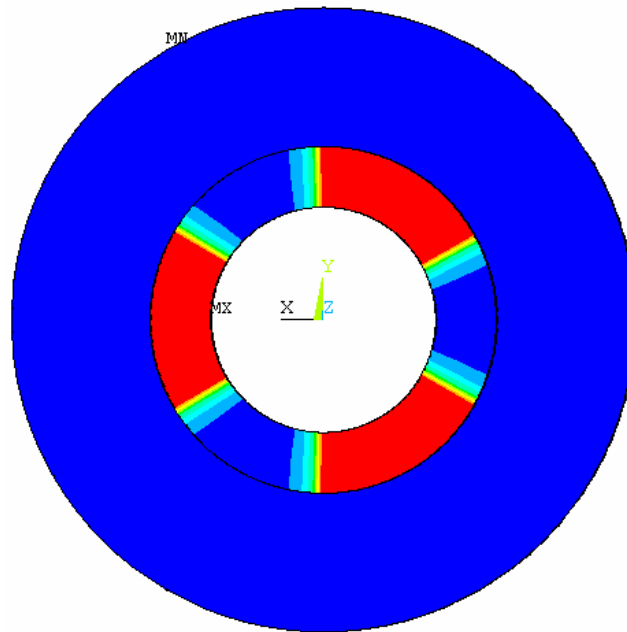


Figure 6.7 Areas of hub subjected to heat in finite element model

6.3 Results

Figure 6.8 shows the temperature distribution in the hub at various times during the heating process. It can be seen that initially only the top part of the hub, where the heat is applied, is at the peak temperature of 1000°F, but as time elapses, other regions of the hub heat up and eventually reach the desired temperature of 350 °F in about 6 hours.

In the context of hub design, the temperature distributions obtained from the thermal analysis (Figure 6.8) are used to determine the thermal stresses developed in the hub. Elements at the bottom of the hub, where the temperature boundary conditions are

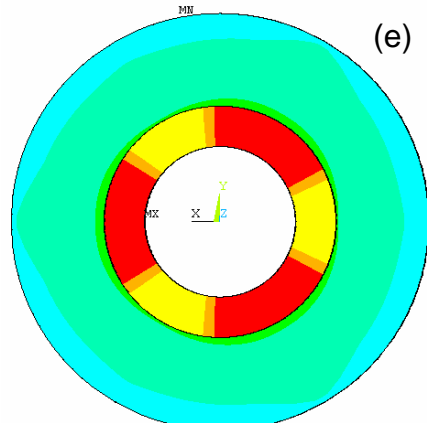
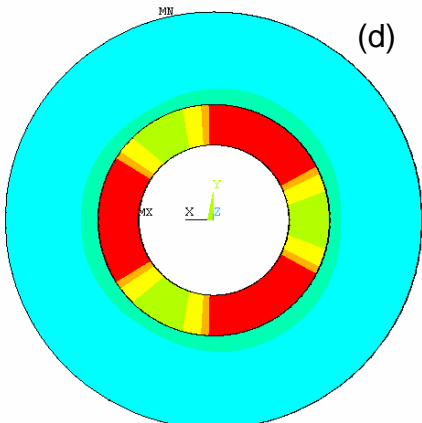
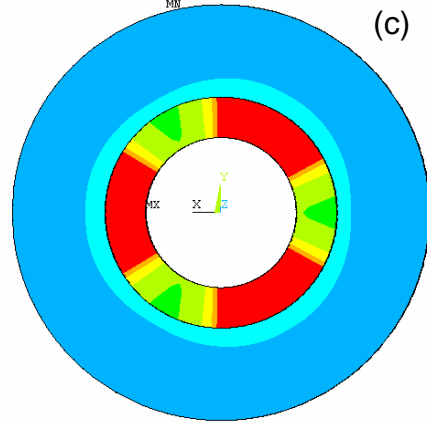
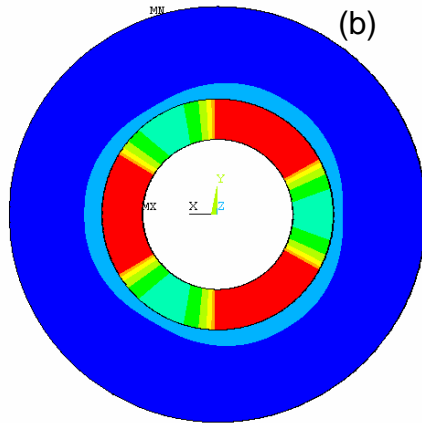
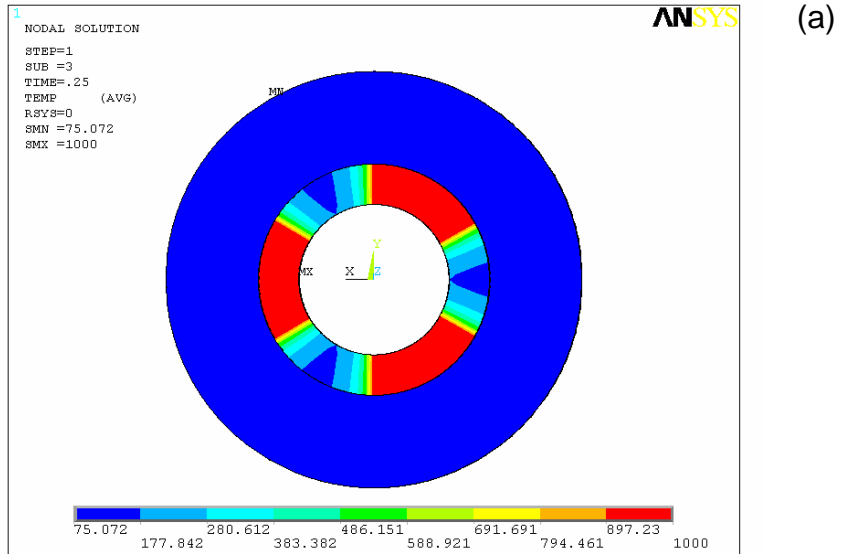


Figure 6.8 Temperature distribution ($^{\circ}\text{F}$) in the hub during heating after (a) 0.25 hours (b) 1.5 hours (c) 3 hours (d) 4.5 hours (e) 6 hours

applied are excluded from structural analysis, since results obtained in this area are unrealistic because of the applied temperature boundary condition.

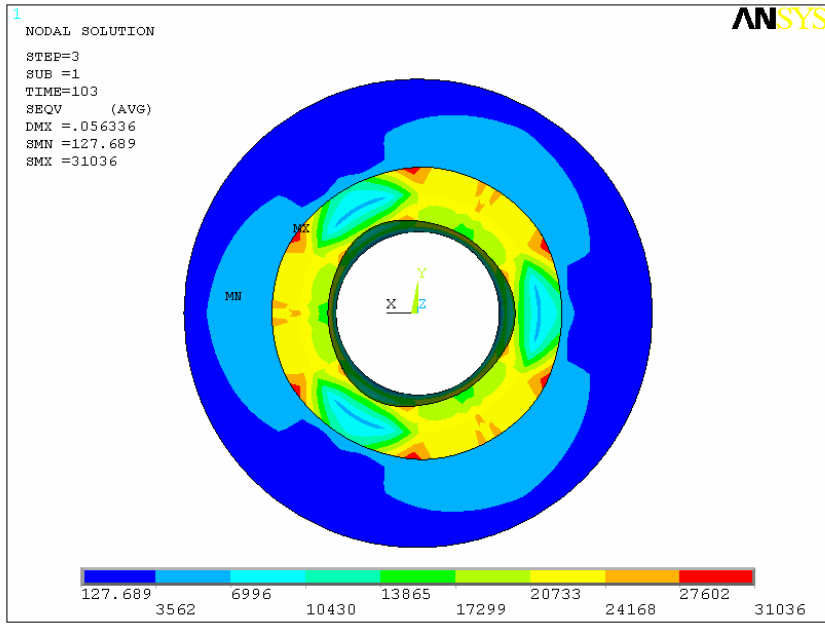
Maximum thermal stresses can be expected at the initial stage when the temperature distribution is highly non-uniform. Figure 6.9 shows Von Mises stress developed at different times during heating of the hub. Von Mises stress is obtained by combining stresses along the different directions, and is found to be a good indicator for failure of ductile materials [49]. It can be seen from Figure 6.9 that the maximum stress occurs at an early stage of heating. The region of high stress is localized around the source of the heat. The thermal stress developed here are below the yield limit of steel at the corresponding temperature, and therefore no permanent deformation is expected.

The main objective of the heating is to obtain sufficient clearance between the hub and the trunnion. Figure 6.10 shows the radial displacement obtained after 6 hours of heating. The results indicate that the deformed shape is not symmetrical due to stiffeners and unsymmetrical heat pattern. In spite of this, it seems feasible to obtain the required clearance of 0.025” at a temperature between 300°F and 400 °F.

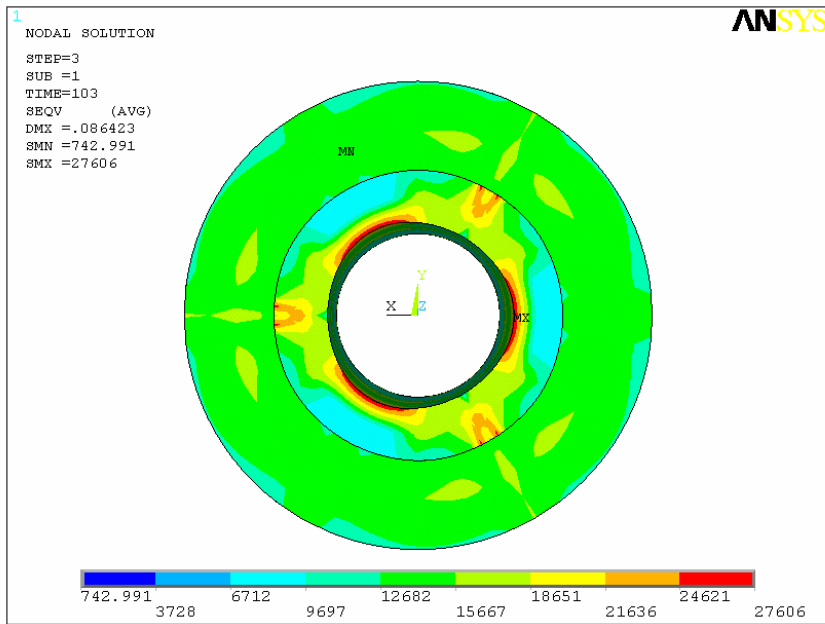
6.4 Effect of Hub Thickness

One of the recommendations from the Chapter 4 was to increase the hub thickness. The effect of this proposed change on thermal stresses developed during shrink fit assembly was determined using a finite element analysis. Items of practical interest are the time required to heat, the maximum stresses developed and maximum radial displacement obtained.

Figure 6.11 shows the Von Mises stress distribution obtained on the thicker hub geometry after 1 hour of heating. The overall stress distribution is higher than that with the thinner hub, but still below yield limit of the steel. The radial displacements shown around the hub bore (Figure 6.12) are also comparable to those obtained earlier. Overall, it can be seen that there is not significant impact on thermal stresses due to the thicker hub.



(a)



(b)

Figure 6.9 Von Mises stress (psi) in the hub during heating after (a) 0.25 hours (b) 1.5 hours

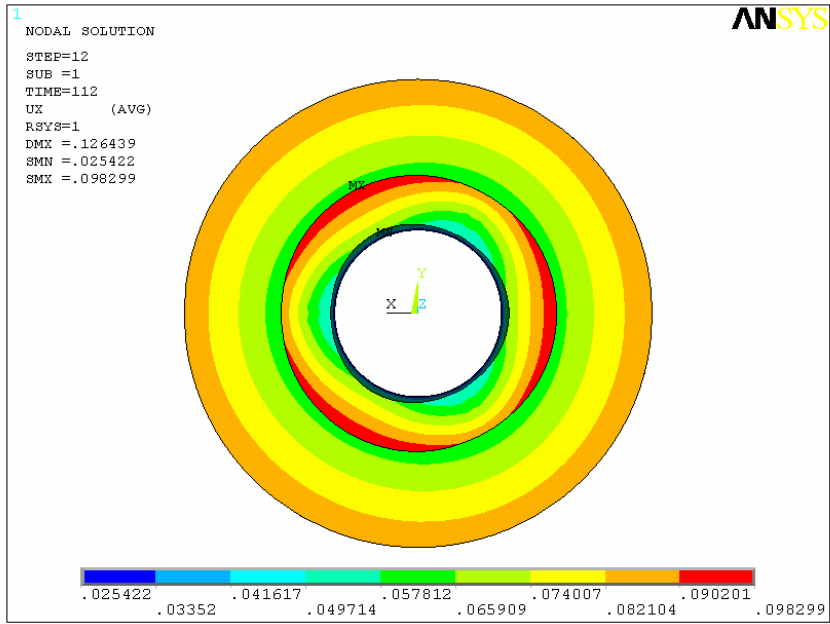


Figure 6.10 Radial displacements (in.) after 6 hours of heating

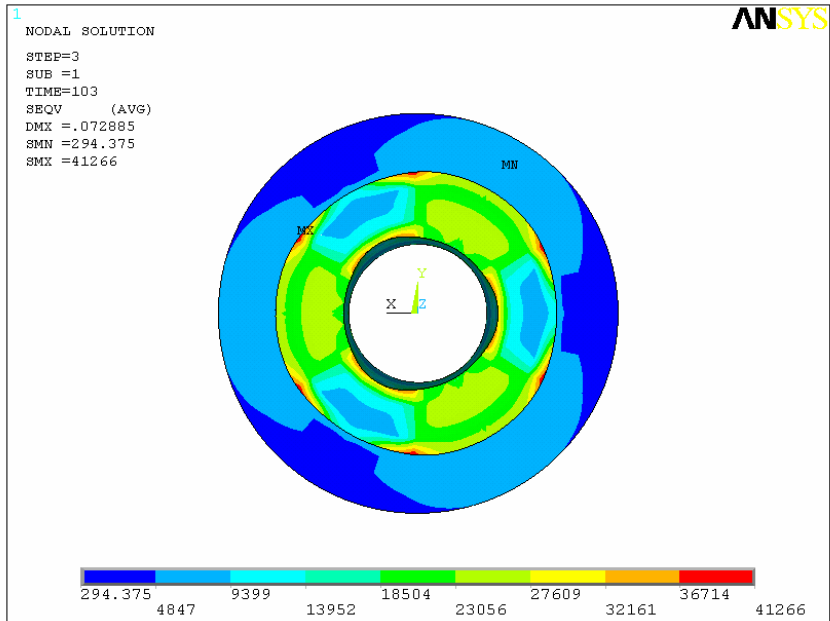


Figure 6.11 Von Mises stress (psi) in the hub during heating after 0.25 hours

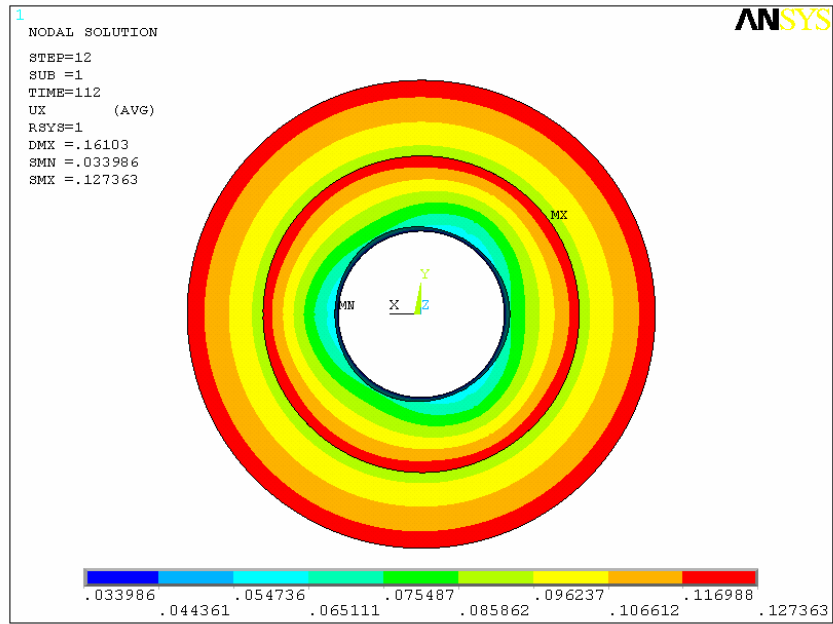


Figure 6.12 Radial displacements (in.) after 6 hours of heating

6.5 Summary

This chapter looked at the implication of using heat for the shrink fit assembly instead of the older practice of cooling with liquid nitrogen. Even without much analysis it is apparent that higher fracture toughness of steel at high temperature is a definite benefit. The analysis performed verified that desired clearances can be achieved through heating while maintaining all stresses within yield limits. The results highlight the need to obtain a uniform temperature through symmetrical heating pattern applied at thick region and by ramping the heat slowly over time.

CHAPTER 7 RECOMMENDATIONS

7.1 Design Recommendations

Based on the analysis presented in Chapters 3 through 6 the following items are recommended to be implemented in hub design for bascule bridges

7.1.1 Castability Considerations

1. Use minimum flange and rib thickness of 1.5”.
2. If feasible, use six ribs instead of eight.
3. Use triangular rib shapes.
4. Provide generous fillet radii at ribs and flanges. Recommended value is 1.5” or more.
5. Include complete casting acceptance criteria as part of the design bid package.

7.1.2 Loading

1. Consider the possibility of plain bearing seizure in design. This can be done by increasing the torsion load by 50% to 100% and ensuring that the torsion capacity of trunnion hub interface (shrink fit + dowels) and hub girder interface (shrink fit + bolted joint) exceed the torsion required to shear the screws used to mount bronze bushings to bearing house and friction due to seized bearings.
2. Design interface at trunnion-hub (shrink + fit) and hub girder interface (shrink fit + bolted joint) to resist applied axial loads. Axial loads may be taken as 15% of trunnion reaction or a computed value considering loads due wind and machine misalignments. If necessary provide a step in the trunnion to resist axial loads.

7.1.3 Geometry & Fit

1. Instead of always specifying FN2 through FN4 for trunnion-hub assembly, select the interference fit based requirements identified in Chapter 4 and computed using the MathCAD worksheet.

2. Hub thickness must also consider interference stresses developed due to trunnion-hub interference and other function requirements. The current SDG recommendation of hub radial being 20% of bore is adequate provided all other requirements identified in Chapter 4 and computed in Appendix B are satisfied.
3. To make load transfer more uniform, if possible, center the girder to the middle of the hub. This is done in practice but not explicitly stated.
4. Make backing ring thickness 30% more than the hub flange thickness. This will lead to nearly uniform load distribution through the hub flange and backing ring.
5. The above recommendations must be followed for all designs, including simple trunnions, Hopkins frame and box girder.

7.1.4 Assembly Procedure

1. Heating of members is preferred means to achieve shrink fit. The heat must be applied uniformly and gradually.

REFERENCES

1. Besterfield, G., A. Kaw, L. Oline and R. Crane. Parametric Finite Element Modeling and Full-Scale Testing of Trunnion-Hub-Girder Assemblies for Bascule Bridges, Final Report, Tampa, FL, 2001.
2. AASHTO. LRFD Movable Highway Bridge Design Specifications, 1st Edition, American Association of State Highway and Transportation Officials, Washington, D.C., 2000.
3. SDO. Structures Design Guidelines for Load and Resistance Factor Design. Florida Department of Transportation Structures Design Office, Tallahassee, FL, 2002.
4. Chen, W. and L Duan (Editors), Bridge engineering handbook, CRC Press, Boca Raton, FL, 2000.
5. Xanthakos, P., Theory and design of bridges, Wiley, New York, 1994.
6. Koglin, T., Movable Bridge Engineering, Wiley, New Jersey, 2003.
7. AASHTO. Standard Specification for Movable Highway Bridges, American Association of State Highway and Transportation Officials, Washington, D.C., 1988.
8. Shigley, J. E. and C. R. Mischke, Mechanical Engineering Design, 5th Edition, McGraw Hill, New York, 1989.
9. Oberg, E., F. D. Jones, H. L. Horton and H. H. Ryffel, Machinery's Handbook, 27th Edition, Industrial Press Inc., New York, 2004.
10. Contract Plans for Bridge No. 157801, Treasure Island Causeway Bascule Bridge (Designed by EC Driver for the City of Treasure Island, Florida, 2004).
11. Contract Plans for Bridge Nos. 170036 & 170167, U.S. 41 Over Gulf Intracoastal Waterway (Designed by EC Driver for FDOT, Sarasota County, 2001).
12. Contract Plans for Bridge Nos. 930506 & 930507, Royal Park Replacement Bridge (Designed by EC Driver for FDOT, Palm Beach County, 2000).
13. Contract Plans for Bridge No. 870662, N.W. 12th Avenue Replacement Bridge over Miami River (Designed by EC Driver for FDOT, Miami Dade County, 2003).
14. Contract Plans for 17th Street Causeway Replacement Bridge (Designed by EC Driver for FDOT, Broward County, November 1997).
15. Contract Plans for 17th Street Causeway Temporary Bridge (Designed by EC Driver for FDOT, Broward County, 1996)

16. Contract Plans for Bridge No. 110077, Astor Bridge Over St. Johns River (Bridge Rehabilitation Plans) (Designed by EC Driver and Associates for FDOT, Lake & Volusia County, 1999).
17. Contract Plans for S.R. 706 Bridge Over Intracoastal Waterway (Designed by Parsons Brinckerhoff for FDOT, Palm Beach County, 1994)
18. Contract Plans for Bridge Nos. 170169 & 170170, U.S. 41 Over Hatchett Creek at Venice (Designed by EC Driver for FDOT, Sarasota County, 2000).
19. Contract Plans for Brickell Avenue over Miami River (Designed by Kunde, Sprecher & Associates for FDOT, Dade County, 1992).
20. Contract Plans for Hillsborough Avenue over Hillsborough River (Designed by DSA Group for FDOT, Hillsborough County, 1994).
21. Contract Plans for S.W. 2nd Avenue Bridge over Miami River (Designed by Kunde Sprecher for FDOT, Dade County, 1999).
22. Contract Plans for Hallandale Beach Blvd. (SR-858) over intracoastal waterway (Designed by Reynold Smith and Hills, Inc for FDOT, Broward County, 1996).
23. Contract Plans for S.R. 44 Over Indian River (Designed by E.C. Driver and Associates for FDOT, Volusia County, 1994).
24. Contract Plans for Bridge Nos. 150253 & 150254, S.R. 699 Over Johns Pass (Designed by Lichtenstein Consulting Engineers for FDOT, Pinellas County, 2004).
25. Design Computations for Bridge Nos. 170169 & 170170, U.S. 41 Over Hatchett Creek at Venice (Designed by EC Driver for FDOT, Sarasota County, 2000).
26. Design Computations for Hallandale Beach Blvd. (SR-858) over intracoastal waterway (Designed by Reynold Smith and Hills, Inc for FDOT, Broward County, 1996).
27. Design Computations for Bridge Nos. 930506 & 930507, Royal Park Replacement Bridge (Designed by EC Driver for FDOT, Palm Beach County, 2000).
28. Design Computations for Bridge No. 870662, N.W. 12th Avenue Replacement Bridge over Miami River (Designed by EC Driver for FDOT, Miami Dade County, 2003).
29. Design Computations for Bridge No. 157801, Treasure Island Causeway Bascule Bridge (Designed by EC Driver for the City of Treasure Island, Florida, 2004).

30. Design Computations for Bridge Nos. 150253 & 150254, S.R. 699 Over Johns Pass (Designed by Lichtenstein Consulting Engineers for FDOT, Pinellas County, 2004).
31. AASHTO. Standard Specification for Highway Bridges, 16th Edition, American Association of State Highway and Transportation Officials, Washington, D.C., 1996.
32. AASHTO. LRFD Bridge Design Specification, 3rd Edition, American Association of State Highway and Transportation Officials, Washington, D.C., 2004.
33. Besterfield, G., A. Kaw, D. Hess and N. Pai. Hub-girder bolt assembly without an interference fit in bascule bridges, Final Report submitted to FDOT, Tampa, FL 2004.
34. Construction Specification Contract Documents for Bridge Nos. 930506 & 930507, Royal Park Replacement Bridge (Designed by EC Driver for FDOT, Palm Beach County, 2000).
35. Construction Specification Contract Documents for Bridge Nos. 170036 & 170167, U.S. 41 Over Gulf Intracoastal Waterway (Designed by EC Driver for FDOT, Sarasota County, 2001).
36. Construction Specification Contract Documents for Bridge No. 870662, N.W. 12th Avenue Replacement Bridge over Miami River (Designed by EC Driver for FDOT, Miami Dade County, 2003).
37. Construction Specification Contract Documents for Bridge No. 157801, Treasure Island Causeway Bascule Bridge (Designed by EC Driver for the City of Treasure Island, Florida, 2004).
38. Hardie-Tynes Co., Inc., Trunnion and Trunnion Hub Installation Procedure Using Heat, Part of contractors documents from for Bridge Nos. 170036 & 170167, U.S. 41 Over Gulf Intracoastal Waterway, Birmingham, Alabama, 2003.
39. Denninger, M., Design Tools for Trunnion Hub Girder Assemblies for Bascule Bridges, Master's Thesis, University of South Florida, Tampa, Florida, August 2000.
40. Collier, N., Benefit Of Staged Cooling In Shrink Fitted Composite Cylinders, Master's Thesis, University of South Florida, Tampa, Florida, March 2004.
41. Berlin, M. W., Innovative Procedure to Install a Trunnion-Hub Assembly in a Bascule Bridge Girder, Master's Thesis, University of South Florida, Tampa, Florida, September 2004.

42. Paul, J., Sensitivity Analysis Of Design Parameters For Trunnion-Hub Assemblies Of Bascule Bridges Using Finite Element Methods, Master's Thesis, University of South Florida, Tampa, FL, January 2005.
43. Shop Drawings for Reconstruction of 145th Street Bridge over the Harlem River, (Casting Map, Drawing No. GN-2), Contract No. HBX1029, City of New York, Department of Transportation, Division of Bridges, October 2004.
44. ASTM, Standard A 609/ A 609M, ASTM International, West Conshohocken, PA, 2002.
45. ASTM, Standard A 802/ A 802M, ASTM International, West Conshohocken, PA, 2001.
46. ASTM, Standard E 165 – 02, ASTM International, West Conshohocken, PA, 2002.
47. ASTM, Standard E 709 - 01, ASTM International, West Conshohocken, PA, 2001.
48. ASTM, Standard E 125 - 63, ASTM International, West Conshohocken, PA, 2003.
49. Ugural, A. and S. K. Fenster. Advanced Strength and Applied Elasticity, 3rd Edition, Prentice Hall, New Jersey, 1995.
50. Blair, M., Stevens, T. L., and Linskey, B., Steel Castings Handbook, 6th Ed., ASM International, Materials Park, Ohio, 1995.
51. Society of Fire Protection Engineers, Handbook of Fire Protection Engineering, 3rd edition, Quincy, MA, 2002.
52. MatWeb.com, <http://www.matweb.com/search/SpecificMaterial.asp?bassnum=MS0001>, 2006.
53. Harper, C. A., Handbook of Building Materials for Fire Protection, McGraw Hill, New York 2004.

APPENDIX A HUB CASTING SHOP DRAWING NOTES [43]

PAGE & PARAGRAPH # FROM ASTM STD IS BELOW	ITEM #		29592.14501	29592.14501
	DESCRIPTION		Track Chair	Center Pivot
N/A	ASTM SPECIFICATION	STD #	A27	A27
1.2.4		GRADE	70-36	65-35
1.2.5		CLASS	I	I
N/A	QUANTITY	VOLUME (M ³)	0.34	1.47334
		DENSITY (Kn/M ³)	77	77
		APPROX. WT (Kn)	26.1813	113.4475
		QUANTITY REQ'D	16	1
A27 SPECS				
1.2.4, 5.1	HEAT TREATMENT	YES OR NO	YES	YES
5.1		PROCEDURE	Manufacturer determines heat treatment parameters to obtain material properties	
6.1	CHEMICAL COMPOSITION	YES OR NO	YES PER A781 5.2	YES PER A781 5.2
6.1		REQUIREMENTS	PER A27 TABLE 1	PER A27 TABLE 1
N/A		AT MILL/BY MILL	AT MILL	AT MILL
N/A		PAID BY/DONE BY	BY CONTRACTOR	BY CONTRACTOR
7.1	TENSILE TESTS	YES OR NO	YES	YES
		REQUIREMENTS	PER A27 TABLE 2	PER A27 TABLE 2
		MIN TENSILE	70 ksi	65 ksi
		MIN YEILD	36 ksi	35 ksi
		MIN ELONGATION	22% / 2"	24% / 2"
		MIN RED. OF AREA	30%	35%
		FREQUENCY OR QUANTITY	1/HEAT	1/HEAT
PAID BY/DONE BY	BY CONTRACTOR	BY CONTRACTOR		
7.2, 7.3	TEST BAR OR COUPON SEE NOTE 7	WHICH ONE	COUPONS CAST INTEGRALLY	COUPONS CAST INTEGRALLY
A781 FIG 1		SIZE SPECS	PER MFR	PER MFR
A370 FIG 4&5		MACHINED DIMS.	PER MFR	PER MFR
7.7	PREPARE PER A732 S3.2	YES OR NO	ONLY IF INVEST. CAST	ONLY IF INVEST. CAST
9	REWORK/RETREA TMENT		SEE NOTE (1)	SEE NOTE (1)
	REPAIRS		SEE NOTES (1), (4)	SEE NOTES (1), (4)
S51	DIMENSIONAL TOLERANCES		PER A27 TABLE 3	PER A27 TABLE 4
A781 SPECS.				
4.1	MELTING PROCESS	(SECTION 4.1)	PER A781 4.1	PER A781 4.1
4.2	HEAT TREATMENT	(SECTION 4.2)	PER A781 4.2	PER A781 4.2
5	CHEMICAL COMPOSITION	(SECTION 5)	PER A781 5.1 AND 5.2	PER A781 5.1 AND 5.3
6	MECHANICAL TESTING	(SECTION 6)	PER A27	PER A28
7	WORKMANSHIP/FI NISH	(SECTION 7)	PER A781 #7	PER A781 #8
8	QUALITY	(SECTION 8)	PER A781 SECTION 8, ALSO SEE NOTES (2) & (4)	PER A781 SECTION 8, ALSO SEE NOTES (2) & (4)
9	REPAIR	(SECTION 9)	PER A488 ALSO SEE NOTES	PER A488 ALSO SEE NOTES
10	INSPECTION	(SECTION 10)	PER A781 #10	PER A781 #10
11	REJECTION	(SECTION 11)	PER A781 #11	PER A781 #11
S1	MAGNETIC PARTICLE INSP.	YES OR NO	YES	YES
		EXTENT OF EXAMINATION	100% PRIOR TO HEAT, TREAT & WELD AREA AFTER REPAIR	b
		BASIS FOR ACCEPTANCE	SEE NOTE (4b)	SEE NOTE (4b)
		PAID BY/DONE BY	CONTRACTOR	CONTRACTOR
S2	RADIOGRAPHIC EXAM	YES OR NO	NO	NO
		PAID BY/DONE BY	CONTRACTOR	CONTRACTOR
S3	LIQUID PENETRANT EXAM	YES OR NO	NO	NO
		PAID BY/DONE BY	N/A	N/A

PAGE & PARAGRAPH # FROM ASTM STD IS BELOW	ITEM #		29592.14501	29592.14501
	DESCRIPTION		Track Chair	Center Pivot
S4	ULTRASONIC EXAMINATION	YES OR NO	YES, ASTM A609, METHOD A	YES, ASTM A609, METHOD A
		EXTENT OF EXAMINATION	SEE NOTE (4C)	SEE NOTE (4C)
		BASIS FOR ACCEPTANCE	QUALITY LEVEL 1 ALSO SEE NOTE (4C)	QUALITY LEVEL 2 ALSO SEE NOTE (4C)
		PAID BY/DONE BY	BY CONTRACTOR - NOTE 3	BY CONTRACTOR - NOTE 4
S5	EXAMINATION OF WELD PREP.	YES OR NO	SEE NOTE (1)	SEE NOTE (1)
		PAID BY/DONE BY	N/A	N/A
S6	CERTIFICATION	YES OR NO	YES	YES
		PAID BY/DONE BY	BY CONTRACTOR	BY CONTRACTOR
S7	PROIR APPROV. OF ALL WELD REPAIRS	YES OR NO	YES, SEE NOTE (1)	YES, SEE NOTE (1)
		PAID BY/DONE BY	BY CONTRACTOR	BY CONTRACTOR
S8	MARKING	YES OR NO	LOW STRESS ROUNDED STAMPS MAY BE APPLIED OR CAST INTEGRALLY IN NON-MACHINED AREA IF DESIRED BY CONTRACTOR, WITH APPROVAL	LOW STRESS ROUNDED STAMPS MAY BE APPLIED OR CAST INTEGRALLY IN NON-MACHINED AREA IF DESIRED BY CONTRACTOR, WITH APPROVAL
		PAID BY/DONE BY	N/A	N/A
S9	CHARPY IMPACT TEST	YES OR NO	NO	NO
		PAID BY/DONE BY	N/A	N/A
S10	HARDNESS TEST	YES OR NO	NO	NO
		PAID BY/DONE BY	N/A	N/A
S11	FERRITE CONTENT RANGE	YES OR NO	NO	NO
		PAID BY/DONE BY	N/A	N/A
S12	TEST REPORT	YES OR NO	YES	YES
		PAID BY/DONE BY	BY CONTRACTOR	BY CONTRACTOR
S13	UNSPECIFIED ELEMENTS	YES OR NO	NO	NO
		PAID BY/DONE BY	N/A	N/A
S14	TENSION TEST FROM CASTING	YES OR NO	NO	NO
		PAID BY/DONE BY	N/A	N/A
S15	ALTERNATE TEST BLOCKS	YES OR NO	NO	NO
		PAID BY/DONE BY	N/A	N/A
S16	WELD REPAIR CHARTS	YES OR NO	YES, SEE NOTE (1)	YES, SEE NOTE (1)
		PAID BY/DONE BY	N/A	N/A
S17	MACROETCH TEST	YES OR NO	NO	NO
		PAID BY/DONE BY	N/A	N/A
S18	HIPing	YES OR NO	NO	NO
		PAID BY/DONE BY	N/A	N/A
S19	CLEANING OF SST	YES OR NO	N/A	N/A
		PAID BY/DONE BY	N/A	N/A
S20	HEAT TREATMENT IN WORKING ZONE OF SURVEYED FURNACE	YES OR NO	NO	NO
		PAID BY/DONE BY	N/A	N/A
A802/802M Specs.				
A802M 2.1.10	Visual Inspection Criteria	A - Surface Texture	A4	A3
2.1.8		B - Non-Metallic Inclusions	B4	B3 Bottom/B2 All Other Surfaces
2.1.4		C - Gas Porosity	C2 Painted Areas/ C3 Bottom Surface	C2
2.1.3.2		D - Laps & Cold Shunts	D2	D2
2.1.1.3		E - Scabs	E3	E1
2.1.5		F - Inserts	F2	F2
1.2		G - Thermal Dressing	G2	G2
1.2		H - Mechanical Dressing	H4 on Bottom / H3 on Exposed Surface	H3
2.1.11		J - Welds	J2 As-Cast/ J3 Bottom Surface	J2

NOTES																		
<p>1.) Contract to Provide WPS and PQR documentation prior to Fabrication.</p> <p>All welds listed below are to be submitted to the Engineer through a weld repair map. Defects shall first be cleaned out to solid metal. Solid metal shall be verified by magnetic particle inspection. Any castings which have been welded without the Engineer's permission will not be accepted.</p>																		
<p>1a) Process Welding (welding done prior to final heat treatment) requires prior APPROVAL from the Engineer when:</p> <ul style="list-style-type: none"> - On the TRACT CHAIR and machined areas of the CENTER PIVOT, the depth of the cavity prepared for welding exceeds 25% of the actual wall thickness or when the extent of the cavity exceeds approximately 10 in² - On the CENTER PIVOT as-cast areas, including the ribs and the area below them, the depth of the cavity prepared for welding exceeds 25% of the actual wall thickness or when the extent of the cavity exceeds approximately 25 in² <p>Final heat treatment shall not be performed until major weld repairs are complete.</p>																		
<p>1b) Repair Welding (welding done after final heat treatment) of castings is permitted only by written permission of the Engineer. Prior to any welding being performed, the Contractor shall submit for Review and Approval the proposed weld repair charts. Any weld repair performed after heat treatment, as Approved by the Engineer, shall be stress-relieved after welding.</p>																		
<p>2) Per Specification "General Specifications for Bridge Machinery" section 2.0.C.1: "All castings shall be free of cracks, cold shunts, shrink holes, blow holes, and porosity" in machined areas, and 2.0.C.2 "All castings shall be cleaned free of loose scale and sand, fins, seams, gates, risers and other irregularities [as directed by the Engineer]. All unfinished edges of castings shall be neatly cast [or ground] with rounded corners, and all inside angles shall have ample fillets."</p>																		
<p>3) Ultrasonic Examination will aid the contractor in determining the suitability of casting prior to machining</p>																		
<p>4) Defects in the casting shall be determined as follows:</p> <ul style="list-style-type: none"> a. Visual examination and based on the criteria listed in the chart. b. Magnetic Particle Examination on all surfaces in accordance with ASTM E125, meeting the following acceptable levels of discontinuities: <table style="margin-left: 40px; border-collapse: collapse;"> <tr> <td style="padding-right: 20px;">Type I</td> <td style="padding-right: 20px;">Cracks/Hot Tears</td> <td>1/4-inch max</td> </tr> <tr> <td>Type II</td> <td>Shrinkage</td> <td>Degree 3</td> </tr> <tr> <td>Type III</td> <td>Inclusions</td> <td>Degree 3</td> </tr> <tr> <td>Type IV</td> <td>Chaplets</td> <td>Degree 2</td> </tr> <tr> <td>Type V</td> <td>Porosity</td> <td>Degree 1</td> </tr> <tr> <td colspan="3">All Flaws in areas to be machined, if not rejected, shall be repaired</td> </tr> </table>	Type I	Cracks/Hot Tears	1/4-inch max	Type II	Shrinkage	Degree 3	Type III	Inclusions	Degree 3	Type IV	Chaplets	Degree 2	Type V	Porosity	Degree 1	All Flaws in areas to be machined, if not rejected, shall be repaired		
Type I	Cracks/Hot Tears	1/4-inch max																
Type II	Shrinkage	Degree 3																
Type III	Inclusions	Degree 3																
Type IV	Chaplets	Degree 2																
Type V	Porosity	Degree 1																
All Flaws in areas to be machined, if not rejected, shall be repaired																		
<ul style="list-style-type: none"> c. Ultrasonic Inspection conforming to ASTM A609 shall be performed on all castings. <ul style="list-style-type: none"> - TRACK CHAIR castings will be UT inspected to Quality Level 1 where possible (areas identified on Shop Drawings) - Center Pivot casting will be UT inspected to Quality Level 2 where possible (areas identified on Shop Drawings) 																		
<ul style="list-style-type: none"> d. Any flaws exposed during machining shall be reported to the Engineer for Approval to repair by welding, blend by grinding or allow as-is. <p>Minor defects shall be defined as any defect that, in the opinion of the Engineer, does not affect the strength of the casting or function of the casting if repaired, and less than 1 square inch in area and 1/8 inch deep in the material that will be left after machining.</p> <p>Major defects shall be defined as any defect that exceeds the dimension for minor defects as noted above, or which, in the opinion of the Engineer, will affect the strength or function of the casting.</p>																		
<p>5) "The MAP table presented herein is not intended to supercede the project specifications. It is a guideline to assess the level of testing effort. The plans and specifications shall govern the criteria for final acceptance of any procedure, material or fabrication."</p>																		
<p>6) <u>The Engineer reserves the Right to perform independent Nondestructive Testing of the castings at any time.</u></p>																		
<p>7) Test bars shall be cast integrally and removed mechanically after heat treatment. No removal by torch or other method that may change properties will be permitted. If coupon is not cast integrally, it is the contractor's responsibility to have the coupon heat treated with the casting it came from. If coupon is not heat treated with casting, that shall be grounds for rejection of the casting.</p>																		

APPENDIX B SAMPLE CALCULATIONS

Preliminary Bascule Hub Assembly Design Tool

*This MathCAD Version 2000 worksheet is intended to assist in developing a **preliminary** design of bascule trunnion hub assembly using simplified assumptions. Typical material properties are assumed. The overall process is as follows:*

- 1. Before using this worksheet, determine the maximum trunnion reaction. This must be determined using the expected live load, dead load, wind load, impact, and any special operational requirements, such as during maintenance.*
- 2. Enter the trunnion load and distance from the centerline trunnion bearing to the centerline girder.*
- 3. All other dimensions are computed based on these two input assuming typical materials.*
- 4. Design equations referred below are from AASHTO LRFD Movable Highway Bridge Design Specifications, First Edition 2000.*
- 5. To account for possibility of bearing seizing, the torsional load is increased by factor 2, and the shrink fit as well as dowels are designed to resist the additional torsion. The bearing must be designed so that the screws mounting the bronze bushing to bearing house shear off before the torsion capacity of the trunnion-hub interface, and hub-girder interface (bolted joint) is exceeded.*

Define Units

$$\text{kip} := 1000 \cdot \text{lbf}$$

$$\text{ksi} := \frac{\text{kip}}{\text{in}^2}$$

$$\text{MPa} := 10^6 \cdot \text{Pa}$$

Minimum Inputs

$$V := 670.5 \cdot \text{kip} \quad \text{Trunnion reaction (per main girder)}$$

$$L := \left(19.25 + \frac{73.5}{2} - \frac{60}{2} \right) \cdot \text{in} \quad \text{Distance between bearing and load (to compute moment arm)}$$

$$\text{Fit} := \text{"FN2"} \quad \text{Desired fit between trunnion-hub}$$

$$T_{\text{amp_rat}} := 2 \quad \text{Amplify the torsion for bearing seizure case}$$

$$C_{\text{CP}} := 1.3 \quad \text{Factor for contact pressure data obtained from FEA}$$

$$N_{\text{H}} := 2 \quad \text{Number of hubs per trunnion (2 for box girders, 1 otherwise)}$$

Trunnion Design

Loads

$$M_a := V \cdot L$$

$$M_a = 1452.75 \text{ kip} \cdot \text{ft}$$

Materials

Assumes typical A668 Class D Material (see Table 6.6.1-1)

$$\sigma_{ut_ksi} := 95 \cdot \text{ksi}$$

$$\sigma_{ut} := \frac{\sigma_{ut_ksi}}{\text{MPa}} \quad \sigma_{ut} = 655.002 \quad \text{Used for endurance limit computations}$$

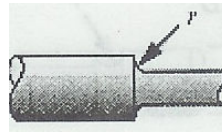
$$\sigma_{yt_ksi} := 70 \cdot \text{ksi}$$

$$\sigma_{yt} := \frac{\sigma_{yt_ksi}}{\text{MPa}} \quad \sigma_{yt} = 482.633 \quad \text{Used for endurance limit computations}$$

$$\tau_a := 52 \cdot \text{MPa}$$

Geometry

$$r_{rat} := \frac{1}{40}$$



Ratio of fillet radius to trunnion diameter (see Figure)

$$D_{ratTB} := 1$$

Ratio of bearing diameter to trunnion diameter. Used for computing torque acting on trunnion

$$T_{rat} := 0.18$$

Friction factor at the bearing for lubricated plain bearing. (Table 5.8.2-1). Used to compute torsion acting on trunnion

$$d_{bore_rat} := 0.2$$

Ratio used to compute bore (20% of diameter per 6.7.4.1)

$$d_{step_rat} := 1.2$$

Ratio used to compute diameter at step

➔ Reference: C:\Bascule\TrunnionFatigue.mcd(R)

Diameter Based on Shear

$$D_s := 1 \cdot \text{mm}$$

Given

$$\tau_a = \frac{V}{\pi \cdot \frac{D_s^2 - (d_{\text{bore_rat}} \cdot D_s)^2}{4}}$$

$$D_s := \text{Find}(D_s) \quad D_s = 10.859 \text{ in}$$

Fatigue Limit Requirement

$$F_{\text{Fatig}}(D, d, d_{\text{bore}}, r, \sigma_{\text{ut}}, \sigma_{\text{yt}}, M_a, T_m) := \begin{cases} I \leftarrow \pi \cdot \frac{(D^4 - d_{\text{bore}}^4)}{64} \\ s \leftarrow \frac{I}{\frac{D}{2}} \\ K_F \leftarrow K_F(D, d, r, \sigma_{\text{ut}}) \\ K_{FS} \leftarrow K_{FS}(D, d, r, \sigma_{\text{ut}}) \\ \frac{1}{s} \cdot \left(\frac{K_F \cdot M_a}{\sigma_e(D, \sigma_{\text{ut}})} + \frac{\sqrt{3} \cdot K_{FS} \cdot T_m}{2 \cdot \sigma_{\text{yt}}} \right) \cdot \frac{1}{\text{MPa}} - 1 \end{cases}$$

Computed Trunnion Geometry

$$D_F := 10 \cdot \text{mm} \quad \text{Arbitrary guess value}$$

$$D_F := \text{root}(F_{\text{Fatig}}(D_F \cdot d_{\text{step_rat}}, D_F, d_{\text{bore_rat}} \cdot D_F, r_{\text{rat}} \cdot D_F, \sigma_{\text{ut}}, \sigma_{\text{yt}}, M_a, T_{\text{rat}} \cdot V \cdot D_{\text{ratTB}} \cdot 0.5), D_F)$$

$$D_F = 21.152 \text{ in}$$

$$D := \max(D_s, D_F) \quad \boxed{D = 21.152 \text{ in}} \quad \text{Trunnion diameter, higher of shear \& fatigue}$$

$$D_{\text{step}} := d_{\text{step_rat}} \cdot D \quad \boxed{D_{\text{step}} = 25.383 \text{ in}} \quad \text{Step diameter}$$

$$r := r_{\text{rat}} \cdot D \quad \boxed{r = 0.529 \text{ in}} \quad \text{Fillet radius at steps}$$

$$D_{\text{bore}} := d_{\text{bore_rat}} \cdot D \quad \boxed{D_{\text{bore}} = 4.23 \text{ in}} \quad \text{Trunnion bore diameter}$$

$$D_{\text{TB}} := D_{\text{ratTB}} \cdot D \quad \boxed{D_{\text{TB}} = 21.152 \text{ in}} \quad \text{Assumed trunnion bearing diameter (used to compute torsion)}$$

Information useful for checking

$$\sigma_e(D, \sigma_{ut}) \cdot \frac{\text{MPa}}{\text{ksi}} = 23.746$$

Endurance limit (ksi)

$$K_F(D_{\text{step}}, D, r, \sigma_{ut}) = 2.071$$

Fatigue stress concentration factor for bending

$$K_{FS}(D_{\text{step}}, D, r, \sigma_{ut}) = 1.782$$

Fatigue stress concentration factor for torsion

Hub Design

Loads

$$V_H := \frac{V}{N_H} \quad \text{Load per hub}$$

$$V_H = 335.25 \text{ kip}$$

$$T := T_{\text{amp_rat}} \cdot T_{\text{rat}} \cdot V_H \cdot \frac{D_{\text{TB}}}{2} \quad \text{Torsion on hub}$$

$$T = 106.369 \text{ kip} \cdot \text{ft}$$

$$P := 0.15 \cdot V_H \quad \text{Axial force on hub}$$

$$P = 50.287 \text{ kip}$$

Material

Hub assumed to be made of A148 Gr 620-415 (see Table 6.6.1-1)

$$\sigma_{a_b} := 145 \cdot \text{MPa} \quad \text{Allowable bearing stress} \quad \sigma_{a_b} = 21.03 \text{ ksi}$$

$$\sigma_{a_t} := 103 \cdot \text{MPa} \quad \text{Allowable tensile stress} \quad \sigma_{a_t} = 14.939 \text{ ksi}$$

$$\tau_a := 52 \cdot \text{MPa} \quad \text{Allowable shear} \quad \tau_a = 7.542 \text{ ksi}$$

$$\mu := 0.33 \quad \text{Friction between Trunnion and Hub}$$

$$E := 29000 \cdot \text{ksi} \quad \text{Modulus of elasticity}$$

 Reference: C:\Bascule\ShrinkFit.mcd(R)

Hub Thickness & Length

Compute optimal length based on allowable bearing. Note allowable bearing stress for trunnion and hub is same (ASTM A668 CL D and ASTM A148 Gr 620-415)

$$L_{\text{Hb}} := 1 \cdot \text{mm}$$

Given

$$\sigma_{a_b} = \frac{V_H}{D_{\text{TB}} \cdot L_{\text{Hb}}}$$

$$L_{\text{Hb}} := \text{Find}(L_{\text{Hb}}) \quad L_{\text{Hb}} = 0.754 \text{ in} \quad \text{This is the hub length required to satisfy bearing stress requirements}$$

Compute required pressure to resist axial and torsional load

$$F_R := \sqrt{P^2 + \left(\frac{T}{D_{TB} \cdot 0.5}\right)^2} \quad \text{Resultant}$$

$$F_R = 130.748 \text{ kip}$$

$$F_{N\text{reqd}} := \frac{F_R}{\mu} \quad F_{N\text{reqd}} = 396.205 \text{ kip} \quad \text{Required normal force at trunnion-hub.}$$

$$C_{\text{PresReqdTorsion}} := \frac{F_{N\text{reqd}}}{(1 \cdot \text{in} \cdot D_{TB} \cdot \pi)} \quad C_{\text{PresReqdTorsion}} = 5.962 \text{ ksi} \quad \text{for 1 inch of hub length}$$

Check for minimum contact pressure to avoid separation

$$\Delta C_{\text{PressDATA}} :=$$

10	-0.0241
11	-0.0226
12	-0.0201
13	-0.0186
14	-0.0172
15	-0.0153

Table provides relationship between trunnion radius(in) and reduction in contact pressure per unit applied load (kip) per unit hub thickness (inch) from FEA results. Bump up this number by factor C_{CP} to ensure sufficient factor safety

$$\Delta C_{\text{pres}} := -\text{linterp}\left(\Delta C_{\text{PressDATA}}^{\langle 0 \rangle}, \Delta C_{\text{PressDATA}}^{\langle 1 \rangle}, \frac{D_{TB}}{2 \cdot \text{in}}\right) \cdot \text{ksi} \quad \Delta C_{\text{pres}} = 0.023 \text{ ksi}$$

$$C_{\text{PresReqdNoSeparation}} := C_{CP} \cdot \Delta C_{\text{pres}} \cdot \frac{V_H}{\text{kip}}$$

$$C_{\text{PresReqdNoSeparation}} = 10.122 \text{ ksi} \quad \text{This is for 1 inch of hub length. Factor } C_{cp} \text{ for safety}$$

$$C_{\text{PresReqd}} := \max(C_{\text{PresReqdTorsion}}, C_{\text{PresReqdNoSeparation}}) \quad C_{\text{PresReqd}} = 10.122 \text{ ksi}$$

Note the contact pressure is computed for 1 inch of hub length. This pressure is divided by the true hub length in the next section while computing the optimal hub-length that meets all functional requirements

Find out limits of interference for specified fit

$$\begin{pmatrix} \delta_{D\text{min}} \\ \delta_{D\text{max}} \end{pmatrix} := \delta_{\text{Range}}\left(\frac{D_{TB}}{\text{in}}, \text{Fit}\right) \cdot 10^{-3} \cdot \text{in} \quad \delta_{D\text{min}} = 0.009 \text{ in}$$

$$\delta_{D\text{max}} = 0.014 \text{ in}$$

Determine the hub outer diameter and hub length that meets the following requirements

1. Bearing stress at hub-trunnion interface within allowable.
2. Hoop stress in the hub within allowable.
3. Hub outer diameter with 1.4 D and 1.8 D (D is trunnion bore)
4. Shrink fit contact pressure sufficient to resist torsion & axial load.
5. Shrink fit contact pressure sufficient to prevent separation of parts under applied load.
6. Interference with specified limits.

The dimensions are optimized arbitrarily by minimizing the sum of hub outer radius and hub length.

Items used by function that computes shrink-fit stresses

$$R_{in} := \frac{D_{bore}}{2} \quad R_{in} = 2.115 \text{ in}$$

$$R_{mid} := \frac{D_{TB}}{2} \quad R_{mid} = 10.576 \text{ in}$$

$$f_{Min}(R_{out}, L_{Hsf}) := R_{out} + L_{Hsf} \quad \text{Function to minimize, change to product or any other suitable form if there is problem minimizing this}$$

$$R_{out} := D_{TB} \quad L_{Hsf} := L_{Hb} \quad \text{Arbitrary guess values}$$

Given

$$\frac{C_{PresReqd}}{\frac{L_{Hsf}}{in}} \leq P_{ShrinkFit}\left(R_{out}, R_{mid}, R_{in}, E, \frac{\delta_{Dmin}}{2}\right) \quad \text{Min. contact pressure reqmt.}$$

$$\sigma_{a_t} \geq \sigma_{\theta} \text{ShrinkFit}\left(R_{out}, R_{mid}, R_{in}, E, \frac{\delta_{Dmax}}{2}\right) \quad \text{Hoop stress requirement}$$

$$R_{out} \leq 0.9 \cdot D_{TB} \quad \text{Preferred size guidelines (based on current data that these work)}$$

$$R_{out} \geq 0.7 \cdot D_{TB}$$

$$L_{Hsf} \geq L_{Hb} \quad \text{Bearing stress}$$

$$\begin{pmatrix} R_{out} \\ L_{Hsf} \end{pmatrix} := \text{Minimize}(f_{Min}, R_{out}, L_{Hsf})$$

$$D_H := 2 \cdot R_{out} \quad \boxed{D_H = 29.613 \text{ in}} \quad \frac{D_H}{D_{TB}} = 1.4 \quad \text{Hub outer diameter}$$

$$\boxed{L_{Hsf} = 3.418 \text{ in}} \quad \text{Hub Length}$$

$$L_H := \max\left(L_{Hsf}, \frac{0.8 \cdot D_{TB}}{N_H}\right) \quad \frac{L_H}{D_{TB}} = 0.4 \quad \text{Here the minimum hub length is set to be 0.8 times the bore diameter for simple & overhang trunnion & half that for box girders}$$

$$L_H = 8.461 \text{ in}$$

Items useful for checking

$$\sigma_{\text{hoop}} := \sigma_{\theta} \text{ShrinkFit} \left(R_{\text{out}}, R_{\text{mid}}, R_{\text{in}}, E, \frac{\delta_{\text{Dmax}}}{2} \right) \quad \sigma_{\text{hoop}} = 14.204 \text{ ksi}$$

$$\sigma_{\text{radial}} := P \text{ShrinkFit} \left(R_{\text{out}}, R_{\text{mid}}, R_{\text{in}}, E, \frac{\delta_{\text{Dmin}}}{2} \right) \quad \sigma_{\text{radial}} = 2.961 \text{ ksi}$$

Hub Flange Outer Diameter

This is based on the bolting requirements. Assume minimum bolt size

$$\sigma_{\text{tbolt}} := 105 \cdot \text{ksi}$$

$$\tau_{\text{bolt}} := \frac{\sigma_{\text{tbolt}}}{6}$$

*Assuming A449 bolts, with factor of safety of 3
(see Section 6.6.1)*

$$N_{\text{ribs}} := 6$$

Number of ribs (6 or 8)

$$T_{\text{ribs}} := 2 \cdot \text{in}$$

Typical rib thickness

$$d_{\text{bolt}} := 1.25 \cdot \text{in}$$

Bolt diameter

$$A_{\text{BoltData}} :=$$

1.000 · 10 ⁰	6.060 · 10 ⁻¹
1.250 · 10 ⁰	9.690 · 10 ⁻¹
1.500 · 10 ⁰	1.405 · 10 ⁰

Tensile stress area of bolts. Will work for 1, 1.25 and 1.5 inch dia bolts

$$A_{\text{Tbolt}} := \text{linterp}\left(A_{\text{BoltData}}^{\langle 0 \rangle}, A_{\text{BoltData}}^{\langle 1 \rangle}, \frac{d_{\text{bolt}}}{\text{in}}\right) \cdot \text{in}^2$$

$$A_{\text{Tbolt}} = 0.969 \text{ in}^2$$

Based on torsion & shear

$$d_{\text{bolt_circle}} := D_{\text{H}} + 1.4 \cdot d_{\text{bolt}}$$

*Not accounted for taper of hub
and fillet at the edge here.*

$$A_{\text{bolt}} := \pi \cdot \frac{d_{\text{bolt}}^2}{4}$$

Area assuming no thread in shear plane

$$F_{\text{per_bolt}} := A_{\text{bolt}} \cdot \tau_{\text{bolt}}$$

$$F_{\text{per_bolt}} = 21.476 \text{ kip}$$

$$F_{\text{bolt_reqdT}} := \frac{T}{d_{\text{bolt_circle}}}$$

$$F_{\text{bolt_reqdT}} = 40.698 \text{ kip}$$

*Two shear planes, so divided by
diameter instead of radius*

$$F_{\text{bolt_reqdV}} := \frac{V_{\text{H}}}{2}$$

Based on two shear planes

$$F_{\text{bolt_reqdTotal}} := F_{\text{bolt_reqdV}} + F_{\text{bolt_reqdT}}$$

*Conservative to add instead of vector addition
of all components along bolt circle*

$$N_{\text{boltTV}} := \text{ceil}\left(\frac{F_{\text{bolt_reqdTotal}}}{F_{\text{per_bolt}}}\right)$$

$$N_{\text{boltTV}} = 10 \quad \text{No. bolts}$$

Based on slip critical connection

$K_s := 0.33$

Surface factor (0.33 or 0.5)

$K_h := 1$

Hole factor = 1 for standard holes

$N_s := 2$

No. slip planes

$$BT_V := \frac{V_H}{2 \cdot K_s \cdot K_h \cdot N_s}$$

$BT_V = 253.977 \text{ kip}$

Bolt Tension to resist Shear

$$BT_T := \frac{\left(\frac{T}{0.5 \cdot d_{\text{bolt_circle}}} \right)}{(2 \cdot K_s \cdot K_h \cdot N_s)}$$

$BT_T = 61.664 \text{ kip}$

Bolt Tension to resist torsion

$BT_{BRF} := 0.2 \cdot BT_V$

$BT_{BRF} = 50.795 \text{ kip}$

Force to overcome backing ring friction. Arbitrarily assume 20% of V

$BT_{Total} := BT_V + BT_T + BT_{BRF}$

$BT_{Total} = 366.437 \text{ kip}$

$$N_{\text{boltSC}} := \text{ceil} \left(\frac{BT_{Total}}{0.7 \cdot 0.76 \cdot \sigma_{\text{tbolt}} \cdot A_{\text{Tbolt}}} \right)$$

$N_{\text{boltSC}} = 7$

$N_{\text{bolt}} := \max(N_{\text{boltTV}}, N_{\text{boltSC}})$

$\text{Circumbolt_reqd} := N_{\text{bolt}} \cdot 3 \cdot d_{\text{bolt}} + N_{\text{ribs}} \cdot T_{\text{ribs}}$

$\text{Circumbolt_avail} := \pi \cdot d_{\text{bolt_circle}}$

$$N_{\text{circles}} := \text{ceil} \left(\frac{\text{Circumbolt_reqd}}{\text{Circumbolt_avail}} \right)$$

$N_{\text{circles}} = 1$

No. bolt circles

$D_{\text{FlangeBolt}} := D_H + 3 \cdot d_{\text{bolt}} \cdot N_{\text{circles}}$

$D_{\text{FlangeBolt}} = 33.363 \text{ in}$

$D_F := \max(D_{\text{FlangeBolt}}, 1.4 \cdot D_H)$

The minimum flange outer diameter is set arbitrarily to 1.4 times the hub diameter to maintain similar proportions to existing hubs

$D_F = 41.458 \text{ in}$

Flange outer diameter

Determine how many bolts can fit in the bolt circle

$$N_{\text{boltFinal}} := \text{floor} \left[\frac{(\text{Circum}_{\text{bolt_avail}} - N_{\text{ribs}} \cdot T_{\text{ribs}})}{3 \cdot d_{\text{bolt}}} \right]$$

$$N_{\text{boltFinal}} = 23$$

Hub Flange Thickness

Conservatively check for flange bending assuming it to be a simply supported beam between two ribs with uniformly distributed axial load. This is highly conservative analysis meant to show that minimum flange thickness as required by castability constraint generally governs (if not refine the analysis)

$$L_B := \pi \cdot \frac{D_F}{N_{\text{ribs}}}$$

$$w_B := \frac{P}{N_{\text{ribs}} \cdot L_B}$$

$$T_{Fb} := 1 \cdot \text{mm}$$

Given

$$\sigma_{a_t} = \frac{\left[\frac{(w_B \cdot L_B^2)}{8} \cdot \frac{T_{Fb}}{2} \right]}{\left(L_B \cdot \frac{T_{Fb}^3}{12} \right)}$$

$$T_{Fb} := \text{Find}(T_{Fb})$$

$$T_{Fb} = 0.649 \text{ in}$$

Determine flange thickness based on resistance to torsion at root of the flange

$$T_{Ft} := 1 \cdot \text{mm}$$

Given

$$\tau_a \cdot (\pi \cdot D_H \cdot T_{Ft}) = \frac{T}{\left(\frac{D_H}{2} \right)}$$

$$T_{Ft} := \text{Find}(T_{Ft})$$

$$T_{Ft} = 0.123 \text{ in}$$

$$T_F := \max(T_{Fb}, T_{Ft}, 1.5 \cdot \text{in})$$

Pick highest of shear, bending or castability requirement

$$T_F = 1.5 \text{ in}$$

Check bolt bearing

$$\sigma_{bb} := \frac{(F_{\text{bolt_reqdT}} + V_H)}{T_F \cdot d_{\text{bolt}} \cdot N_{\text{boltFinal}}} \quad \sigma_{bb} = 8.718 \text{ ksi}$$

"BEARING STRESS OK" if $\sigma_{bb} < \sigma_{a_b}$ = "BEARING STRESS OK"
 "BEARING STRESS NO GOOD" otherwise

If bearing stress is exceeded, it is recommended the number of bolts be increased in the final design.

Rib Thickness

Axial load must be resisted by flange bending and shear and rib shear. Assume 100% axial load must be resisted by rib shearing (discount flange cross-section). This is extremely conservative, but generally castability will govern in any case. Refine analysis if required.

$$T_G := T_F$$

Conservatively assume girder thickness = flange thickness

$$L_R := \frac{L_H}{2} - \frac{T_G}{2} - T_F \quad \text{Length of ribs}$$

$$L_R = 1.98 \text{ in}$$

$$T_{RS} := 1 \cdot \text{mm} \quad \text{Arbitrary guess}$$

Given

$$\tau_a = \frac{P}{N_{\text{ribs}} \cdot L_R \cdot T_{RS}}$$

$$T_{RS} := \text{Find}(T_{RS})$$

$$T_{RS} = 0.561 \text{ in}$$

$$T_{RS} := \max(T_{RS}, 1.5 \cdot \text{in}) \quad \text{Minimum dimension of 1.5" based on castability requirements.}$$

$$T_{RS} = 1.5 \text{ in}$$

Dowels

$$F_{\text{Dowel}_T} := \frac{T}{\frac{D}{2}}$$

$$F_{\text{Dowel}_T} = 120.69 \text{ kip}$$

$$F_{\text{Dowel}_A} := P \cdot 1$$

$$F_{\text{Dowel}_\text{Total}} := \sqrt{F_{\text{Dowel}_A}^2 + F_{\text{Dowel}_T}^2}$$

$$\tau_{a_dowel} := 440 \cdot \frac{\text{MPa}}{3}$$

Assume unhardened ASTM 108 Grade 1040 with 440 MPa shear strength, factor safety 3

$$\tau_{a_dowel} = 21.272 \text{ ksi}$$

$$A_{\text{dowel}} := \frac{F_{\text{Dowel}_\text{Total}}}{\tau_{a_dowel}}$$

$$A_{\text{dowel}} = 6.146 \text{ in}^2$$

$$N_{\text{dowel}} := 2$$

$$d_{\text{dowel}} := 1 \cdot \text{mm}$$

Given

$$N_{\text{dowel}} \cdot \pi \frac{d_{\text{dowel}}^2}{4} = A_{\text{dowel}}$$

$$d_{\text{dowel}} := \text{Find}(d_{\text{dowel}})$$

$$d_{\text{dowel}} = 1.978 \text{ in}$$

If diameter is too high, increase the number of dowels to 3

$$L_{\text{dowel}_b} := 1 \cdot \text{mm}$$

Arbitrary guess value

Given

$$\sigma_{a_b} = \frac{F_{\text{Dowel}_\text{Total}}}{(N_{\text{dowel}} \cdot L_{\text{dowel}_b} \cdot d_{\text{dowel}})}$$

$$L_{\text{dowel}_b} := \text{Find}(L_{\text{dowel}_b})$$

$$L_{\text{dowel}_b} = 1.571 \text{ in}$$

$$L_{\text{dowel}} := \begin{cases} L_{\text{dowel}_b} & \text{if } L_{\text{dowel}_b} \geq 2 \cdot d_{\text{dowel}} \\ (2 \cdot d_{\text{dowel}}) & \text{otherwise} \end{cases}$$

$$L_{\text{dowel}} = 3.956 \text{ in}$$

Note: In addition to bearing due to torsion, there will be bearing due to contact pressure from the shrink fit. The general rule of thumb is to provide 1.5 to 2 times the dowel diameter as the length.

Backing Ring

Note: Bolt bearing case is not checked since the check is similar to that for the hub flange

$$T_{BRf} := 1.3 \cdot T_F$$

Bearing on hub. It was shown using FEA that the backing ring carries less than 50% of the net shear. However, conservatively assume entire load acts through the backing ring

$$T_{BRb} := 1 \cdot \text{mm}$$

Given

$$\sigma_{a_b} = \frac{V}{T_{BRb} \cdot D_H}$$

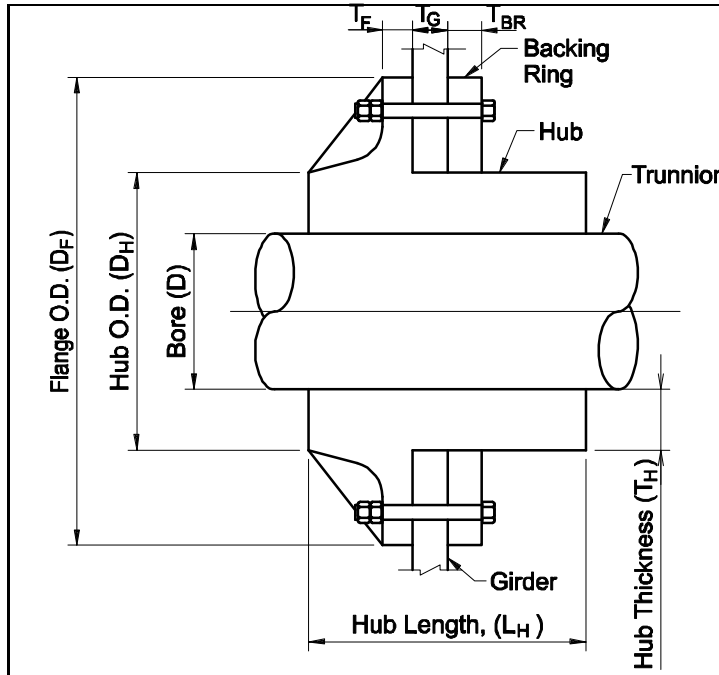
$$T_{BRb} := \text{Find}(T_{BRb})$$

$$T_{BRb} = 1.077 \text{ in}$$

$$T_{BR} := \max(T_{BRb}, T_{BRf})$$

$$T_{BR} = 1.95 \text{ in} \quad \textit{Backing ring thickness}$$

Summary



This figure is provided only to show the nomenclature and is not to scale. Scaled representation of the hub can be obtained using the Excel worksheet developed for bolting spacing checks.

$D = 21.152 \text{ in}$

(if time use only)

$D_H = 29.613 \text{ in}$

$\frac{D_H}{D} = 1.4$

If this is 2, there was an error find the optimum solution using the minimize function

$D_F = 41.458 \text{ in}$

$\frac{D_F}{D} = 1.96$

$\sigma_{\text{hoop}} = 14.204 \text{ ksi}$

$\sigma_{\text{radial}} = 2.961 \text{ ksi}$

$L_H = 8.461 \text{ in}$

$\frac{L_H}{D} = 0.4$

Fit = "FN2"

$N_{\text{ribs}} = 6$

$T_F = 1.5 \text{ in}$

$T_{RS} = 1.5 \text{ in}$ *Rib thickness*

$T_G = 1.5 \text{ in}$

$T_{BR} = 1.95 \text{ in}$

$d_{\text{bolt_circle}} = 31.363 \text{ in}$

$N_{\text{circles}} = 1$

$d_{\text{bolt}} = 1.25 \text{ in}$

$N_{\text{boltFinal}} = 23$

Note: The bolting requirements are preliminary and can be further refined to meet all spacing requirements using the Excel worksheets developed as part of the project.

This following functions are used to determine stress concentration factors for torsion and bending for fatigue, and also endurance limit used for trunnion design

$$\sigma_{ut} \text{ (MPa)} \quad a^{1/2} \text{ (mm)}^{1/2}$$

Table 6.7.3.2-1

NeuberData :=

420.00	0.54
630.00	0.35
840.00	0.25
980.00	0.20
1260.00	0.12

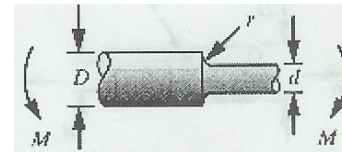
$$a_{\text{interp}}(\sigma_{ut}) := \text{linterp}\left(\text{NeuberData}^{\langle 0 \rangle}, \text{NeuberData}^{\langle 1 \rangle}, \sigma_{ut}\right)^2 \cdot \text{mm}$$

$$q(\sigma_{ut}, r) := \frac{1}{\left(1 + \frac{\sqrt{a_{\text{interp}}(\sigma_{ut})}}{\sqrt{r}}\right)} \quad \text{Eqn. 6.7.3.2-3, values should be in MPa and mm (but have no Mathcad units)}$$

K_tData :=

D/d	A	b
6	0.87868	-0.33243
3	0.89334	-0.3086
2	0.90879	-0.28598
1.5	0.93836	-0.25759
1.2	0.97098	-0.21796
1.1	0.9512	-0.23757
1.07	0.97527	-0.20958
1.05	0.98137	-0.19653
1.03	0.98061	-0.18381
1.02	0.96048	-0.17711
1.01	0.91938	-0.17032

See pg. A6-3, Fig. A6-2-4



$$K_{t\text{Data}} := \text{csort}(K_{t\text{Data}}, 0)$$

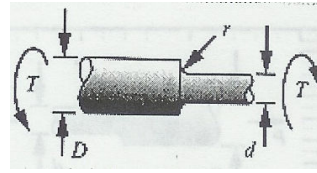
$$K_t(D, d, r) := \begin{cases} A \leftarrow \text{linterp}\left(K_{t\text{Data}}^{\langle 0 \rangle}, K_{t\text{Data}}^{\langle 1 \rangle}, \frac{D}{d}\right) \\ b \leftarrow \text{linterp}\left(K_{t\text{Data}}^{\langle 0 \rangle}, K_{t\text{Data}}^{\langle 2 \rangle}, \frac{D}{d}\right) \\ A \cdot \left(\frac{r}{d}\right)^b \end{cases}$$

Geometric Stress Concentration factor for Shaft with Shoulder Fillet in Bending (pg. Fig. A6.2-4, pg. A6-3, LRFDM)

$$K_F(D, d, r, \sigma_{ut}) := 1 + q(\sigma_{ut}, r) \cdot (K_t(D, d, r) - 1) \quad \text{Eqn. 6.7.3.2-1}$$

$$K_{tsData} := \begin{array}{c|ccc} & D/d & A & b \\ \hline & 2 & 0.86331 & -0.23865 \\ & 1.33 & 0.84897 & -0.23161 \\ & 1.2 & 0.83425 & -0.21649 \\ & 1.09 & 0.90337 & -0.12692 \end{array}$$

See pg. A6-4, Fig A6-2-5



$$K_{tsData} := \text{csort}(K_{tsData}, 0)$$

$$K_{ts}(D, d, r) := \begin{cases} A \leftarrow \text{interp}\left(K_{tsData}^{(0)}, K_{tsData}^{(1)}, \frac{D}{d}\right) \\ b \leftarrow \text{interp}\left(K_{tsData}^{(0)}, K_{tsData}^{(2)}, \frac{D}{d}\right) \\ A \cdot \left(\frac{r}{d}\right)^b \end{cases}$$

*Geometric Stress
Concentration factor for
Shaft with Shoulder Fillet in
Torsion (pg. Fig. A6.2-5, pg.
A6-4, LRFDM)*

$$K_{FS}(D, d, r, \sigma_{ut}) := 1 + q(\sigma_{ut}, r) \cdot (K_{ts}(D, d, r) - 1)$$

Eqn. 6.7.3.2-2

The following function computes endurance limit

$$\alpha := 0.5$$

Sec. 6.6.3.2

$$C_D(D) := \left(\frac{\frac{D}{\text{mm}}}{7.6}\right)^{-0.113}$$

$$C_S(\sigma_{ut}) := \begin{cases} a \leftarrow 4.51 \\ b \leftarrow -0.265 \\ a \cdot (\sigma_{ut})^b \end{cases}$$

*Eqn. 6.6.3.2-4
a & b from Table 6.6.3.2-1
for machined surface*

$$C_R := 1 \quad \text{Sec. 6.6.3.2}$$

$$C_T := 1$$

$$C_M := 1$$

$$\sigma_e(D, \sigma_{ut}) := \alpha \cdot \sigma_{ut} \cdot C_D(D) \cdot C_S(\sigma_{ut}) \cdot C_R \cdot C_T \cdot C_M$$

The following functions compute contact pressure and hoop stress resulting from shrink fit on the hub using solutions for compound cylinders presented in "Advanced Strength and Applied Elasticity", 3rd Edition by A.C. Ugural & S.K. Fenster, pg. 337

$$P_{\text{ShrinkFit}}(R_{\text{out}}, R_{\text{mid}}, R_{\text{in}}, E, \delta_R) := \frac{E \cdot \delta_R}{R_{\text{mid}}} \cdot \frac{(R_{\text{mid}}^2 - R_{\text{in}}^2) \cdot (R_{\text{out}}^2 - R_{\text{mid}}^2)}{2 \cdot R_{\text{mid}}^2 \cdot (R_{\text{out}}^2 - R_{\text{in}}^2)}$$

$$\sigma_{\theta \text{ShrinkFit}}(R_{\text{out}}, R_{\text{mid}}, R_{\text{in}}, E, \delta_R) := P_{\text{ShrinkFit}}(R_{\text{out}}, R_{\text{mid}}, R_{\text{in}}, E, \delta_R) \cdot \frac{R_{\text{mid}}^2 + R_{\text{out}}^2}{R_{\text{out}}^2 - R_{\text{mid}}^2}$$

The following functions are based on ANSI standard fits for shaft and hole

$$\text{FN1}_{\text{min}}(D) := \begin{cases} 4.4 & \text{if } D \geq 17.72 \wedge D \leq 19.69 \\ 6.0 & \text{if } ((D \geq 19.69 \wedge D \leq 24.34)) \\ 7.0 & \text{if } (D \geq 24.34 \wedge D \leq 30.09) \\ 7.5 & \text{if } (D \geq 30.09 \wedge D \leq 35.47) \\ 9.5 & \text{if } (D \geq 35.47 \wedge D \leq 41.49) \\ 11.0 & \text{if } (D \geq 41.49 \wedge D \leq 48.28) \\ 13.0 & \text{if } (D \geq 48.28 \wedge D \leq 56.19) \\ 14.0 & \text{if } (D \geq 56.19 \wedge D \leq 65.54) \\ \text{"Diameter out of range"} & \text{otherwise} \end{cases}$$

These functions return the minimum diametral interference (in 1000th of an inches) for a given diameter D (inches)

$$\text{FN2}_{\text{min}}(D) := \begin{cases} 7.5 & \text{if } D \geq 17.72 \wedge D \leq 19.69 \\ 9.0 & \text{if } ((D \geq 19.69 \wedge D \leq 24.34)) \\ 11.0 & \text{if } (D \geq 24.34 \wedge D \leq 30.09) \\ 14.0 & \text{if } (D \geq 30.09 \wedge D \leq 35.47) \\ 16.0 & \text{if } (D \geq 35.47 \wedge D \leq 41.49) \\ 17.0 & \text{if } (D \geq 41.49 \wedge D \leq 48.28) \\ 20.0 & \text{if } (D \geq 48.28 \wedge D \leq 56.19) \\ 24.0 & \text{if } (D \geq 56.19 \wedge D \leq 65.54) \\ \text{"Diameter out of range"} & \text{otherwise} \end{cases}$$

$$\text{FN3}_{\text{min}}(D) := \begin{cases} 11.5 & \text{if } D \geq 17.72 \wedge D \leq 19.69 \\ 15.0 & \text{if } ((D \geq 19.69 \wedge D \leq 24.34)) \\ 17.0 & \text{if } (D \geq 24.34 \wedge D \leq 30.09) \\ 21.0 & \text{if } (D \geq 30.09 \wedge D \leq 35.47) \\ 24.0 & \text{if } (D \geq 35.47 \wedge D \leq 41.49) \\ 30.0 & \text{if } (D \geq 41.49 \wedge D \leq 48.28) \\ 35.0 & \text{if } (D \geq 48.28 \wedge D \leq 56.19) \\ 39.0 & \text{if } (D \geq 56.19 \wedge D \leq 65.54) \\ \text{"Diameter out of range"} & \text{otherwise} \end{cases}$$

$$\text{FN1}_{\max}(D) := \begin{cases} 7.0 & \text{if } D \geq 17.72 \wedge D \leq 19.69 \\ 9.2 & \text{if } ((D \geq 19.69 \wedge D \leq 24.34)) \\ 10.2 & \text{if } (D \geq 24.34 \wedge D \leq 30.09) \\ 11.6 & \text{if } (D \geq 30.09 \wedge D \leq 35.47) \\ 13.6 & \text{if } (D \geq 35.47 \wedge D \leq 41.49) \\ 16.0 & \text{if } (D \geq 41.49 \wedge D \leq 48.28) \\ 18.0 & \text{if } (D \geq 48.28 \wedge D \leq 56.19) \\ 20.5 & \text{if } (D \geq 56.19 \wedge D \leq 65.54) \\ \text{"Diameter out of range"} & \text{otherwise} \end{cases}$$

These functions return the maximum diametral interference (in 1000th of an inches) for a given diameter D (inches)

$$\text{FN2}_{\max}(D) := \begin{cases} 11.6 & \text{if } D \geq 17.72 \wedge D \leq 19.69 \\ 14.0 & \text{if } ((D \geq 19.69 \wedge D \leq 24.34)) \\ 16.0 & \text{if } (D \geq 24.34 \wedge D \leq 30.09) \\ 20.5 & \text{if } (D \geq 30.09 \wedge D \leq 35.47) \\ 22.5 & \text{if } (D \geq 35.47 \wedge D \leq 41.49) \\ 25.0 & \text{if } (D \geq 41.49 \wedge D \leq 48.28) \\ 28.0 & \text{if } (D \geq 48.28 \wedge D \leq 56.19) \\ 34.0 & \text{if } (D \geq 56.19 \wedge D \leq 65.54) \\ \text{"Diameter out of range"} & \text{otherwise} \end{cases}$$

$$\text{FN3}_{\max}(D) := \begin{cases} 15.6 & \text{if } D \geq 17.72 \wedge D \leq 19.69 \\ 20.0 & \text{if } ((D \geq 19.69 \wedge D \leq 24.34)) \\ 22.0 & \text{if } (D \geq 24.34 \wedge D \leq 30.09) \\ 27.5 & \text{if } (D \geq 30.09 \wedge D \leq 35.47) \\ 30.5 & \text{if } (D \geq 35.47 \wedge D \leq 41.49) \\ 38.0 & \text{if } (D \geq 41.49 \wedge D \leq 48.28) \\ 43.0 & \text{if } (D \geq 48.28 \wedge D \leq 56.19) \\ 49.0 & \text{if } (D \geq 56.19 \wedge D \leq 65.54) \\ \text{"Diameter out of range"} & \text{otherwise} \end{cases}$$

$$\delta_{\text{Range}}(D, \text{Fit}) := \begin{cases} \begin{pmatrix} \text{FN1}_{\min}(D) \\ \text{FN1}_{\max}(D) \end{pmatrix} & \text{if Fit = "FN1"} \\ \begin{pmatrix} \text{FN2}_{\min}(D) \\ \text{FN2}_{\max}(D) \end{pmatrix} & \text{if Fit = "FN2"} \\ \begin{pmatrix} \text{FN3}_{\min}(D) \\ \text{FN3}_{\max}(D) \end{pmatrix} & \text{if Fit = "FN3"} \\ \begin{pmatrix} \text{"Out of range"} \\ \text{"Out of range"} \end{pmatrix} & \text{otherwise} \end{cases}$$

```

FN(D,δD) := "FN1" if (D ≥ 17.72 ∧ D ≤ 19.69 ∧ δD ≤ 7)
            "FN2" if [D ≥ 17.72 ∧ D ≤ 19.69 ∧ (δD > 7 ∧ δD ≤ 11.6)]
            "FN3" if [D ≥ 17.72 ∧ D ≤ 19.69 ∧ (δD > 11.6 ∧ δD ≤ 15.6)]
            "FN4 or above" if (D ≥ 17.72 ∧ D ≤ 19.69 ∧ δD > 15.6)
            "FN1" if (D ≥ 19.69 ∧ D ≤ 24.34 ∧ δD ≤ 9.2)
            "FN2" if [D ≥ 19.69 ∧ D ≤ 24.34 ∧ (δD > 9.2 ∧ δD ≤ 14)]
            "FN3" if [D ≥ 19.69 ∧ D ≤ 24.34 ∧ (δD > 14 ∧ δD ≤ 20)]
            "FN4 or above" if (D ≥ 19.69 ∧ D ≤ 24.34 ∧ δD > 20)
            "FN1" if (D ≥ 24.34 ∧ D ≤ 30.09 ∧ δD ≤ 10.2)
            "FN2" if [D ≥ 24.34 ∧ D ≤ 30.09 ∧ (δD > 10.2 ∧ δD ≤ 16)]
            "FN3" if [D ≥ 24.34 ∧ D ≤ 30.09 ∧ (δD > 16 ∧ δD ≤ 22)]
            "FN4 or above" if (D ≥ 24.34 ∧ D ≤ 30.09 ∧ δD > 22)
            "FN1" if (D ≥ 30.09 ∧ D ≤ 35.47 ∧ δD ≤ 11.6)
            "FN2" if [D ≥ 30.09 ∧ D ≤ 35.47 ∧ (δD > 11.6 ∧ δD ≤ 20.5)]
            "FN3" if [D ≥ 30.09 ∧ D ≤ 35.47 ∧ (δD > 20.5 ∧ δD ≤ 27.5)]
            "FN4 or above" if (D ≥ 30.09 ∧ D ≤ 35.47 ∧ δD > 27.5)
            "FN1" if (D ≥ 35.47 ∧ D ≤ 41.49 ∧ δD ≤ 13.6)
            "FN2" if [D ≥ 35.47 ∧ D ≤ 41.49 ∧ (δD > 13.6 ∧ δD ≤ 22.5)]
            "FN3" if [D ≥ 35.47 ∧ D ≤ 41.49 ∧ (δD > 22.5 ∧ δD ≤ 30.5)]
            "FN4 or above" if (D ≥ 35.47 ∧ D ≤ 41.49 ∧ δD > 30.5)
            "FN1" if (D ≥ 41.49 ∧ D ≤ 48.28 ∧ δD ≤ 16.0)
            "FN2" if [D ≥ 41.49 ∧ D ≤ 48.28 ∧ (δD > 16.0 ∧ δD ≤ 25.0)]
            "FN3" if [D ≥ 41.49 ∧ D ≤ 48.28 ∧ (δD > 25.0 ∧ δD ≤ 38.0)]
            "FN4 or above" if (D ≥ 41.49 ∧ D ≤ 48.28 ∧ δD > 38.0)
            "FN1" if (D ≥ 48.28 ∧ D ≤ 56.19 ∧ δD ≤ 18.0)
            "FN2" if [D ≥ 48.28 ∧ D ≤ 56.19 ∧ (δD > 18.0 ∧ δD ≤ 28.0)]
            "FN3" if [D ≥ 48.28 ∧ D ≤ 56.19 ∧ (δD > 28.0 ∧ δD ≤ 43.0)]
            "FN4 or above" if (D ≥ 48.28 ∧ D ≤ 56.19 ∧ δD > 43.0)
            "FN1" if (D ≥ 56.19 ∧ D ≤ 65.54 ∧ δD ≤ 20.5)
            "FN2" if [D ≥ 56.19 ∧ D ≤ 65.54 ∧ (δD > 20.5 ∧ δD ≤ 34.0)]
            "FN3" if [D ≥ 56.19 ∧ D ≤ 65.54 ∧ (δD > 34.0 ∧ δD ≤ 49.0)]
            "FN4 or above" if (D ≥ 56.19 ∧ D ≤ 65.54 ∧ δD > 49.0)
            "Diameter out of range" otherwise

```

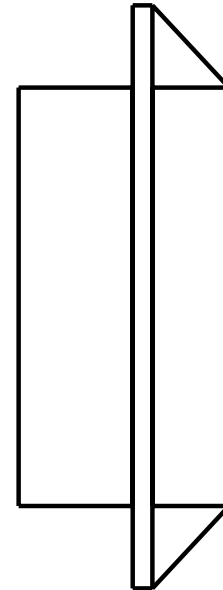
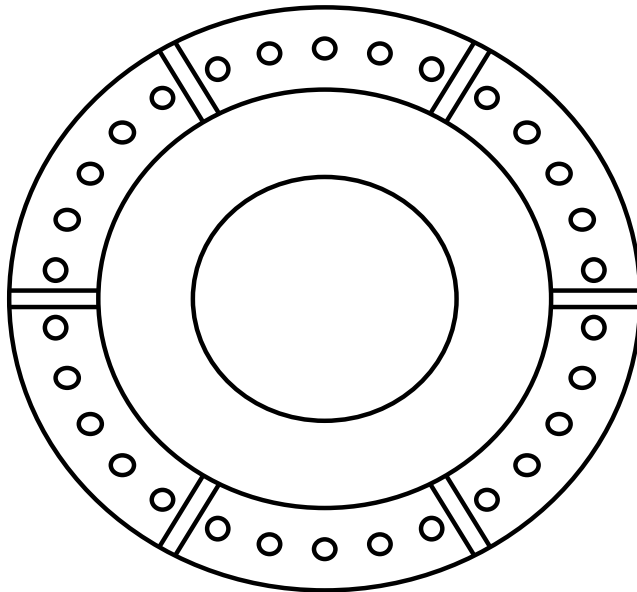
This function returns the type of fit that can provide the desired interference or more for a shaft of given diameter (inches) and diametral interference (in 1000ths of an inch)

$$\delta_{\text{Range}}(D, \text{Fit}) := \begin{cases} \begin{pmatrix} \text{FN1}_{\min}(D) \\ \text{FN1}_{\max}(D) \end{pmatrix} & \text{if Fit = "FN1"} \\ \begin{pmatrix} \text{FN2}_{\min}(D) \\ \text{FN2}_{\max}(D) \end{pmatrix} & \text{if Fit = "FN2"} \\ \begin{pmatrix} \text{FN3}_{\min}(D) \\ \text{FN3}_{\max}(D) \end{pmatrix} & \text{if Fit = "FN3"} \\ \begin{pmatrix} \text{"Out of range"} \\ \text{"Out of range"} \end{pmatrix} & \text{otherwise} \end{cases}$$

	Project				
	Designed	Checked	Project No.	Date	Sheet of

Subject: Hub-Girder Assembly Design

Task: Bolt Analysis



Bore	21.152
Hub flange Inner diameter	36.312
Hub flange outer diameter	50.837
No. of ribs	6
Effective rib thickness (including fillet)	1.5
Bolt diameter	1.25
No. of bolt circles	1
Bolt circle 1 - Diameter	43.575
Bolt circle 1 - No. of bolts between 2 ribs	5
Angle from rib axis to first bolt	6.64
Bolt circle 2 - Diameter	
Bolt circle 2 - No. of bolts between 2 ribs	
Angle from rib axis to first bolt	
Bolt circle 3 - Diameter	
Bolt circle 3 - No. of bolts between 2 ribs	
Angle from rib axis to first bolt	

Hub Length	16.9216
Flange Thickness	1.5
Total # Bolts Reqd.	28

Draw

Distance between bolts **OK**
 Bolt Edge Distance **OK**
 Bolt End Distance **OK**